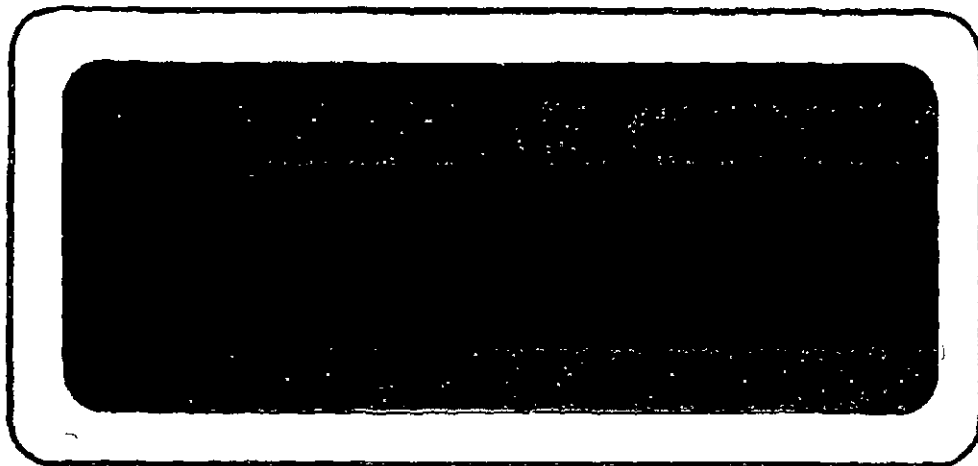


7
X



~~N71-18713~~



Get DRA

FACILITY FORM 602	N71-18713 (ACCESSION NUMBER)	(FORM) B
	153 (PAGES)	(CODE) 07
	CR-116789 (NASA CR OR TMX OR AD NUMBER)	(CATEGORY)

TRW
SYSTEMS GROUP

ONE SPACE PARK • REDONDO BEACH CALIFORNIA

Reproduced by
**NATIONAL TECHNICAL
INFORMATION SERVICE**
Springfield, Va 22151



SUMMARY REPORT
TASK IV SPACE STORABLE PROPELLANT MODULE
ENVIRONMENTAL CONTROL TECHNOLOGY
November 16, 1970


Report No. 14051-6005-T0-00

SUMMARY REPORT
TASK IV SPACE STORABLE PROPELLANT MODULE
ENVIRONMENTAL CONTROL TECHNOLOGY
Contract No 7-750

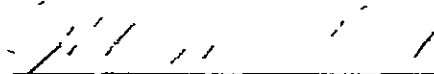
Report No. 14051-6005-T0-00

by

O O Haroldsen



J. F. Bevans, Manager
Heat Transfer and Thermodynamics Dept.



W. R. Wannlund, Manager
Engineering Design Laboratory

TRW SYSTEMS
One Space Park
Redondo Beach, California

Table of Contents

	<u>Page</u>
SUMMARY	1
1.0 INTRODUCTION	1
2.0 MODULE DESCRIPTION	2
3.0 MISSION PROFILE	15
3.1 Groundhold	15
3.2 Launch and Parking Orbit	15
3.3 Jupiter Transfer Phase	15
3.4 Jupiter Orbit	16
3.5 Module Operating Requirements	16
4.0 METHOD OF ANALYSIS	21
4.1 Thermal Analysis Models	21
4.2 Propulsion Analysis Models	29
5.0 RESULTS OF ANALYSIS	36
5.1 Groundhold Thermal Control	36
5.2 Flight Thermal Control	41
5.3 Propulsion System Results	56
6.0 CONCLUSIONS and RECOMMENDATIONS	84
REFERENCES	89
Appendix A Thermal Computer Model Details	90
Appendix B Propulsion System Analysis Equations	126

List of Figures

<u>Figure</u>		<u>Page</u>
2-1	Schematic Diagram of $\text{OF}_2/\text{B}_2\text{H}_6$ System	7
2-2	Engine Thrust Support Design	8
2-3	Schematic of Propellant Line Insulation	9
2-4	Louver Internal Effective Emissivity	10
3-1	Off-Pointing Angle During Mission	18
3-2	Solar Flux at Spacecraft	19
5-1	Equilibrium Temperature as a Function of LN_2 Coolant Flow Rate	60
5-2	Transient Warm-up and Cooldown During Groundhold	61
5-3	Fluid Temperature Characteristics with Cyclic Control	62
5-4	Tank Temperature with 2000 Btu/hr Heat Addition	63
5-5	Steady-State Temperatures for Varying Solar Radiation	64
5-6	Relative Solar Heating Rate on a Black Surface During Normal Mission	65
5-7	Module Temperatures after Launch on Normal Mission	66
5-8	Module Frame Temperatures after Launch on Normal Mission	67
5-9	Sources of Module Heating while in Earth Orbit	68
5-10	Effect of Orienting from 0° Off-Pointing to 90° Off-Pointing while Near Earth	69
5-11	Temperature History of Bipropellant Valve Immediately After Launch	70
5-12	Outside Surface Temperature of Engine During Operation	71
5-13	Helium Temperature Drop During Engine Firing	72
5-14	Temperature Histories During and After Engine Operation	73

List of Figures (Con't)

<u>Figure</u>		<u>Page</u>
5-15	Steady-State Fuel Temperatures for Varying Off-Pointing Angles	74
5-16	Thermal History of Major Components During Normal Mission	75
5-17	Thermal Histories of Major Components During Normal Mission	77
5-18	Effect of Varying RTG Temperature on Quasi-Steady-State State Module Temperature	80
5-19	Steady-State Temperatures for Varying Solar Radiation	81
5-20	Mixture Ratio vs Propellant Temperatures	82
5-21	Chamber Pressure vs Propellant Temperatures	83

List of Tables

Table		<u>Page</u>
2-1	Summary of Estimated Subsystem Weight	11
3-1	Recommended Component Temperature Ranges	20

SUMMARY

The objective of Task IV was to make a detailed analysis of the B_2H_6/OF_2 propulsion module established by the work of Tasks I, II, and III. The results of this analysis are given in this report.

The analysis considered all phases of the mission, including groundhold. The approach used was to first establish by analysis the thermal characteristics and temperature histories of the propulsion module during its life. This was followed by an analysis of the propulsion system which accounted for the thermal environment as established by the thermal analysis.

This investigation shows that the thermal control system, as designed, maintains the required thermal environment throughout the mission. It also shows that considerable mission variations can be accommodated without ill effects. Where it was originally believed that exposure to the sun for only one or two hours could be accepted, as much as 20° off-pointing may be acceptable during the first days of the mission even if no special shielding is provided. After day 100 of the mission, continuous 90° off-pointing is acceptable.

The investigation shows that, though louvers aid in controlling the module temperature, they are not very effective. For this reason, unless a remotely controlled louver mounted on the RTG is acceptable, it is recommended that a totally passive thermal control system (replace the louvers with radiator plates) be utilized.

Finally, it is concluded that, in the light of the accuracy of spacecraft thermal analyses, an experimental program should be initiated. The test program objectives should be to 1) prove the validity of the analysis during groundhold and flight, and 2) obtain sufficient information concerning the module thermal characteristics that the thermal control system may be "trimmed" for particular missions.

1 0 INTRODUCTION

This is the Task IV Summary Report of the Space Storable Propulsion Module Environmental Control Technology Project accomplished under Contract No NAS 7-750. Task IV had as its objective the thermal analysis of a propulsion module designed during Task III, Reference 1. Section 2 of this report describes in detail the propulsion module and Section 3 describes the mission profile and constraints.

The analyses were broken into two separate parts

- o The temperature history and thermal characteristics of the module were determined
- o The effects of the module thermal environment on the operation of the propulsion system were determined

Section 4 describes the computer programs used in this work and the basis of these programs. Section 5 lists the results of the analysis and Section 6 gives the conclusions which can be drawn from the investigation.

2 0 MODULE DESCRIPTION

The basic module design is as shown in Drawing SK 406876, sheets 1 and 2, and the schematic for the propulsion system as given in Figure 2-1.

The propulsion system is comprised of three types of equipment tanks, engine and plumbing. Two propellant tanks, one for each propellant, are used. Each tank is constructed of boron filament and lined with 0.010 inch aluminum. Each tank is 36 inches in diameter and utilizes hemispherical ends having an eccentricity of 0.784. The support attachments for each tank provide both axial and shear restraint at the bottom while only shear restraint at the top. To avoid the transmission of any moments into the tanks, universal joints are used at both ends.

Internal to each propellant tank is a capillary-type propellant acquisition device (exact details to be established by JPL) and a ground-hold heat exchanger. The heat exchanger consists of a 1/2-inch diameter aluminum tube, 8 feet long, formed into a coil having a diameter of approximately 5 inches. Through this coil will pass LN₂ during ground-hold for propellant cooling purposes.

The helium tank is also constructed of boron filament. This tank is suspended at the top by an aluminum cross beam and is laterally stabilized at the bottom by boron filament tubes running from the tank to the engine support frame. A cooling coil, similar to those in the propellant tanks is installed in the helium tank.

Other than a weight penalty, there is no technical reason why the boron filament tanks cannot be replaced with metal tanks. The thermal characteristics of the module would be essentially the same since the thermal conductivity of the walls of the tanks is very large compared to the insulation conductivity.

The engine, as indicated in the drawing, is supported below the helium tank by a small triangular frame which is, in turn, suspended from the main frame by boron filament tubular members. For purposes of analysis, it was assumed that the engine is held in place by a classic gimbal, comprised of an outer ring fixed with respect to the spacecraft, a floating

inside ring and appropriate crossed axes which are perpendicular to each other and the engine centerline. The gimbal assembly is held by a thrust assembly as shown in Figure 2-2

At the direction of JPL, a film cooled columbium engine, having a 40:1 expansion ratio, has been assumed. Other engine parameters assumed are:

Mixture Ratio	3 0
Chamber Pressure	100 psia
I_{sp}	400 sec
Thrust	1000 lbs

Components are clustered in order to facilitate access and the fuel and oxidizer connections are separated for safety reasons. All gas circuitry is 1/4-inch except for the vent and relief lines which are 1/2-inch. All propellant circuitry is 3/4-inch except for the fill lines which are 1/2-inch. All tubing is assumed to be 300 series stainless steel with welded or brazed connections, except where bolted or flanged joints are necessary for assembly and/or test purposes.

Where flexibility in the lines is necessary, short bellows or corrugated inconel hoses are used. All propellant lines have been routed to facilitate passivation and drainage. In addition, the following design provisions are shown on the drawings:

- o A separate helium filter upstream of the regulator is utilized
- o The propellant valve solenoid pilot valve is made a part of the gimbaling portion of the engine to improve response
- o The feedline isolation and relief return valving is positioned as close to the tank as is possible in order to minimize the length of liquid filled line
- o Injector purge solenoid and check valves are included
- o Gas supply lines to the pilot and purge valves are looped to provide flexibility.

There are three main control panels, one propellant tank pressurization control panel for each propellant and one helium control panel. The helium control panel contains the helium squib valves, regulator,

filter and fill valve. All of the fluid line disconnect fittings have been mounted directly on one of these three panels. This places them all approximately 30 inches inside the shroud line. If it becomes desirable for reasons of shroud design or groundhold procedures to mount these fittings nearer the shroud, special mounting brackets will be required.

A space truss structure is utilized to support the propulsion hardware and also the spacecraft. The reasons for this choice are given in Reference 2. The entire module and spacecraft are supported, when attached to the boost vehicle, by 16 boron filament tubular struts having aluminum fittings. These struts remain with the boost vehicle upon separation. The separation fittings (pyrotechnic devices) are located on the main platform.

Both propellant tanks, the helium tank, and all propellant-filled lines are insulated with 3/4-inch of two-pound density, closed-cell polyurethane foam¹. This foam is extended to cover all metallic hardware (frame, gas circuitry, etc.) which contact the tanks to a distance of one foot from the point of contact. Non-metallic members are similarly insulated for a distance of 4 inches. In addition, the aluminum beam which supports the helium tank is entirely insulated with foam.

Aluminized Mylar blanket insulation is also utilized in several places. A 10-layer blanket, attached to the lower surface of the electronics package (spacecraft) which extends down on to the spacecraft support struts, is required. Three other blankets of insulation are shown in Drawing 406876, one around each of the propellant tank helium vent panels and one around the helium control panel. The purpose of these blankets is to maintain the temperature of the enclosed equipment near propellant temperatures during flight and also at or near ambient temperature during the groundhold phase. These blankets have flap-type doors to allow easy access to the enclosed equipment.

¹As specified by North American Rockwell Specification MBO 130-077, "Specification for Two-Pound Density Polyurethane Spray Foam."

In order to maintain most of the fluid circuitry lines at the prescribed temperatures, the tubes in question are routed along the surface of adjacent propellant or pressurant tank insulation and then overlaid with 20 layers of aluminized Mylar. Where no such adjacent tank exists, the tube is insulated around its entirety with the aluminized Mylar. A sketch of this arrangement for one of the propellant lines is given in Figure 2-3. Since in flight, conductivity of the foam is much higher than the conductivity of the aluminized Mylar, the tube adopts the temperature of the tank in the region where the tube is adjacent to the tank.

In all cases, the aluminized Mylar is installed with the Mylar side out. In addition, a 10-layer blanket of aluminized Kapton attached to the lower meteoroid shield on the helium tank side, is necessary. Kapton must be used in place of Mylar since, during engine operation, the allowable temperature for Mylar is exceeded.

Two openings are left in the foam insulation on each propellant tank to accommodate either radiator plates or louver assemblies. If louvers are used, they will be secured to the tanks by bonding the flanges of the assemblies frame to the tank wall.

Louver assemblies consist of a frame within which is mounted bimetallic springs. A radiator plate covered with second-surface silvered mirrors having an emittance of 0.8 is attached to the outside of the frame. Thus, when the insulation discussed above is removed, the mirrored surface "sees" space and the aluminum louvers see the back of the radiator plate on one side and the tank surface on the other.

Louver assemblies are designed such that the actuator springs sense the tank surface temperature and thus actuate (rotate) the louvers open or closed, depending on the tank temperature. The effective emissivity of the assemblies as a function of tank temperature are assumed to be as given in Figure 2-4. This assumption is based on previous TRW spacecraft designs (Pioneer, OGO).

If only radiator plates are used, they will merely consist of a section of tank wall to which is bonded second-surface silvered mirrors.

To prevent frost formation within and on the louvers after propellant loading, a sophisticated insulation cover, which is removable after launch,

is provided. This cover is shown on Drawing SK 406876, sheet 2 and is described in Reference 1. As mentioned in Reference 1, the major problem in providing a cover for louvers is to provide a way of allowing the louvers to "breathe" through the cover without allowing frost to accumulate on the louvers. If a radiator plate is used, the necessity of providing for the breathing disappears and the cover then becomes a relatively simple removable section of insulation.

For purposes of this analysis, it has been assumed that the spacecraft, or else a platform mounted between the module and the spacecraft, will partially shield the module from solar heating. In a portion of the analysis, this shield was considered to be 10 feet in diameter (shroud diameter is 11 feet). The effect of reducing this shield diameter is also considered.

The total weight of the propulsion module is approximately 3348 pounds. Approximately 27 pounds is attributable to the thermal control system. A detailed weight breakdown of the module is given in Table 2-1.

One general comment is appropriate at this point. Every effort was made to avoid peculiar design requirements or exotic materials. The objective was to produce the most simple design commensurate with the mission requirements. Thus, such things as special coatings were avoided where possible. It will become obvious through the discussion, that there are places (for example, the frame) where minor changes could be made to reduce temperatures. When mission requirements or module limitations are further defined, it may become necessary to institute some changes, but within the mission constraints as they are now specified, these changes are not necessary.

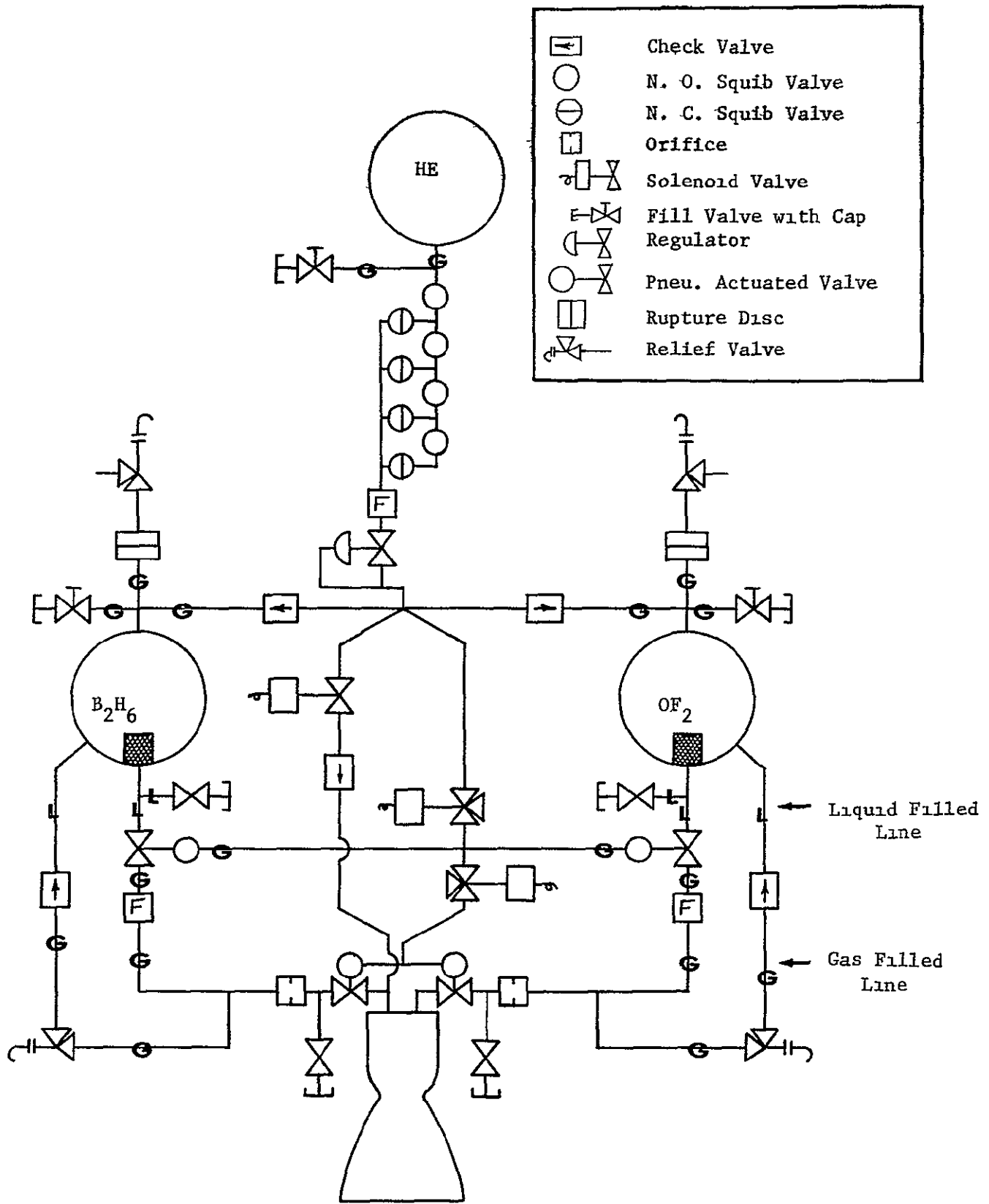


Figure 2-1 Schematic Diagram of OF_2/B_2H_6 System

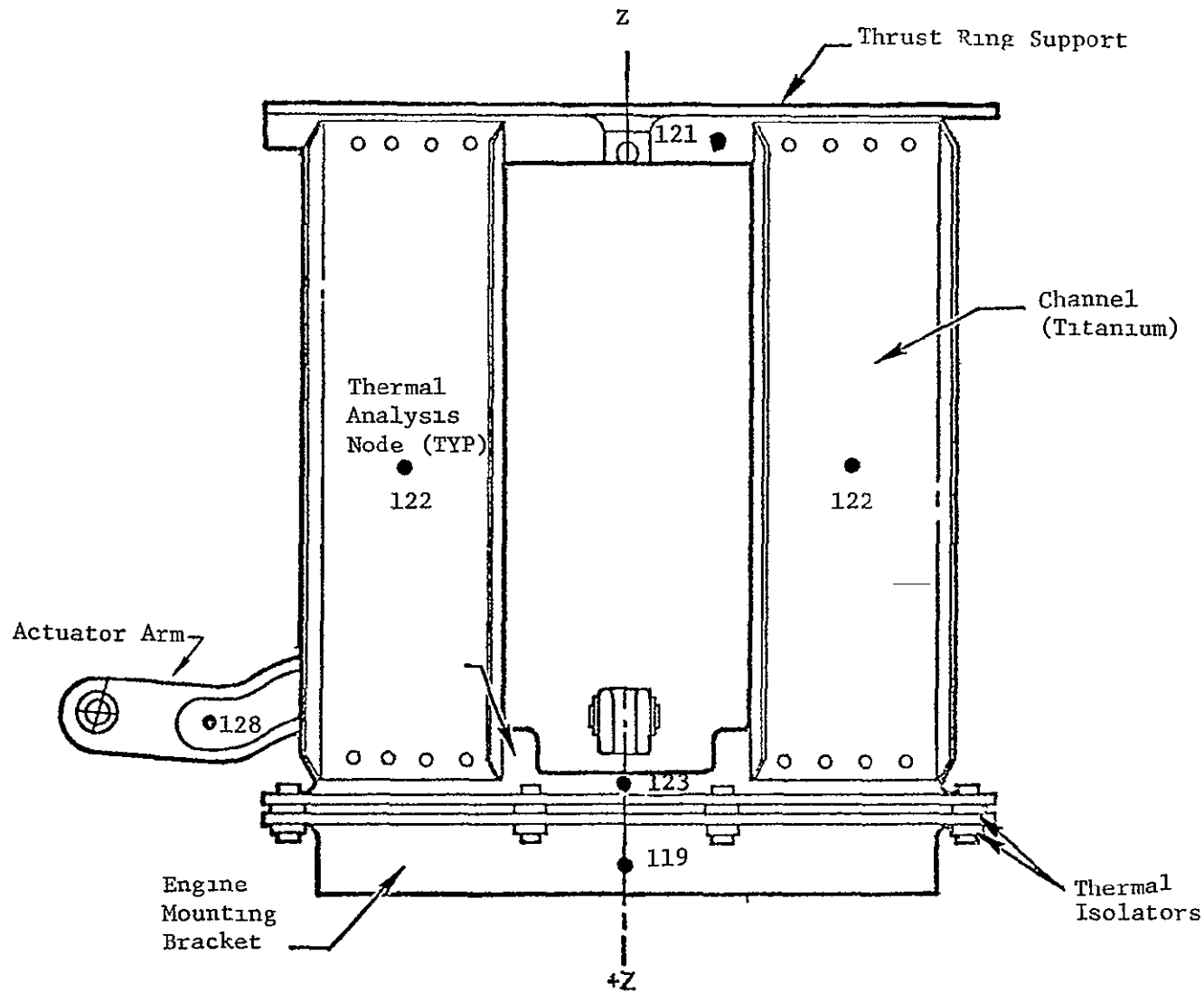


Figure 2-2 Engine Thrust Support Design

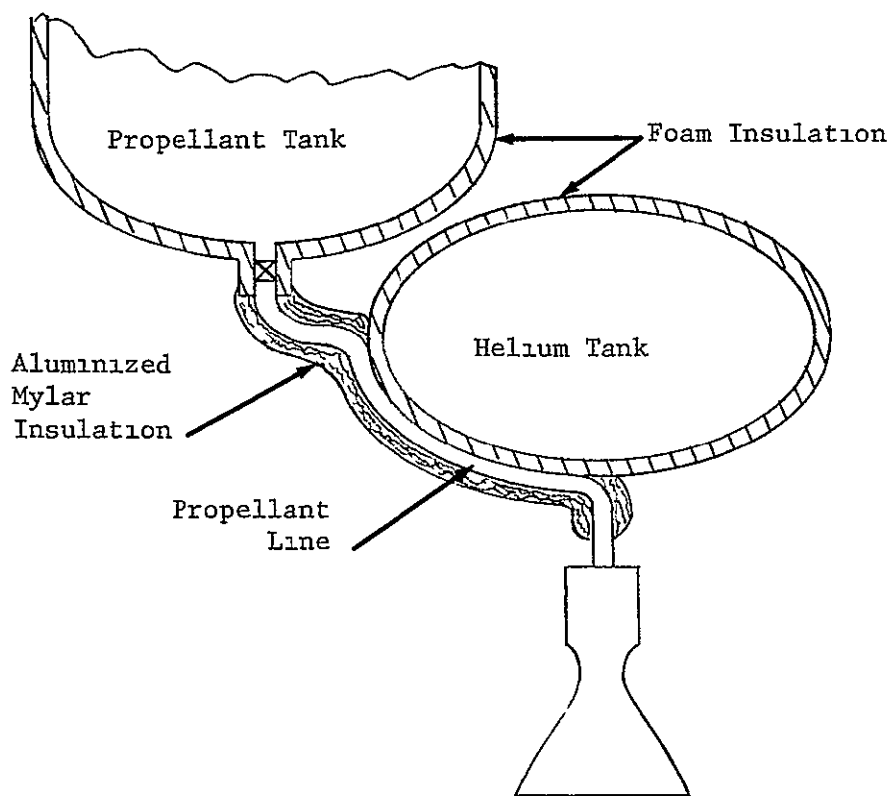


Figure 2-3 Schematic of Propellant Line Insulation

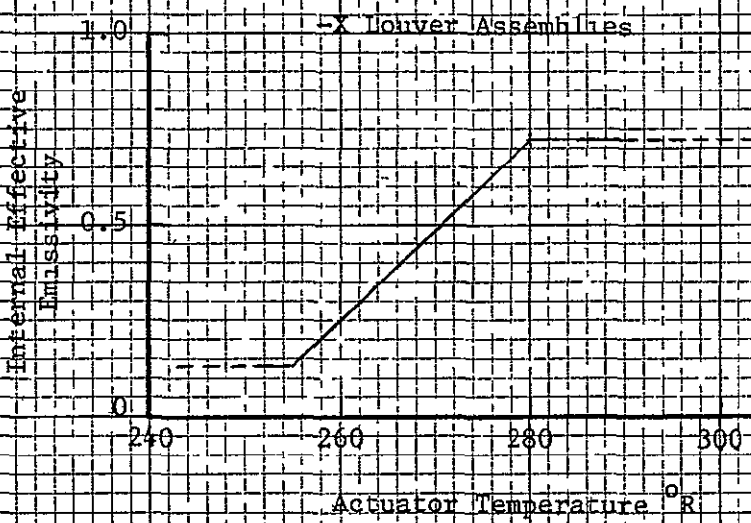
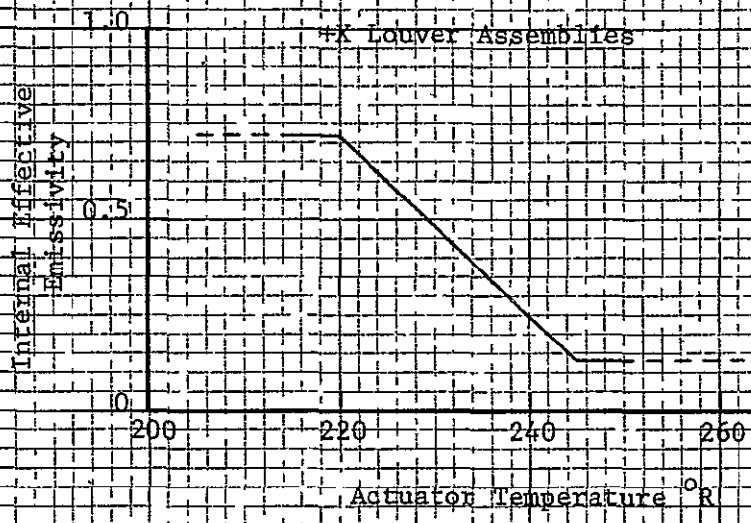


Figure 2-4 Louver Internal Effective Emissivity

Table 2-1

Summary of Estimated Subsystem Weight

Tankage

1 - helium tank at 90 lb each	90 0 lb
2 - propellant tanks at 59 6 lb. each	119 2 lb
2 - propellant surface tension screens at 2 lb each	4 0 lb
Total	<u>213 2 lb</u>

Liquid Circuits

2 - passivation valves at 1 lb each	2 0 lb
2 - fill valves at 1 lb each	2 0 lb
2 - isolation valves at 2 lb each	4 0 lb
2 - filters at 1 lb each	2 0 lb
2 - relief modules at 1 2 lb each	2 4 lb
2 - check valves at 1 lb each	2 0 lb
Total	<u>14 4 lb</u>

Gas Circuit

1 - fill valve at 1 lb each	1 0 lb
4 pr - explosive valves at 3 lb each	12 0 lb
1 - filter at 1 lb each	1 0 lb
1 - regulator at 1 lb each	2 0 lb
2 - check valves at 0 5 lb each	1 0 lb
2 - relief modules (disc plus valve) at 1 lb each	2 0 lb
2 - pre-pressurization and vent valves at 1 lb each	2 0 lb
2 - solenoid valves at 2 lb each	4 0 lb
Total	<u>25 0 lb</u>

Thrust Chamber Assembly

1 - thrust chamber w/gimbal mount at 45 5 lb	45 5 lb
2 - gimbal actuators at 2 25 lb each	4 5 lb
1 - propellant valve w/pilot solenoid valve at 7 lb each	7 0 lb
1 - purge check valve at 0 5 lb each	0 5 lb
2 - mixture ratio trim orifices and flanges at 0 5 lb each	1 0 lb
Total	<u>58.5 lb</u>

Fluids

Oxidizer (OF_2)	2107 0 lb
Fuel (B_2H_6)	702 0 lb
Helium (He)	31 7 lb
Total	<u>2840 7 lb</u>

Structure - Above Separation Plane

Upper truss members	20 67 lb
Tank upper support members	1 44 lb
Spacecraft attachment fittings	4 25 lb
Platform members	8 37 lb
Platform fittings	5 25 lb
Engine support truss members	1 68 lb
Engine support platform	2 87 lb
Tank end fittings	2 70 lb

Table 2-1 (Continued)

Valve assembly brackets	6.80 lb
Meteoroid shield	18.23 lb
Total	<u>72 26 lb</u>
<u>Structure - Below Separation Plane</u>	
Truss members	44 22 lb
Fittings (separation)	2 50 lb
Stabilizing frame	1 00 lb
Total	<u>47 72 lb</u>
<u>Miscellaneous</u>	
Lines and fittings	20 00 lb
Instrumentation	4 00 lb
Command and squib harness	8 00 lb
Contingency	16 00 lb
Total	<u>48 00</u>
<u>Thermal Control</u>	
Foam - 2 propellant tanks	16 20 lb
Foam - pressurant tank	2 66 lb
Cooling coils	1 00 lb
Louvers	6 0 lb
Mylar	2 0 lb
Total	<u>27 86 lb</u>
GRAND TOTAL	<u>3347 6</u>

3.0 MISSION PROFILE

The general system requirements on thermal control is to maintain the propulsion module components within design temperature limits during all phases of the mission. For purposes of thermal analysis, the mission can be considered as composed of four distinct phases

1. Groundhold
2. Launch and Parking Orbit
3. Jupiter Transfer Phase
4. Jupiter Orbit

3.1 Groundhold

Groundhold is that period from initiation of passivation to launch which may last as much as one month. In addition to the passivation process which must be followed (Reference 6 specifies the recommended passivation procedure and equipment), the stage must be maintained at specified temperature limits during this phase. It is also necessary to prevent frost or water accumulation on any flight hardware. The three fluid control panels and the thrust chamber with its related valves and lines may remain at ambient temperature during the groundhold phase.

3.2 Launch and Parking Orbit

The vehicle will be launched into a 100 nautical mile parking orbit by a Titan/Centaur/Kick stage. It is assumed that there are no restrictions as to the time of launch and that the protective shroud will be jettisoned at approximately 225,000 feet altitude. Maximum coast time in the parking orbit will be one hour. Sun exposure of the propulsion module during the launch and parking orbit is assumed to be random.

3.3 Jupiter Transfer Phase

During this phase, the spacecraft will be oriented with the propulsion module nearly shaded except for one-hour reorientation maneuvers during each of the mid-course correction firings. It is expected that up to three such mid-course corrections firings may be required with an aggregate

firing time of 44 seconds. For purposes of this thermal analysis, however, it is assumed that only one firing occurring on the seventh day which accomplishes a 100 meter/sec trajectory correction, will be required.

A single Jupiter orbit insertion firing of 533 seconds is assumed to occur 716 days after launch. Prior to this firing, the spacecraft orientation for a normal mission is assumed as given in Figure 3-1. During this transit period, the solar intensity at the vehicle will be as given in Figure 3-2.

3 4 Jupiter Orbit

A final engine firing will occur at some arbitrary time after Jupiter encounter plus 23 days (773 days after launch). The purpose of this correction is to change the Jupiter orbit inclination angle. This will require about 528 seconds of engine operation. The initial Jupiter orbit will be 4 x 98 8 R inclined to the Jupiter equator at an angle of less than one degree. The orbit period will be approximately 45 4 days.

3 5 Module Operating Requirements

As indicated above, during groundhold it is only necessary to hold the propellant and pressurant temperatures within specified limits. These limits are 250 $\begin{matrix} +30 \\ -40 \end{matrix}$ °R for the propellants and nominally 280 $\begin{matrix} +0 \\ -100 \end{matrix}$ °R for the helium. It is not necessary to maintain any of the component temperatures at any given value solely for the sake of the component. Only to the extent that such components temperatures affect the fluid temperatures within the tanks will such component temperatures be held near 250°R.

During flight, it is also necessary to maintain the propellant temperatures within the specified limits. However, as shown in Reference 2, it is also necessary that, at engine operation, the two propellants be at nearly the same temperature and that various components be within specified limits. Note carefully that these additional requirements exist only during and just prior to engine firing. Table 3-1 lists the various component temperature requirements.

A comment is in order concerning the helium temperature requirements. Upon helium tanking, it is necessary to keep the temperature of the helium at or below 280°R or else a severe over-pressure will be experienced.

However, there are distinct advantages if the helium temperature is maintained above propellant temperatures. First, it allows a more efficient utilization of the pressurant and second, it reduces the chances of over-pressurization because the warmer helium is subsequently cooled by the propellant when it enters the propellant tank. Thus, there is no apparent reason why the helium could not be allowed to exceed 280°R , provided maximum helium tank pressure is not exceeded. This means that the helium temperature after the first firing can exceed 280°R .

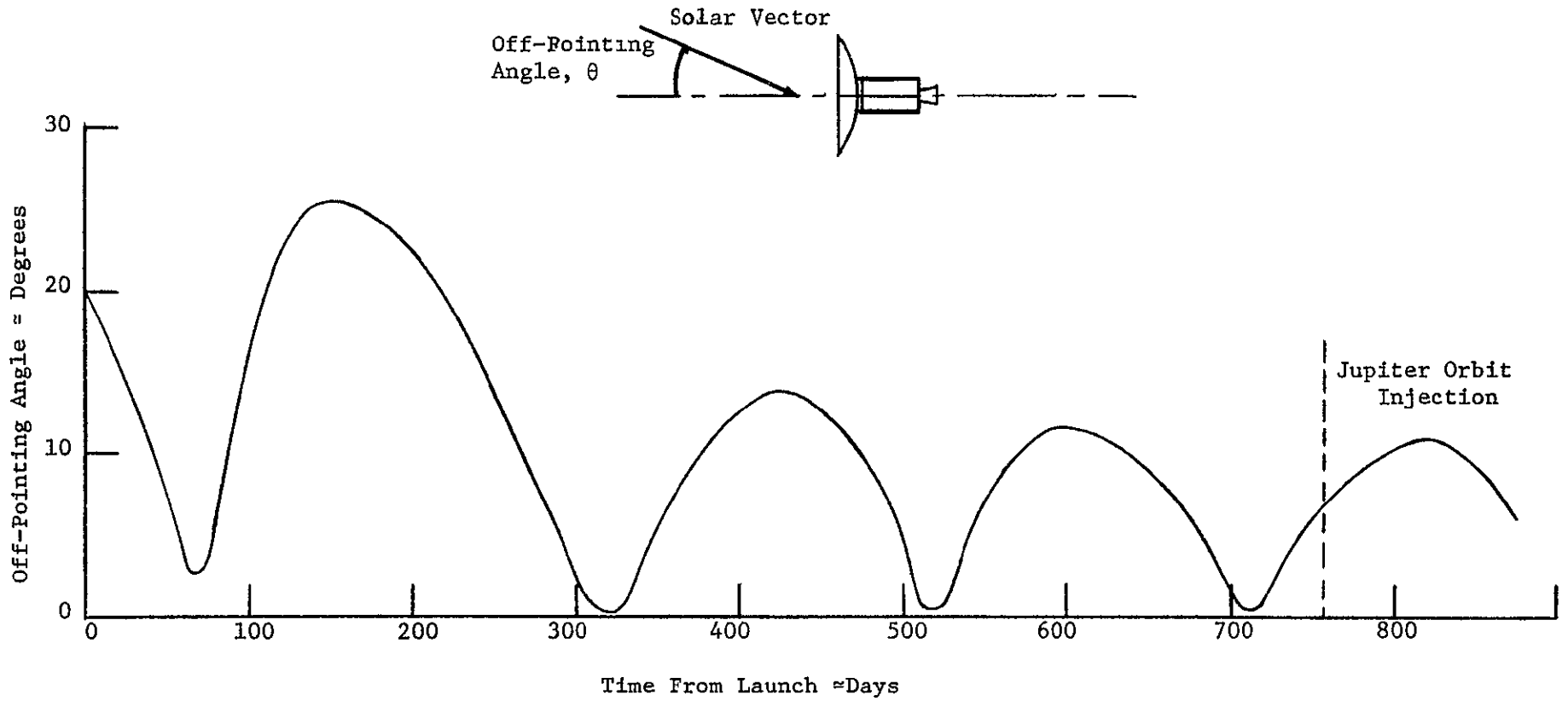


Figure 3-1 Off-Pointing Angle During Mission

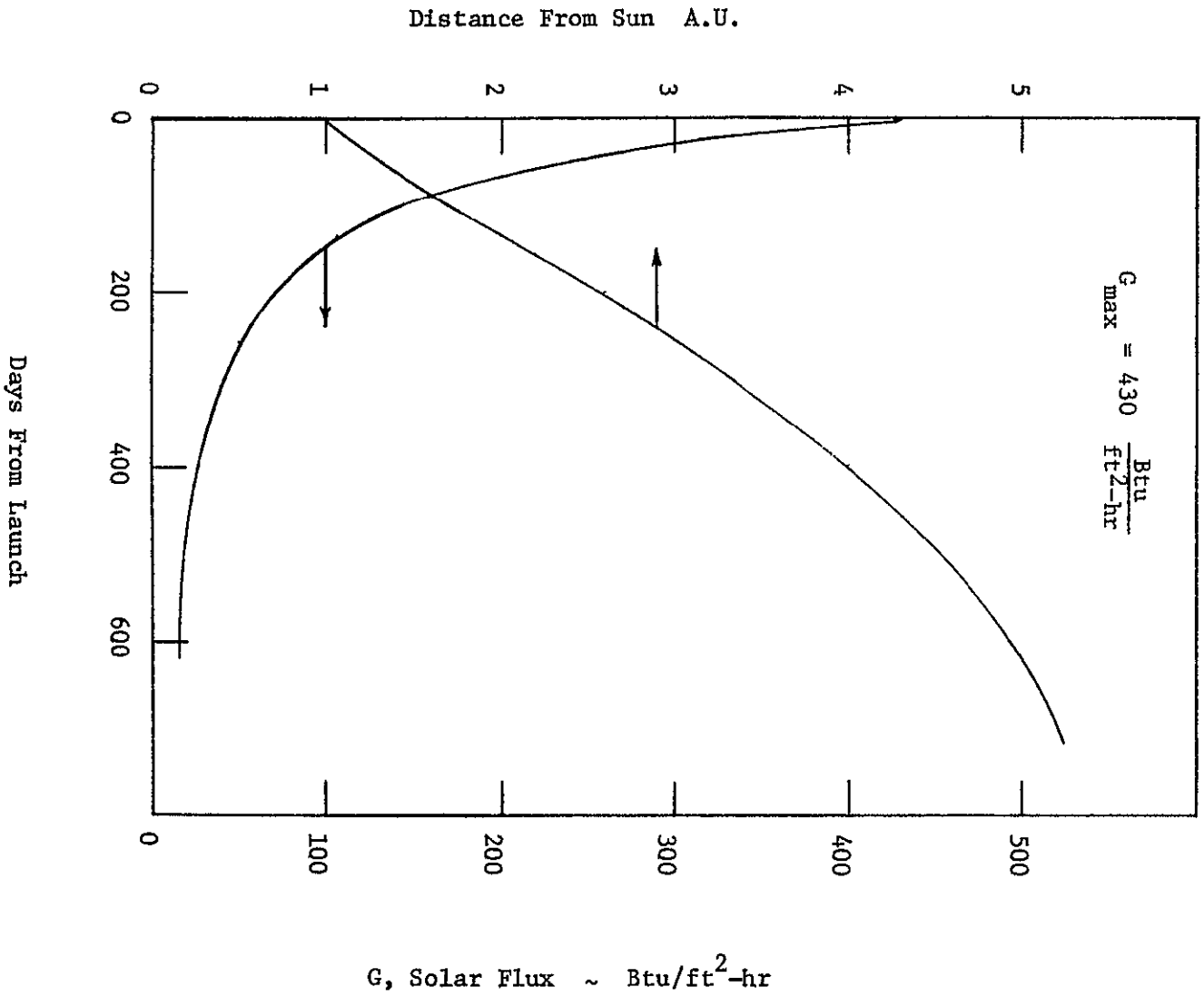


Figure 3-2 Solar Flux at Spacecraft

Table 3-1 Recommended Component Temperature Ranges

Component	Operating Temperature (a)		Probable Effect of Operation at Temperatures above Recommended Maximum	Initiation of Operation of Temperatures above Maximum (b)
	Minimum, °R	Maximum, °R		
Helium Fill Valve	150	560	Essentially none	ok
Helium Explosive Valves	200	560	Essentially none	ok
Helium Filter	200	560	Negligible change in pore rating	ok
Regulator	200	300	Regulated pressure will be 5 to 10% low	avoid
Helium Check Valves	200	300	Seating pressure will be 5 to 10% low	ok
Tank Relief Modules	200	300	Cracking pressure will be 5 to 10% low	ok
Propellant Fill and Vent Valves	150	560	Essentially none	ok
Propellant Isolation Valves	210	280	Propellant heating and vaporization	avoid
Propellant Filters	200	290	Negligible change in pore rating, propellant heating	avoid
Passivation Valves	200	290	Propellant heating and vaporization	avoid
Mixture Ratio Trim Orifices	200	290	Negligible change in area, propellant heating	avoid
Engine Propellant Valve	200	290	Propellant heating and vaporization slower response	avoid
Injector	200	290	Propellant heating and vaporization	avoid
Feedline Relief Modules	200	290	Cracking pressure will be 5 to 10% low, propellant heating	avoid
Feedline Relief Check Valves	200	280	Propellant heating and vaporization	avoid
Actuation Pressure Valve	200	300	Slowed response - probably not critical	ok
Purge Actuation Valve	200	300	Slowed response - probably not critical	ok
Purge Check Valve	200	300	Reduced seating pressure (5 to 10%)	ok

(a) "Operating" implies preparation for and execution of a firing

(b) "Initiation" implies these temperatures will quickly decrease to the recommended maximum, or lower, immediately upon firing

4.0 METHOD OF ANALYSIS

The analysis of the module is divided into two parts. First, a thermal analysis of the complete module is made for the various phases of the mission. These investigations provide module fluid and component temperatures at any time during the mission and they consider such variables as spacecraft position relative to the sun, RTG operation, insulation properties, weight of propellants on board, etc.

The second step of the overall analysis is to use the results of the thermal investigation, i.e., fluid and component temperatures, to determine the performance of the propulsion system during operation.

4.1 Thermal Analysis Models

The propulsion module temperatures are calculated by representing the physical system by an equivalent electrical network which is solved by the CINDA computer program on the Univac 1108 computer. The equivalent electrical network is referred to as an analytic, mathematical, or computer model.

For purposes of this analysis, two computer models of the module were formulated: the basic model for analysis of all flight conditions and the revised model for analysis of groundhold conditions.

The basic computer model assumes the propulsion module and its environment may be represented by 163 uniform temperature elements, or nodes, connected by appropriate radiation and conduction resistances. Appendix A gives a detailed description of these nodes and the conduction and radiation heat transfer conductances between the various nodes. Thermal characteristics and property values of the various components were obtained from published data or from developmental tests conducted on previous programs at TRW Systems.

The revised model was obtained by making changes to the basic model which account for groundhold conditions. The specific changes were as follows:

- o Atmospheric convection heat transfer to all external nodes was provided.

- o Background radiation level was changed from 0°R to 525°R.
- o Nodes were added to account for the cooling coils inside the fluid tanks.
- o RTG in a stowed position.
- o Louver nodes were deleted to account for insulation over the top of the louvers.
- o All separation assembly interfaces were assumed to be held at 530°R.

As developed, the revised model had 168 nodes. In order to simplify the revised model, three assumptions were made. First, it was assumed that the external film coefficient used in determining the atmospheric convection heat transfer was independent of temperature. Ordinarily, this coefficient is proportional to $(\Delta T)^{0.25}$ in natural convection where ΔT is the temperature difference between the surface being heated or cooled and the ambient air. However, in this case, the effect of temperature variation upon the film coefficient will be small because the temperature difference between the air and module surfaces will remain small, 5° to 15°F, and fairly constant. More to the point, however, the coefficient is more dependent upon the velocity of the ambient air. For quiescent natural convection, the film coefficient may be as low as 0.25 Btu/hr-ft²-°F. But for high velocity gas, i.e., 35 fps, the coefficient may reach 10 Btu/hr-ft²-°F. Even such a wide variation in film coefficient has little effect upon the overall operation of the module during groundhold since the film coefficient presents very little resistance to heat flow compared to the foam insulation. Thus, for sake of convenience, a constant value of 1 Btu/hr-ft²-°F was used in the computer program for most parts of the analysis. However, as will be seen, the effect of larger film coefficients was considered.

The second assumption made was that the tank walls are at the same temperature as the internal fluid which is in contact with the tank wall. Within the accuracy of calculations, this is sufficiently correct. For normal conditions, the heat transfer rate through the walls will be shown to be of the order of 50 Btu/hr-ft²-°F. A hand calculation will show that, for the propellants under study, such a heat transfer rate

will result in less than a 3°F temperature drop across the film at the wall. This assumption is also the most conservative because it results in answers indicating higher heat transfer rates into the tank than will actually occur

This is not the same assumption that is made for the analysis of the operation of the propulsion system during engine operation. As will be shown below, during engine operation a thermal gradient at the wall is assumed.

The third assumption has to do with the film coefficients at the surfaces of the cooling coils. As was pointed out in Reference 1, it has been found that the principles of physical similitude and the scaling laws are valid for cryogenic application, and that the applicable empirical equation for the external film coefficient is

$$h_o = 0.72 \frac{k}{D} \left[\frac{D^3 \rho^2 \beta g \Delta T}{\mu^2} \frac{c\mu}{k} \right]^{.25}$$

where h_o = external coefficient of heat transfer, Btu/hr-ft²-°R

D = tube diameter, ft

k = propellant thermal conductivity, $\frac{\text{Btu-ft}}{\text{hr-ft}^2\text{-}^\circ\text{R}}$

ρ = propellant density, lb/ft³

β = propellant coefficient of volumetric expansion, 1/°R

ΔT = temperature difference between tube and propellant ($T_B - T_t$)

g = constant, 4.17×10^8 ft/hr²

μ = propellant viscosity, lb/ft-hr

c = propellant specific heat at constant pressure, Btu/lb-°R

Theoretically, several of the variables of this equation are temperature dependent and should be evaluated at some temperature between the propellant bulk temperature and the tube surface temperature. A hand calculation will show that the maximum error induced by assuming temperature independent properties is 12%. Since the properties of the propellants are not known to a high degree of accuracy, it is hard to justify accounting for temperature variations present in the analysis. Even if the properties of the propellants were known accurately as a function of temperature, it is not logical to try to improve the accuracy of analysis by

including temperature dependent variables in the analysis because the greatest uncertainty in the analysis stems from unknowns about the convection currents within the propellants.

The film coefficient on the outside of the cooling coil is highly dependent upon the motion of the natural convection currents which will be set up in the tank. However, these currents are influenced not only by the propellant properties but also by tank shape, tank size, and, in this case, most importantly by the shape and size of the propellant acquisition device. The equation listed for h_o is a generalized empirical equation obtained by correlating experimental results from tests in which cooling coils were immersed in containers of fluids. Though the equation is the best available, it obviously will not predict accurately ($\pm 20\%$) the film coefficient on the outside of the coils since it is taken from generalized data. It is also obvious that attempts to make it more accurate by using temperature dependent properties in its solution is not logical. To obtain a more accurate knowledge of the heat transfer properties in the region of the coils, it is mandatory to conduct experimental investigations using the tank configuration of the flight module.

For these reasons, the approach taken in this analysis has been to use the equation listed and then show from the results that the design is sufficiently conservative to accommodate any errors introduced by the equation. Thus, h_o is made a function of only ΔT in the revised computer program. The actual values of h_o as a function of ΔT were hand calculated and are inserted in the program as a table.

The equation chosen in Reference 1 for the coil internal coefficient is

$$h_i = 0.029 \frac{k}{D} \left[\frac{DV\rho}{\mu} \right]^{0.8} \left[\frac{c\mu}{k} \right]^{0.4}$$

where h_i = internal coefficient of heat transfer, Btu/hr-ft²-°R

D = tube diameter, ft

k = thermal conductivity of liquid coolant, Btu/hr-ft²-°R

V = liquid coolant velocity, ft/hr

ρ = liquid coolant density, lbs/ft³

μ = liquid coolant viscosity, lbs/hr-ft

c = liquid coolant specific heat at constant pressure, Btu/lb-°R

Although this equation contains variables which are influenced by a temperature change, no consideration needs to be given to this problem for the following reasons. As reported in Reference 3, the modified Colburn equation

$$\frac{hD}{k} = 0.023 \left[\frac{VD\rho}{\mu} \right]^{0.8} \left[\frac{c\mu}{k} \right]^{0.4}$$

correlates within 10% the data obtained from tests of heat transfer to a turbulent fluid flowing inside a tube provided no boiling takes place and the viscosity of the fluid is not greater than twice that of water. This correlation was made with all properties evaluated at the initial bulk temperature except viscosity, which was evaluated throughout the cooling tube at the film temperature, T_f

$$T_f = T + 0.5 (T_s - T)$$

where T_s is the local saturation temperature and T is the local bulk temperature. However, data for the case of saturated liquids being boiled showed that for runs in which the Reynolds numbers exceed 65,000, the true mean coefficient, h_m , for the entire tube based on the mean temperature (saturation temperature minus bulk temperature) throughout the tube length, averaged 1.26 times the value predicted by the modified Colburn equation. Thus, for boiling liquids inside tubes, the coefficient in the Colburn equation is changed to 0.029.

In the present investigation, the Reynolds Number of the LN_2 will be in excess of 65,000 except for the very low flows. If, in addition, it is assumed that the LN_2 enters the tube at its saturation temperature, the mean temperature (the temperature at which all the properties should be evaluated) is identical to the bulk temperature and it is, for all practical purposes, constant throughout the tube.

If the major method of heat transfer ceases to be heat transfer to a turbulent vapor, not only does the constant temperature assumption fail but the coefficient, 0.029, reverts back to 0.023. The data used in Reference 3 shows that the coefficient of 0.029 holds within 10% for a coolant quality at the tube exit of 7% or less vapor by weight provided the Reynolds number is in excess of 65,000. If the quality increases to 50% vapor at the exit, the accuracy of the coefficient drops to $\pm 25\%$. As

will be shown later, for all normal situations, the quality of the coolant in the case under study will be less than 30%, and in all probability will be less than 10%

Again, it should be clearly noted that it is not wise to attempt to infuse additional accuracy into the analysis by either using more accurate propellant property information or performing additional analytical work. Experience in this field of heat transfer has shown that the additional accuracy can only be achieved by testing.

With these assumptions (constant temperature and sufficient flow), h_1 is reduced to a function of liquid velocity (coolant flow rate). In the program, h_1 is treated as a constant, the value of the constant being chosen according to the following hand calculated table

<u>LN₂ (Coolant) Flow Rate, lb/hr</u>	<u>h_1 Btu/hr-ft²-°R</u>
0	0
123	123
247	214
1317	2470

Due to a lack of adequate theory and, more particularly, due to the wide variety of conditions which may exist, both programs are undoubtedly somewhat in error in their representation of temperature gradients within the three fluid tanks. Both computer models assume that the fluid and walls of each tank may be divided into three discrete nodes. In the flight model, it is assumed that there is no convective heat transfer between the nodes (no convective fluid currents), only conductive heat transfer. This assumption is the most conservative because it results in answers which indicate large thermal gradients. During zero-g flight, it is generally assumed that only conduction heat transfer occurs, but it seems logical that if any spacecraft maneuvering occurs, the fluid will be "stirred" up. It follows that the temperature of a given propellant entering the engine upon engine operation will be near the average of the three propellant nodes.

There is the added problem of accounting for the position of the propellants within the tanks during zero-g flight. A detailed study of this problem is beyond the scope of this present investigation, but the following

generalized comments are pertinent to this investigation.

The location and condition of the propellants within the tank during zero-g is dependent upon the propellant properties, tank shape and size (including propellant acquisition device), heat transfer rate, and locality of heat transfer. It is conceptually possible for the vapor and liquid to be interspersed into a homogenous mixture completely filling the tank. It is highly unlikely this will be the situation. Rather, the vapor and liquid will usually be separated such that the liquid will form a continuous media with a pocket (or pockets) of gas. Since the configuration is highly susceptible to change when the location of heat transfer to the tank changes, it is difficult to predict the fluid configuration with a high degree of accuracy. This is part of the problem here since, for a normal mission, the location and level of heat transfer varies appreciably with time.

It was, therefore, assumed for purposes of the flight thermal analysis that the fluid is evenly distributed around the surface of its tank and that all the ullage gas is contained in a single pocket of gas centrally located inside the liquid. This is the most conservative assumption for two reasons.

1. It results in the lowest calculated temperatures when no external heating exists and in the highest calculated temperatures when solar heating exists. This is because no thermal resistance between the tank wall and propellant is considered.
2. It results in the greatest calculated thermal gradient within the propellant. This is because higher heat transfer rates occur when no internal vapor film exists adjacent to the wall and because the assumed configuration results in the maximum length and minimum area heat transfer path between the several propellant nodes.

As was indicated above, during groundhold operations, convective currents within the propellants will be established but the exact mode of the currents is difficult if not impossible to predict. But the fact that the currents do exist makes the assumption used in the flight analysis of only conductive heat transfer within a propellant tank invalid. To directly account for convective currents inside a tank in a computer program is essentially impossible. Such a program would be correct only to the

extent the convection currents are known. Not only would the current paths have to be known, but the current velocities would have to be known. In addition, the correct nodal arrangement would be totally dependent upon the convection current paths and velocities. Thus, for even minor changes in the heat transfer pattern (for example, a shift in the external air currents), a change in nodal arrangement would have to be made.

It is possible to indirectly account for the convective heat transfer by increasing the thermal conductivity of the propellant by an amount such that the apparent heat transfer rate indicated by conduction only would be the same as that which actually occurs with both conduction and convection. This approach results in a distorted picture of the temperature profiles within a tank. But, from an overall point of view, the error is negligible and therefore, this approach was adopted. References 3 and 4 were used to estimate the apparent conductivity used in this analysis.

Recounting the approximations and assumptions made in formulating the thermal computer models, it will be seen that errors introduced into the computations can be grouped into three classes:

1. Errors due to the nodal configuration used to simulate the module
2. Errors due to unknowns in material properties and hardware construction (conductivities, reflectivities, interface thermal resistance, etc.)
3. Errors due to lack of information concerning the dynamic and heat transfer characteristics of fluids in zero gravity fields

Errors of the first type can be reduced to any desired level by using a sufficiently small nodal grid. In reality, this reduces to a trade-off between the degree of accuracy necessary and the resulting complexity in the computer program which results. Judgement derived from other programs (Pioneer, OGO, MSS) indicated that little would be gained by increasing the model complexity over that which exists in the formulated programs. Though a detailed error analysis of this particular aspect of the programs was not made, analysis from other programs would indicate the error due to this source is about $\pm 5^{\circ}\text{F}$.

An analysis of the second type of errors was made for this program. This was done by first estimating the extreme limits which could logically

exist for each of the conductances of the programs, and then determining the resulting temperature shift which would result if all these extremes were to occur simultaneously. This analysis showed that if all the extremes "lined up" to shift the module temperature in one direction, the average module temperature would shift some 21^oF. If the possible variations in the conductances occurred in a 3 σ random pattern, which is much more likely to be the case, the temperature error due to this source will be no more than $\pm 7^{\circ}$ during groundhold and $\pm 11^{\circ}$ during flight. This is comparable with experience from past TRW thermal control projects. To obtain a better prediction of actual performance, actual tests must be run.

Errors of the third type, as discussed above, are difficult to assess due to a lack of both theory and experimental data. Without an indepth analysis, it is impossible to assign a value to this error. Based upon theory which is available and the particular nature of the module, we believe that temperature variations caused by these unknowns will not be major, less than 5^oF for the heat transfer rates existing in this case.

4.2 Propulsion Analysis Models

Two digital computer programs were written and used to calculate system pressures, flow rates, temperatures, etc., as a function of initial propellant and gas temperatures. The first program simulates firing conditions. It is comprised of a set of equations in which time is one of the variables so that "time-advancing" calculations can be made of the progressive changes in temperatures and masses which will occur with time during firings. The second program simulates cruise periods. It is a set of equations, which are unrelated to time, that calculate the equilibrium propellant tank pressure for any combination of physically compatible values of temperature, propellant mass, and helium mass.

It was assumed that the propellant and gas circuitry would be properly calibrated to deliver nominal performance at 250^oR (i.e., mixture ratio would be 3.0 and chamber pressure would be 100 psia). Calculations were made to determine the mixture ratio and chamber pressure excursions.

if the propellants were conditioned to temperatures other than the nominal design point temperature by the thermal control system. Also, calculations were made of the ullage gas temperature, helium sphere temperature, and pressure histories during the nominal temperature (250°R) mission firings and post-firing cruise periods.

Firing durations were calculated for the nominal mission based on a delivered specific impulse of 400 lb_f-sec/lb_m and a spacecraft mass of 4400 lbs at launch. Velocity increments (ΔV's) of 100 m/s (meters per second), 1460 m/s and 2320 m/s were used for the midcourse, orbit insertion, and orbit inclination maneuvers, respectively. The midcourse ΔV represents the maximum total for three firings but these were lumped together since one long firing is a "worst case" compared to three shorter firings. Burn times for these firings were calculated according to the equation

$$\theta_b = \frac{M_o}{\dot{M}_p} \left[1 - \frac{1}{\ln^{-1} \frac{\Delta V}{g I_s}} \right]$$

where θ_b = burning time, seconds

M_o = spacecraft mass at start of firing, lb_m

ΔV = velocity increment, ft/sec

g = gravitational constant, 32 174 ft/sec²

I_s = specific impulse, lb_f-sec/lb_m

\dot{M}_p = propellant consumption rate, lb_m/sec

A nominal propellant consumption of 2.5 pounds per second yields firing durations of 44, 533, and 528 seconds for the three maneuvers. These conditions require total propellant masses which are larger than those given in the work statement; however, the propellant loads given in the work statement (and the resultant tank sizes) were used in the calculations since the differences are small.

4 2 1 Discussion of Method of Analysis

The entire sequence of calculations utilized in the propulsion system analysis is included in Appendix B. However, certain comments concerning the method of analysis are in order at this point. As a matter of introduction, it should be recognized that a simpler or more complex method of analysis could have been chosen. The method chosen represents a judgement as to the optimum between useful results and complexity.

4 2.1.1 Helium Supply

Calculations of helium consumption rates are only as accurate as the solubilities, heat transfer rate models and helium properties used. In this case, solubility equations were obtained by curve fitting to the empirical data contained in Reference 7. No attempt was made to predict the rates at which the helium would go into or come out of solution, but instead it was judged that these rates were relatively slow so that no significant changes would occur during firing periods.

For the calculations made in this study, it was assumed that the propellants contain no dissolved helium until after the midcourse firing (seven days). After each firing, the helium in the ullages partially dissolves in the liquid propellant until an equilibrium concentration is reached. Prior to each firing, the ullages are brought up to regulated pressure in sufficient time for the helium tank and ullage gases to return to equilibrium temperatures prior to start, yet soon enough before the firing that no change occurs in the amount of helium dissolved in the liquids. Should pressurization occur only until immediately prior to the firings, a greater consumption of helium would result.

The sudden withdrawal of the amounts needed to both raise the tanks to operating level and to expell the propellant causes the temperature in the helium tank to drop to a lower level than in the case with an interim warm-up period.

During the two longer firings, the temperatures of the ullage gases drop below equilibrium temperature. This is because the helium in the helium tank becomes colder as a firing proceeds due to the fact that the withdrawal part of the helium allows the remaining helium to expand

Therefore, helium drawn from the tank is progressively colder and so chills the ullage gases as it mixes with them, reducing the average temperatures of these mixed ullage gases to below the initial temperature by the end of a long firing (It was assumed, however, that the liquid propellant temperatures remained unchanged during firings). Therefore, there is a post-firing warming to equilibrium temperature which results in a pressure rise above regulated pressure unless a substantial fraction of the helium is dissolved in the liquid propellant. After the orbit insertion burn, the propellants already contain an appreciable fraction of the equilibrium concentration of helium so that little of the newly added helium goes into solution. After the orbit inclination burn, the nearly saturated propellant absorbs very little helium and, therefore, the warming to equilibrium temperature will cause the pressure to exceed regulated pressure in some cases by 9 psi.

The amount of helium which is required to expell the propellants is influenced by the amount of heat transferred to the gas within the helium tank, hence, the importance of the convective heat transfer coefficient. Despite the widespread use of stored, high-pressure gas supplies, no proven, generalized analytical method of predicting the rate of heat transfer from a vessel wall to a diminishing gas supply has been developed.* For the present program, a greatly simplified free convection model was adopted to simulate the gas film coefficient together with a simple, three-slab representation of the tank wall. It was assumed that no significant amount of heat was transferred to the tank from outside during the firing period (i.e., the only external energy available to the gas during firings was that stored in the tank wall)** Constant values of conductivity and heat capacity were used in all cases. The errors introduced by this simplification are probably smaller than the errors in the presently available physical constant values for the tank wall material. Small errors are also introduced by the use of constant

* Apparently, Reynolds and Kays worked only with low pressures (Reference 8), and Keith covered very rapid blowdown rates (Reference 9). See also Reference 10.

** Originally, the planned program also was to account for heat extracted from the helium system components but this was not included due to the exigencies of time available. Were this energy available, the ullage gas temperature might be slightly higher than now calculated.

"average" values for the thermal properties of helium.

4.2.1.2 Ullage Conditions

No attempt was made to account for less-than-perfect mixing of the ullage gases. Analytical models of diffusion and convective mixing are rather complex and of mediocre accuracy so it was not deemed worthwhile to attempt using them. A point of interest is that the incoming helium will be more dense than the saturated propellant vapors in most cases. This means that the acceleration produced by the engine will tend to promote convective mixing of the ullage gases. Therefore, during such periods, substantial mixing may be expected. Nevertheless, it must also be expected that temperature, density and concentration gradients will be present in real tanks to some extent.

The equations were derived on the assumption that the ullage gases are always uniformly mixed and that the vapor pressures and densities are the saturation values at the average ullage temperature. This relation is essentially true when ullage temperatures fall below the liquid surface temperature. An initial difficulty did develop because originally the enthalpy balance, used to calculate ullage temperature change, was based on the assumption that the vapor flux entering the ullage is at the average ullage temperature (i.e., that the liquid surface is at the average ullage temperature, an assumption consistent with the dependency of vapor pressure upon ullage temperature). The mutual dependency of the vapor flux enthalpy and ullage temperature upon each other caused solution instability. By assuming the vapor flux to be at the liquid bulk temperature, the ullage temperature becomes dominated by the influence of the increasingly colder helium temperature. This is borne out by experience.

A remaining shortcoming is the lack of any accounting for the latent heat of condensation within the enthalpy balance equations. This is considered to be of minor importance.

4.2.1.3 Liquid Propellant Flow

Liquid temperature is important because it affects the flow rates and therefore thrust and mixture ratio. Liquid temperature was assumed constant during each firing period. As will be seen in Section 5, this

assumption is correct as far as external heat transferred to the bulk liquids is concerned. The initial flow to the engine will be heated or cooled somewhat if the lines, valves, filters and injectors are not at the same temperatures as the liquids. But these parts have a relatively limited heat capacity and the turbulent flow conditions will promote rapid adjustment of their temperatures to that of the liquids

The major source for significant liquid temperature changes are the thermal interactions of the liquid-to-ullage interfaces. Vaporization and heat transfer are the two important mechanisms. For the higher temperature cases, the vapor mass evolved during the orbit insertion firing becomes sizable, enough in fact to change the average bulk temperature of the fuel by more than 2 degrees if the heat of vaporization were to be uniformly drawn from all the liquid. Contrwise, if convective currents are real, thermal stratification could develop zones of relatively colder and denser liquid at the interface. A sudden initiation of convection could conceivably carry this denser propellant to the tank outlet port. The likelihood of this is uncertain. More probably, there would be a gradual commencement of circulation within the liquid before substantial gradients have developed. This tendency is less pronounced in the oxidizer tank. During the orbit inclination firing, when the interfaces drop close to the outlet ports and much of the colder propellant would be consumed, the tendency for such action to occur appears greater. However, as will be shown later, the consequences of this occurring are small. The thrust and mixture ratio could shift one or two percent, but no harm to the engine would result.

Heat transfer between the ullage gases and the liquids will also tend to chill the liquid surface towards the end of the larger firings. The magnitude of this effect was not investigated.

Resistance to propellant flow to the engine depends upon the design geometry. Several kinds of resistance relations are likely. Some components have discharge coefficients which are essentially constant over the range of Reynolds Numbers involved. For the present calculations, it was assumed that the injector was designed with this characteristic. The injector nominal design point chosen for these calculations was a fuel velocity of 140 ft/sec, a total oxidizer orifice

area of 1.4383 times the fuel orifice area, and an orifice C_D of 0.75 on both sides. (These values were derived from data supplied by JPL.)

Flow resistances in pipes and many fluid components are commonly approximated by a term which includes the product of a "friction factor" term (which is a non-linear function of Reynolds Number) and an equivalent pipe length-to-diameter ratio. All of the feedline losses, including the valving losses, were assumed to be characterized by a relation of this form. In the calculations, total resistances, inversely proportional to the squares of the flow rates, were selected which would give the rated flows at 250°R with nominal tank pressure (300 psia) and chamber pressure (100 psia). The injector resistances were subtracted from these to leave the total resistances presented by the lines, valves, filters, etc. Calculated resistances for typical valve, filter and line designs yielded total resistances less than these differences, therefore, the remainders can be attributed to the trimming orifices.

The foregoing simplifications contain departures from reality. For example, the corrugated metal hoses which comprise much of the feedline lengths would have resistances following totally different relations to Reynolds Number than do smooth-bore pipes. Friction factors for such hoses are constant up to transition ranges of Reynolds Number. Above the transition range, the friction factors increase to new constant values, Reference 11. Calculations show that the oxidizer hose will operate in a Reynolds Number range over which the friction factor is constant, but that the fuel hose's friction factor will vary by as much as 60%. The absolute magnitudes of the hose losses are fairly low, however, so the errors introduced by assuming "pipe flow" are small. Filters typically impose pressure losses which are directly proportional to the flow rate rather than following the square law. And the trimming orifices may operate in the constant C_D range, whereas they were treated as equivalent L/D ratios in the present calculations.

4 2.1.4 Engine

Very small errors were introduced by assuming that the specific impulse is a function of mixture ratio alone, in practice, specific impulse will be slightly sensitive to chamber pressure as well.

5.0 RESULTS OF ANALYSIS

5.1 Groundhold Thermal Control

All of the results from the analysis show that the thermal control system functions very well during the groundhold phase. Those module components which must be kept cold can indeed be maintained at the required low temperatures. Also, such components as the frame, insulation outside surface, helium control panel, and bipropellant valve act as relatively constant temperature components by remaining within 10°F of the ambient temperature. The valve and filter located at the bottom of each propellant tank will, of course, remain within 20°F of the tank temperature. The actual thermal characteristics of those components which must be kept cold after propellant loading are best demonstrated by the curves of Figures 5-1 through 5-4.

Figure 5-1 is a plot of the equilibrium temperature of the three tanks as a function of LN_2 coolant flow rate in each tank for an outside film coefficient of $1.0 \text{ Btu/hr-ft}^2\text{-}^{\circ}\text{F}$ (the film coefficient for still air would be about $0.35 \text{ Btu/ft}^2\text{-hr-}^{\circ}\text{F}$). It can be seen that it is no problem to keep the fluid temperature within limits. In fact, for the design established, that is, an 8-foot coil of 1/2-inch tubing 8 feet long, the problem may be one of excess cooling to the point that freezing of the B_2H_6 may occur. With a pressure drop across the coil of only 25 psia, the coolant flow rate capability is considerably in excess of 1000 lbs/hr. Yet, it can be seen from Figure 5-1 that a continuous flow rate of only 40 lbs/hr will result in a coil surface temperature which may be low enough to cause freezing on the surface of the coil (190°R). Resolution of this problem, through coolant flow control, will be discussed later.

The temperature of any particular tank is relatively independent of the temperature of the other two tanks. For example, a variation in the oxidizer tank temperature of 50°F will result in a shift in the fuel temperature of less than 3°F .

If the oxidizer and helium tanks are maintained at 250°R and all coolant to the fuel tank is eliminated, the resulting equilibrium fuel tank temperature would be near 480°R . The dependency of the helium tank temperature upon the combined effects of the other tank temperature is

slightly more pronounced. No coolant to the helium tank will result in an equilibrium helium tank temperature in excess of 440°R , depending on the ambient wind conditions. These temperatures apparently preclude an ambient access to a particular tank while the others are conditioned.

* Also, this limited interdependence results in a certain characteristic which should be noted. If the propellants are loaded, but the helium is not, there will be a tendency for the helium tank pressure to drop since the helium tank temperature will fall in response to the propellant tanks. Therefore, attention must be given to preventing the collapse of the helium tank. Unless the helium tank is designed to withstand negative pressures, additional helium must be added during the tanking of the propellants.

The extent to which all coolant flow may be eliminated is indicated in Figure 5-2. As should be expected, the rate of temperature rise of each tank is closely related to the mass and specific heat of that tank. Thus, the temperature response of the helium tank is most pronounced because of its low heat capacitance. Obviously, the time during which cooling may be eliminated is also related to the initial temperature. Assuming an initial helium temperature of 225°R , coolant to the helium may remain off only 9 hours before its maximum temperature occurs. In comparison, it will take some 40 hours for the OF_2 or B_2H_6 temperature to rise 40°F .

The characteristics described above make it possible to utilize a simple on-off technique for controlling the propellant temperatures which will, at the same time, solve ground support equipment problems. At most launch sites, the LN_2 supply is some distance away and for purposes such as proposed here, the lines are generally insulated with a mineral-type insulation such as Armaflex. Lengthy transport lines for the LN_2 will require high flow to obtain high quality liquid coolant at the tanks without necessitating vacuum jacketed lines. As noted above, high flow rates in the fuel tank coolant coil could cause local freezing of the fuel. Therefore, in the present design, the coolant to the fuel tank will have to be operated on an intermittent basis with two different sensors controlling. A temperature sensor attached to the coil, stops flow to prevent freezing and a sensor immersed in the fluid near its surface initiates coolant flow.

If groundhold thermal control is accomplished by flowing large quantities of LN₂ for relatively short periods of time, cyclic thermal response similar to that shown in Figure 5-3 may be expected. Graph A is for the particular case of LN₂ flowing at 1000 lbs/hr in each coil. Graph B is for the case of LN₂ flowing at 35 and 200 lb/hr in the fuel tank coil.

In this analysis, it was assumed that the LN₂ flow in the helium and oxidizer tanks is controlled by thermocouples immersed in the fluid and that LN₂ coolant flow would be initiated when the fluid temperatures exceed 270°R and is stopped when the fluid temperatures drop below 220°R. It was also assumed that the coolant flow in the fuel tank is initiated when the bulk temperature exceeds 270°R but that the coolant flow is stopped when the coolant coil temperature drops below 190°R, the temperature at which freezing on the coil could conceivably start.

The effect of controlling the fuel temperature in this manner is clearly demonstrated in Figure 5-3. At a flow rate of 1000 lbs/sec, the minimum bulk temperature of the fuel is about 252°R. This is because at the high coolant flow rate, the coil is substantially colder than the surrounding liquid. In comparison, if the flow rate is 35 lbs/hr and the lower control temperature is kept at 190°R at the coil, the fuel bulk temperature will drop to approximately 203°R. This clearly points out three facts:

1. The cooling response rate and rate of temperature drop is not materially affected by the LN₂ flow rate because the outside film coefficient is the controlling parameter, not the inside coil coefficient.
2. There is a maximum LN₂ flow rate which may be accommodated, approximately 1500 lbs/hr. A higher flow rate will result in the low temperature sensor (coil temperature) giving a signal to stop LN₂ flow in order to prevent possible local freezing when the bulk temperature is still in excess of 270°R. The actual result would be that the LN₂ flow control valve would turn on and off fairly rapidly (possibly several times each hour) without any effective cooling of the fuel resulting.
3. There is also a minimum allowable LN₂ flow rate which is required to maintain the bulk fuel temperature above 210°R if a constant control temperature of 190°R is maintained. This rate is about 175 lbs/hr.

With OF_2 , the cooling capacity is insufficient to cause freezing and there is no freezing problem with helium

It should be noted that it is not clear whether local freezing on the coil is objectionable. On refrigeration coils operating in the air, local freezing of atmospheric vapor is undesirable since the frost formed may be fluffy and act as an insulator. Whether freezing of B_2H_6 would be objectionable for the same reason depends on the magnitude of the thermal conduction of the "ice" in comparison to the film coefficient on the outside of the "ice"

In addition to the problem of ice reducing the efficiency of the fuel cooling coil, there is the possible problem of loose ice being injected into the propulsion system upon engine operation. This is not a serious problem. If the LN_2 is turned off while the bulk temperature is still above $210^{\circ}R$, any ice formed will melt within hours. Only if the bulk fuel temperature is very near the freezing point and/or a very large quantity (tens of pounds) of ice has been formed will more than a few hours be required to melt the ice. This characteristic, however, may be an important consideration when the time of first engine firing is scheduled.

This problem of freezing could be overcome by reducing the size of the cooling coil. However, such a size reduction also reduces the capability of accommodating unusually large heating loads which might occur in an emergency such as insulation failure. As will be indicated below, the present design is well suited to handle such emergencies and considering the chemical characteristics of the propellants, it is considered wise to retain this emergency capability.

There is one point which must be given serious thought and planning. As will be shown later, there are distinct advantages to launching with all fluids at their minimum temperatures. But, from Figure 5 3, it can be seen that using a purely automatic system will

result in all the fluid tanks thermally cycling at different frequencies. It would thus be difficult to assure that all temperatures are at their minimum at the time of launch. This problem may be overcome in either of two ways, but in either case, a manual override in the thermal control system would be required. The most obvious way is to include in the launch count-down a step for initiating a "last cooling" sequence for each tank. The coolant to each tank would be turned on at a time such that given the cooling characteristics of that tank, it will just reach its lowest temperature at the time of launch. A second way to handle the problem is to lower the upper control temperature limits to very near the minimum allowable temperatures. This approach would be wasteful of LN_2 but could be done 48 hours prior to launch to reduce the waste.

All of the discussion heretofore is applicable regardless of the location of the coils within the tanks provided the coils are submerged. But, if it becomes necessary to locate the coils near the bottom of the propellant tanks in order to accommodate requirements established by the propellant acquisition devices, the average temperature of an entire tank will be somewhat higher. This is because cooling occurring near the tank top aids in setting up natural convection currents, whereas cooling at the bottom leads to thermal stratification. An engineering estimate, based on the characteristics of the propellants, indicates that the average propellant tank temperature will be raised some $10^{\circ}F$ if the coil is relocated from the top to the bottom.

The capacity of the system to accommodate variations in the heat transfer rates to the tanks is excellent. Such an increase would be caused by the following.

- o Increase in outside film coefficient
- o Degradation of the foam insulation
- o Failure of the insulation by separation from the tank(s)

The first cause is of little concern since its relative contribution to the overall resistance to heat flow is minor compared to the resistance of the foam. For example, a 500% increase in h_o results in only a 1°R increase in the propellant temperature. In comparison, a 50% increase in the insulation conductivity will result in approximately an 18°F temperature rise if the coolant flow rates are maintained constant. Either of these variations is readily counteracted by slight changes in the coolant flow rate.

The extent to which increased heat transfer rates may be overridden by increased coolant flow is indicated by Figure 5-4. This figure gives the tank temperatures which would result for varying coolant flow rates if an additional 2000 Btu/hr were added to each tank. Recalling that the coolant coils can readily pass 1000 lbs/hr of LN_2 it can be seen that a very sizable heat transfer rate increase can be accommodated.

To experience an additional heat load of 2000 Btu/hr into a given tank, a major insulation failure would have to occur. Reference 5 reported that the overall conductance of an uninsulated, thin walled (0.05 inches) metal tank containing LN_2 varied from 0.81 to 3.53 Btu/ft²-hr- $^\circ\text{F}$ as the outside wind velocity varied from 0 to 20 fps. These experimental data were apparently obtained after some frost had collected on the outside surface. If it is assumed that the conductance is doubled in the absence of frost and that the heat transfer properties of LN_2 and the propellants under study are similar then a heat addition of 2000 Btu/hr could be experienced if approximately 1 ft² of insulation were removed.

It should be realized that the results of Figure 5-4 assumes that no propellant vapor is formed or, if it is formed, it immediately condenses back as a part of the liquid bulk. As such, the results cannot be used if boiling without recondensing occurs. The extent to which severe local boiling could not be handled can only be established by test.

5.2 Flight Thermal Control

The general approach used in the flight thermal analysis was to investigate discrete sections of the mission with an eye not only to determining the operation of the particular vehicle under study but also to establishing general principles which may be applicable to other vehicles.

having similar propellants and missions. Thus, the results and discussion below consider both normal operation and the effects of changes in design and mission.

There are several major factors which bear upon the module temperatures. They are

- o Off-pointing angle, θ (see Figure 3-1)
- o Solar radiation intensity, G (see Figure 3-2)
- o Transient factors including module temperatures at launch, mass of fluids on board, trajectory, and engine operation
- o Extent of sun shielding by spacecraft (size and shape of sun shield)
- o RTG temperature

In order to fully understand the influence of these factors, it is necessary to consider them somewhat independent of each other and then combine them in building block fashion to show their combined effects

5 2 1 Solar Radiation and Off-Pointing Angle Effects

The effect of the first two items can be seen from Figure 5-5. In this plot, the effects of constant, but different, solar intensities and/or off-pointing angles are accounted for in the abscissa where G is the solar radiation intensity at any time during the mission and G_{\max} is the solar constant at 1 A.U. (430 Btu/ft²-hr). For example, at a distance of 2 A.U., where the solar intensity is roughly 100 Btu/ft²-hr, the average fuel temperature will be approximately 250°R if the off-pointing angle is held constant at 30°. Note carefully that this plot applies only for a design which utilizes an abbreviated sun shield as indicated in Figure 5-5 and a normal RTG temperature of 960°R.*

* The curves of Figure 5-5 are applicable only to the extent that the solar heating is a continuous function of the off-pointing angle. If a shield were present, such that a given component were shielded from the sun for a quantum of off-pointing and then became exposed to the sun for increased off-pointing angles, the effects of both G and θ could not be combined into the single function $\frac{G \sin \theta}{G_{\max}}$. For the case

in which an abbreviated shield is assumed, this criteria is effectively met.

Three points should be noted from these curves

1. Steady state operation in the shade, either 0° off-pointing or in the shade of Jupiter, will result in major component temperatures of approximately 225°R .
2. For radiation from the +X (or -X) side, the helium and propellant temperature differentials remain small.
3. The propellant valve responds to solar radiation much more readily than do the propellants and helium

The reason that the valve responds differently is that it is strongly coupled with the engine bell and thus, its temperature is very strongly controlled by the engine bell temperature

Because of these characteristics, it is apparent that the orientation which could be accommodated with an abbreviated shield, that is, the amount of solar radiation that is allowable, is determined by the propellants, particularly the OF_2 . However, the tendency of the valve to run hot would dictate that certain maneuvers be made prior to engine start in order to drop the valve temperature. If, during the initial stages of the mission when the sun intensity is high, the craft were to be oriented such that the relative solar intensity were about 0.2, the propellant temperatures would be within limits, but the valve temperature would be too high. Therefore, if an engine start were attempted at such a time, either the off-pointing angle would have to be reduced long enough to allow the valve to cool or a "hot" start would have to be made. Of course, the valve temperature will be near the propellant temperature within a short time after propellant flow is initiated.

Similar data exists for the propellant feed lines, the insulation valves, and the helium control panel. Except for those portions of the two propellant feed lines adjacent to the bipropellant valve, the temperature of these two lines will follow within 5°F of the respective propellant tank temperature. Obviously, the ends of the lines which attach to the main valve will follow the valve temperature.

As indicated above, the isolation valves located below each tank may be as much as 20°F above the temperature of the tank to which it is attached during groundhold. During flight, however, the heat transfer rates to these valves are much smaller and consequently the isolation

valve temperatures follow the propellant tank temperatures within 4^oF

The helium control panel temperature follows substantially the temperature of the OF₂ tank but because of its position and attachment method it does fluctuate somewhat. If it receives no solar radiation, its temperature will be approximately 11^oF below the OF₂ tank temperature. But if the module were to be oriented such that the -X side is exposed to solar radiation at a relative intensity of 0.3, the helium panel will exceed the OF₂ temperature by approximately 22^oF.

5.2.2 Transient Factors

By itself, Figure 5-5 does not give a totally clear picture of the module temperature characteristics when an abbreviated shield is used since it gives only quasi-steady-state temperatures, that is, it does not account for the heat capacitance of the module or the varying nature of the solar heating.

The varying nature of the solar heating is indicated in Figure 5-6. The solid curve gives the relative solar radiation intensity on a black surface located in a Y-Z plane if it were to have the mission parameters given in Figures 3-1 and 3-2 (the normal mission for this study). This curve shows that solar heating decreases rapidly and is highly dependent upon the off-pointing angle. If no shading were provided, not even the abbreviated shield, and the surface were constantly perpendicular to the solar rays, the relative intensity would be as given by the dashed curve of Figure 5-6. A comparison of these two curves indicates the increase in solar heating which is caused by off-pointing only when no side shielding is provided.

Using hand calculated data of solar heating (similar to that of Figure 5-6) for the various components which can receive solar heating during a normal mission when only the abbreviated shield is used, a series of computer runs were made to ascertain the module temperature characteristics during various phases of the mission. These runs established one point which is extremely important to an understanding of the thermal analysis. That is, except for those situations in which sudden changes take place, the results given in Figure 5-5 are correct. Stated differently, the environmental conditions surrounding the craft change

slowly enough such that the module may be considered in a thermally quasi-steady-state condition during all phases of the mission except for the following four conditions.

1. Approximately the first 20 days after launch when the module is adjusting to the flight environment.
2. Immediately after and during a major module orientation maneuver which shifts its position relative to the sun.
3. Upon entering or leaving the shadow of Jupiter
4. During and after an engine firing

The typical thermal response which can be expected immediately after launch is given in Figures 5-7 and 5-8. Note that these results do not consider the effect of ascent heating (or cooling), engine operation, or earth radiation and albedo. The ascent heating or cooling will have no effect upon the fluid temperatures since, in the extreme, this phase lasts only a few minutes and, as shown in the groundhold analysis, the module will not respond even to severe environmental changes in such a short interval. Also, for a normal mission, earth effects are small and last for only one or two hours. Only if the mission includes an extended period of time in a near earth orbit, will earth effects be appreciable.

If the mission did include an extended period of time in earth orbit, the effect would be highly dependent upon the orientation of the craft. The worst condition would occur if the module were non-spinning and oriented in a 90° off-pointing angle. Since earth emission is approximately $68 \text{ Btu/ft}^2\text{-hr}$, and albedo is approximately $168 \text{ Btu/ft}^2\text{-hr}$, it is obvious that the module temperatures will rise towards totally unacceptable levels, $> 325^\circ\text{R}$. The best orientation would be in a 0° off-pointing angle. Here, the heating of the tanks would be predominately due to earth emission since the tanks would be shadowed by the aft shield from the albedo during those periods that the view of albedo is largest. And of course, albedo heating occurs for only about half the orbit time for low altitude orbits and it is small for high altitude orbits. These characteristics are shown in Figure 5-9.

A very conservative approximation of the equilibrium temperature of

the tanks during a 0° off-pointing earth orbit can be had by assuming that the tanks are exposed to a constant heating load of half the albedo plus half the earth emission, or $118 \text{ Btu/ft}^2\text{-hr}$. This is a relative solar intensity of 0.275 ($118/430$). From Figure 5-5, the equilibrium temperature of the OF_2 tank is indicated as 283°R , 3°R over the allowable limit. A more rigorous solution would show a maximum temperature somewhat lower. In addition, when the effects of the shadowing produced by the standard 10-foot diameter shield are considered, the equilibrium temperature would be even lower.

Note, however, that even a 0° off-pointing angle will result in an excessive bipropellant valve temperature if a low earth orbit is maintained because the engine will receive a substantial amount of heat from the earth.

Regardless of whether an extended time period is spent in an earth orbit, several important points are demonstrated by the curves of Figures 5-7 and 5-8. First, the assertion made previously that the curves of Figure 5-5 can be used in determining module temperatures during most of the mission because the environment is only slowly changing is well demonstrated. Figure 5-6 shows that the relative intensity at 20 days is 0.22. Using this value to enter Figure 5-5 to obtain the quasi-steady-state temperatures results in temperatures very close to those given in Figure 5-7 at 20 days. The oxidizer temperature at 20 days is approximately 5°F below quasi-steady-state and from the temperature trend shown it appears it will not reach equilibrium until about day 22.

It is logical that the oxidizer should take longer to come to quasi-equilibrium since it has a higher heat capacity, w_c . In comparison, the bipropellant valve is in quasi-equilibrium by day 6. The reason it does not come to quasi-equilibrium sooner is that its quasi-equilibrium is directly dependent upon the engine.

Figure 5-8 shows that the very low heat capacity components will be in quasi-equilibrium within one day.

Looking again at Figure 5-7, it will be noticed that the thermal histories of the helium and propellants during the initial days after

launch are highly dependent upon the launch temperature. It is this characteristic which makes it possible to keep the propellants within the specified limits during the initial days of the normal mission if only an abbreviated shield is used. The reason for this is as follows. If the module were launched with propellant and helium temperatures around 270°R to 280°R , the quasi-equilibrium temperatures should be reached within four days. But at four days, the relative sun intensity is sufficiently high to cause overheating of the OF_2 . The point to be gained from this is that to avoid propellant overheating, quasi-equilibrium must be delayed until about day 14 or sun shielding must be provided. The necessary delay can be accomplished either by launching with cold propellants or reducing the off-pointing angle during the first 13 days. But as will be shown later the standard design provides sufficient shielding to eliminate this problem.

Figure 5-7 and Figures 5-5 and 5-6 also show that with only the abbreviated shielding, an engine firing may not be initiated within the first 33 days without first orienting in such a manner as to cool the bipropellant valve unless firing with a hot valve is permissible. The requirements of such a pre-firing maneuver is dependent upon the time of firing and the required orientation at time of firing.

Figure 5-10 shows the typical thermal response of the module if it were to move from a 0° off-pointing angle to a 90° off-pointing angle in 15 minutes, stay at 90° for 34 hours and then move back to a 0° angle in 5 minutes. As should be expected, the valve readily responds to the solar radiation whereas the fuel responds very slowly. The oxidizer, having a higher heat capacitance, responds more slowly than does the fuel.

Applying this data, it is possible to see that if an engine firing were to be made on the 7th day when the valve is 307°R , the craft would first have to be maneuvered to 0° off-pointing and held in that position for approximately 11 or 12 hours in order to reduce the valve temperature to 280°R , the maximum temperature limit for the oxidizer. Even if the craft were launched into a 0° off-pointing position and held there, Figure 5-11 shows that it would be approximately two days before the valve would reach 280°R .

There may be one possible way to decrease the valve temperature when the engine is exposed to solar radiation and that would be to coat the engine surfaces which see the sun with a material having a low α/ϵ . However, it would be necessary that the material burn off after the first burn. The disadvantage of such an approach is that if the off-pointing which occurs prior to the first burn is not sufficient the valve would then be too cold at the time of the first firing

Figure 5-10 is for the specific case of 90° off-pointing near earth, and full tanks. If the tanks should happen to be only partially filled, the response rate at any given temperature will be inversely proportional to the mass of the tanks. If the reorientation should happen to occur at a later date in the mission when the solar intensity is reduced, the response rate will be reduced in proportion to the intensity reduction

The ability to continuously accommodate solar intensities ranging from 0 to that which exists near earth necessarily includes variations which will be encountered while in orbit around Jupiter. For the Jupiter orbit given (for the normal mission), the effects of Jupiter emission and albedo are negligible since the view factor of Jupiter is less than 0.05 and the Jupiter emission and albedo are only 2 Btu/fr²-hr and 8 Btu/fr²-hr respectively. If, however, the orbit diameter around Jupiter were to be reduced so that the view factor of that planet increased to an appreciable value, say 0.3, the module temperatures could rise significantly. Particularly, if the module were oriented with the -X side always towards Jupiter, the temperature rise would be large since the module would be "boxed in" with the warm RTG on the +X side and the relatively warm Jupiter on the -X side

The remaining normal mission transient condition to be discussed is the time during engine firing.

Data supplied to TRW Systems indicates that during steady-state engine operation, the outside temperatures on the engine will be approximately as given in Figure 5-12. However, for purposes of analysis, the entire bell (from the throat to the exit) was assumed to be at 2600°R and the remainder of the engine was assumed to be at 1000°R .

It was assumed that during the firing, the bipropellant valve would be maintained at the propellant temperature because of the cooling effects of the propellant flowing through it.

As will be shown later in the propulsion system analysis, during a firing the helium will drop in temperature about as indicated in Figure 5-13. Therefore, in the thermal analysis of the engine firing, the helium temperature was constrained to follow the curve of Figure 5-13.

It may be argued that this approach is not adequate in that during the firing, radiated and conducted heat from the engine may prevent the helium from dropping as far as indicated by Figure 5-13. To establish that, at least during the firing, the helium temperature is independent of the engine temperature, a computer run was made in which all parameters were as they are for a quasi-steady state analysis except the engine was assumed to be at 3000°R . That run showed that the helium temperature did not noticeably respond to this perturbation for over an hour. It was therefore concluded that the approach described above was justified.

The results of this portion of the analysis are shown in Figure 5-14. As was expected, the firing of the engine has only a small effect upon the propellant temperatures, and its effect upon the helium temperature, other than through the helium consumption process, is not severely large. A hand calculation reveals this characteristic more clearly. For example, if it is grossly assumed that all the thermal energy contained in the hot engine at shut down is transferred directly into a half full B_2H_6 tank, the resulting temperature rise in the fuel tank is only 17°F .

There are two areas which are affected, however. First, it should be noticed that the aft shield reached 824°R . This is sufficiently warm to dictate that the multilayer insulation blanket which rests against the shield be made of aluminized Kapton instead of aluminized Mylar.

The second affected area is the propellant feed lines. The valve temperature rises after shut down to approximately 596°R because of the heat soak back from the engine. The propellant feed lines will, in turn, rise in temperature. Consequently, propellant held in the feed lines at shut down will be boiled to a certain extent. A return relief line which

dumps the propellant vapor so formed back into the tank is provided, but the extent of this boiling process is unknown. The computer program does not consider this problem at all since to do so would require a detailed knowledge of transient boiling heat transfer in zero gravity. A hand calculation which assumed that all the heat which caused the temperature rise in the lines at shut down was instead used to vaporize propellants indicated that approximately 0.05 lbs of B_2H_6 and 0.11 lbs of OF_2 would be vaporized. How the system would function if these quantities of vapor were vented back into the tanks is not known but it appears it would be recondensed immediately unless the entire propellant bulk were at the saturation temperature.

5.2.3 Effects of Sun Shielding

Up to this point, it has been necessary to eliminate the effects of solar shielding as much as possible in order to discern the effects of the other variables. Shielding effects will now be considered.

In general, the presence of a surface near the module has two distinct effects. It may prevent the module from being exposed to solar radiation (this depends on the module orientation relative to the sun) and it does reduce the module's view factor of space. For the case of an abbreviated amount of shielding at the top of the module as considered in the previous discussion, these effects are minimized. If an extended shield is incorporated into the module design, the effects can be very substantial. Such is the situation with the present module design in which a 10-foot diameter flat shield is assumed to exist at the spacecraft/module interface. Where any off-pointing resulted in all the tanks, the engine and the frame receiving solar radiation when the abbreviated shield was assumed, no solar radiation is received by any of the module for off-pointing angles of up to 22° when the standard shield is considered. In addition, an off-pointing angle of 36° results in only the frame, helium tank and engine receiving solar radiation when the normal shield is used. The general effect of this shield is to cause the module to function as if it were the shade for off-pointing angles up to 22° . From 22° to 90° , the various components receive varying amounts of solar radiation depending on their location.

Unfortunately, it is impossible to graphically represent the steady-state thermal characteristics of the shielded module by a single set of curves similar to those presented in Figure 5-5. Instead, several families of curves similar to the family for B_2H_6 , shown in Figure 5-15, are required. The value of G/G_{\max} in Figure 5-15 is as given by the dashed line of Figure 5-6

The point to observe from Figure 5-15 is that regardless of G/G_{\max} , the quasi-steady-state fuel temperature is constant because the fuel is always shielded from the sun. Since this is the case, it is readily apparent that the RTG should be adjusted to cause the fuel to run at about $250^\circ R$. This can be accomplished by increasing the RTG temperature to approximately $1100^\circ R$ or moving the RTG about 1 foot closer to the module.

5.2.4 Mission Operation

Utilizing all of the information and techniques which have now been discussed, it is possible to construct the temperature histories of the module components for an entire mission. In order to fully demonstrate the thermal characteristics of the module, this has been done for both a module which has only an abbreviated shield and one which has the normal shield. The results are presented in Figures 5-16 and 5-17. The major differences between the two configurations are two

1. The spacecraft with the normal 10-foot shield does not need to be reoriented prior to the first engine operation since the shielding aids the valve to attain operational temperature limits
2. The module temperatures will remain constant once the initial launch transient is overcome.

The 10-foot diameter shield does add a substantial safety factor to the thermal control system design. Figure 5-16 shows that the module operates near its maximum temperatures immediately after launch and at its minimum temperatures when the off-pointing is zero if an abbreviated shield is used. But with the larger shield, module temperatures remain constant once the initial transient is overcome. In fact, if the LN_2 coolant flow rate during groundhold is properly adjusted, the propellant temperatures will remain constant during the entire mission. Thus, it is possible to

accommodate, within limits, additional unforeseen variations such as shifts in RTG temperature. However, for large off-pointing angles, $>50^{\circ}$, for long periods of time, the large shield would actually be a slight detriment because it reduces the module's view of space.

Curves similar to those of Figures 5-16 and 5-17 can be constructed for almost any conceivable mission to Jupiter (except ones which included extended orbit time near earth or low altitude orbits around Jupiter) by using just the curves presented to this time. Such results would necessarily be less reliable but they would serve as excellent first order approximations. For example, suppose the mission were to be altered to the extent that instead of the module being pitched to allow solar heating on the +X side, it was pitched to allow the off-pointing solar heating on the -Y side. That is, only the fuel tank would receive solar heating. If the lift-off temperatures were as the case of Figure 5-7, the results would be approximately as follows:

Module with Abbreviated Shield

- o The fuel temperature history would approximate the temperature history during a normal mission, Figure 5-16, since solar heating would be about the same.
- o The oxidizer temperature would remain at about 225°R since it will effectively operate as if it were continuously in the shade.
- o The helium tank will substantially act as it does during a normal mission since it will receive about the same amount of solar heating and the "hot" fuel and "cold" oxidizer will counterbalance each other relative to the heat conduction through the aluminum support structures.
- o The bipropellant valve will function as it will during a normal mission since the engine bell receives about the same amount of solar heating regardless of the direction of the sun, and it is predominately the bell which controls the valve temperature.

Module with Regular Shield

- o The temperatures would be as indicated by Figure 5-17 since the module will still remain shaded

The reason such an approximation of module operation can be made is that the various parts of the module are, to a limited degree, thermally

independent. The errors involved in making such an approximation stem from two sources. First, the extent of shadowing is not entirely independent of the direction of the sun even though the off-pointing is held constant. Second, and more important, whether a -X louver or a +X louver, or no louver at all, receives solar heating affects the tank temperature. If, for example, the -X side were to be exposed to the sun, it would be through that louver that a significant amount of heat would be added to the module tank.

5 2.5 Effects of RTG and Louver Changes

To this point, the discussion has considered variations in the mission and variations in the foam insulation qualities. However, no consideration has been given to the consequences of varying the RTG temperature or replacing the louvers with totally passive radiators. These two variations will now be considered.

The sensitivity of the module to variations in the RTG temperature depends upon the amount and location of solar heating which is occurring. The module is most sensitive to RTG changes for the condition of 0° off-pointing, that is, no solar heating. Figure 5-18 is a plot showing the sensitivity at this condition. This plot indicates that the RTG temperature could be increased to approximately 1135°R before the maximum allowable propellant temperature of 280°R is exceeded. This is indeed true for 0° off-pointing, but with any appreciable solar heating, the maximum allowable temperatures would then be exceeded.

At the other extreme, the curves show that the RTG temperature must not be less than approximately 800°R if the fluid temperatures are to be maintained at all times above 220°R . Of course, the RTG temperature can drop considerably without harm if solar heating occurs.

The module was designed to function properly when the RTG is at about 960°R . It could have been designed to operate with a different nominal RTG temperature. It should also be noted that it could have been designed to maintain the propellants at different temperatures. This could prove to be a decided advantage should a clearer definition of the mission may indicate that one propellant tank will receive more solar heating.

than the other. Such changes in the design are readily handled by moving and/or rotating the RTG only minor amounts relative to the module.

In line with this last comment, it should be noted that the design established is not necessarily the optimum. This design, however, does permit sufficient temperature control for the normal mission specified, but it may prove wise to vary the mission, or RTG temperature or even a combination of several variables in order to accommodate a specific objective of the overall project. To arrive at the optimum design, it would be necessary to make an exhaustive parametric study which would consider the following variables:

- o Off-pointing angle during the first 40 days
- o Module orientation during the first 40 days
- o Time of first firing
- o RTG temperature
- o RTG temperature variation
- o Louver area

As for replacing the louvers with radiator plates, the effects are not as striking as might be expected. A series of computer runs were made to establish how a totally passive system with an abbreviated shield would function when exposed to different intensities of solar radiation. The results are given in Figure 5-19. This plot is similar to Figure 5-5 and may be compared directly to establish the effectivity of louvers as opposed to radiator plates. It will be seen that replacing the louvers with radiators of equal area reduces the allowable solar intensity to the propellants by about 25%. It should also be noted that the equilibrium temperature for no solar heating is slightly higher, 5°R . By decreasing the +X radiator area slightly (the radiator which sees the RTG), the curves could be made to shift down slightly. As it turns out, radiator plates having the same area as the louvers are not the optimum size. If the radiator area were changed to the optimum size, the allowable solar intensity to the propellants would be only 10% less than it is when louvers are used. Thus, where a semi-passive system can withstand a

relative solar intensity of 0.34, the passive system can withstand an intensity of 0.31.

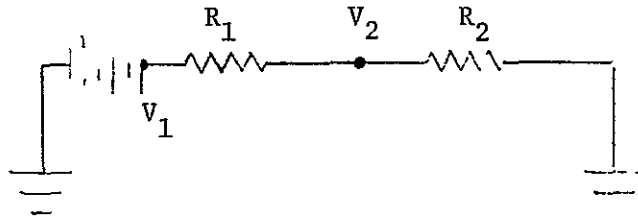
Of course, the louvers also make it possible to accommodate a larger fluctuation in RTG temperature. However, it can be seen that the louvers do not increase the flexibility of the thermal control system as much as might be expected. The reason the louvers have such a minimal effect stems from their locations.

The -X louvers, those which do not see the RTG, transfer less than 15 Btu/hr when fully open because of their low radiating temperature. The +X louvers, when fully open, receive less than 35 Btu/hr from the RTG because of the view factor. In comparison, the propellants may lose as much as 110 Btu/hr to space through the insulation and they can gain as much as 120 Btu/hr from the RTG through the insulation. In essence, the thermal control exerted by the louvers is only a partial control.

The choice of putting the louvers on the tanks was dictated by the ground rule that no active thermal control can be utilized. Obviously, the ideal place to locate the louvers is on the RTG with a sensor attached to the tanks so that the louvers, though located on the RTG, would function according to propellant temperatures. With this arrangement, heat loss to space through the insulation would be about 100 Btu/hr but the heat gain from the RTG could be made to vary from essentially 0 to 200 Btu/hr. It must be clearly understood that the louvers so located would have to operate from tank sensors since the louvers would have no way to compensate for varying solar heating, or, in the alternative, 100% sun shading would have to be provided.

There is, of course, the possibility of eliminating the radiator plates also and having only insulation on the tanks. This can be done theoretically, but the thermal control system would have very little capability to accommodate normal variations in fabrication (normal material variations) let alone mission variations. Where the louvers give a control range of approximately 44 Btu (variation in heat transfer via the louvers) and the radiator plates give a control range of about 32 Btu, the insulation has a control range of less than

10 Btu The reason for this becomes apparent if the last two cases are compared to the simple circuit given below



For the case of insulation, the resistance of the insulation, R_1 is constant but the radiation resistance, R_2 , is somewhat smaller and is inversely proportional to V_2^4 . Thus, when R_1 is very large compared to R_2 the network acts as a simple linear network in which the current is directly proportional to the voltage (heat transfer is directly proportional to the temperature). For the case of a radiator plate, however, R_1 is zero and the current is proportional to V_2^4 (heat transfer is proportional to temperature to the fourth power)

Considering the nature of this propulsion system, an engineering judgement would dictate the use of radiator plates since they are less complicated than the louvers and yet they provide sufficient control which only insulation does not

5.3 Propulsion System Results

Before describing the results of the propulsion analysis, it should be recalled from Section 4 that the following assumptions are made

1. The propulsion system is calibrated to deliver 100 psia chamber pressure at a mixture ratio of 3.0 when both propellants are at 250°R and pressurized to 300 psia
2. The propellants are not saturated with helium prior to launch.
3. The propellant tank ullages are not pressurized for the first time until shortly before the midcourse firing

- 4 For all firings, the ullages are not suddenly pressurized just prior to firing. Rather, they are pressurized soon enough before the firing that both ullages and the helium tank may return to thermal equilibrium prior to the firing

These assumptions were made on the belief that they represent the best compromise between standard pre-launch handling requirements and helium conservation during flight. The practicality of the sequence of Item 4 will be discussed later.

As shown above, the predicted propellant and helium equilibrium temperatures are very nearly constant during the normal fully-shaded mission. A set of computations were made to reveal the system performance and operating points during this type of mission. Fuel and oxidizer temperatures were assumed to be a constant 250°R and equilibrium temperature was set at 256°R.

With the propellant equilibrium temperatures held constant throughout the period from before the midcourse firing to the end of the orbit inclination maneuver, the mixture ratio and chamber pressure will be the same during each firing for constant tank pressures (assuming no degradation in propellant or hardware). At the end of a single 44-second midcourse maneuver, the oxidizer ullage temperature is calculated to be 252.5°R and the fuel ullage temperature is 251.7°R. A total of 27.18 pounds of helium at 251.5°R is left in the helium tank.

During the following cruise period, the propellant tank ullage gases will return to 250°R. Since the liquid propellants were free of helium until the firing, a portion of the helium in the ullages will dissolve into the liquids. When equilibrium helium concentration at 250°R is attained, the total pressures (vapor pressure plus partial pressure of helium) will be 291.8 psia in the fuel tank and 248.9 psia in the oxidizer tank. Prior to the orbit insertion firing, these ullages must again be pre-pressurized to 300 psia.

At the conclusion of the 533-second orbit insertion firing, the oxidizer ullage is at 245.4°R and the fuel ullage is at 242.3°R. At this point, the temperature of the 17.07 pounds of residual helium is 215.8°R

The post-firing cruise period allows the propellant tank ullage gases to return to equilibrium temperatures. This causes the pressures to rise above operating level since the propellants have become saturated during the previous cruise period. Hence, the propellants absorb very little additional helium at the new equilibrium conditions. Oxidizer tank pressure at equilibrium cruise condition is 208.3 psia, the fuel tank pressure is 308.4 psia.

Starting the orbit inclination firing at these elevated pressures generates a momentary surge in chamber pressure to 102.1 psia and the mixture ratio drops to 2.976 to 1. In less than 20 seconds, both of the tank pressures decline to regulated levels (300 psia) and engine performance is again nominal. At the end of the 528-second firing, the oxidizer ullage is at 241.2°R and the fuel is at 240.5°R. The final residual helium mass is 7.14 pounds at 205.6°R, this corresponds to a final pressure of 821 psia. These results are given in Figure 5-17.

Of course, it is possible to analyze any given mission and obtain a picture similar to that given for the normal mission.

In order to obtain a generalized picture of what may occur relative to engine performance should the fuel and oxidizer temperatures be other than 250°R, computations were done for a matrix of cases. The results are given in Figures 5-20 and 5-21. These plots show the effect of propellant temperatures on mixture ratio and chamber pressures. It will be seen that mixture ratio never exceeds 3.16 nor falls below 2.88. The extreme values of chamber pressure are 104.3 and 96.5 psia. These values occur when the oxidizer temperature falls to 200°R or rises to 290°R, with corresponding fuel temperatures of 210 and 270°R. If neither propellant exceeds the 210 or 270°R limitations, then the mixture ratio range is approximately 3.13 to 2.93, and the chamber pressure range is 103.6 to 98.2 psia.

No generalized data is presented which indicates the helium consumption for various arbitrary missions simply because the range of variables is nearly limitless. Not only is helium consumption dependent upon propellant temperatures, but also upon mission profile.

From the comments and data presented, it can be seen that the module propulsion system performance is relatively insensitive to propellant temperatures. Neither mixture ratio nor chamber pressure changes more than 1% from the nominal design points if the propellants are kept at the same temperature and within 12°R of the nominal (250°R) temperature. Under the worst conditions, that is, either propellant at the extreme limits and the other propellant temperature differing from it by a full 20°R, the mixture ratio and chamber pressure will be within 5% of the nominal values. (All of these conclusions relate to firings with both propellant tanks at 300 psia.)

It should be recalled that the basic module design results in an off-set between the module centerline and the spacecraft centerline of approximately 10.62 inches. One concern has been the possibility of a shift in spacecraft C.G. should the mixture ratio not remain nominal. Calculations show that for the normal mission, the C.G. shift after the last burn will be approximately 0.25 inches towards the fuel tank. Only a minor shift should be expected for the normal mission since the engine operation is very nearly constant. If a peculiar mission were attempted, however, the C.G. shift could become considerably larger.

One last point should be noted. The present helium tank volume is adequate for normal mission temperatures, but lower temperatures (approximately 245°R) probably would cause sufficient helium depletion that the final moments of the orbit inclination firing would occur in a blowdown mode within the propellant tanks. This should not be viewed with great alarm since it is rather easy to adjust the thermal design slightly and obtain a higher average helium temperature.

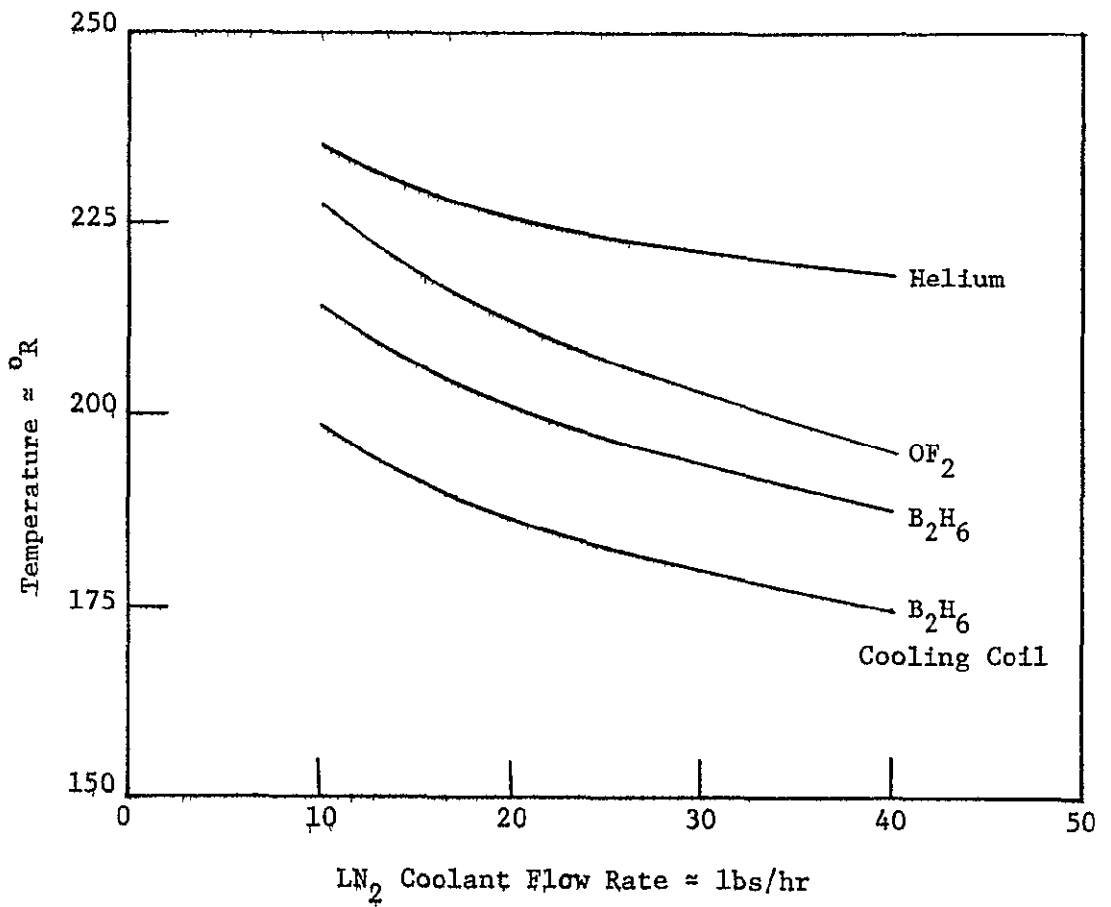


Figure 5-1 Equilibrium Temperature as a Function of LN₂ Coolant Flow Rate. Outside Film Coefficient = $1.0 \frac{\text{Btu}}{\text{ft}^2\text{-hr-}^\circ\text{F}}$

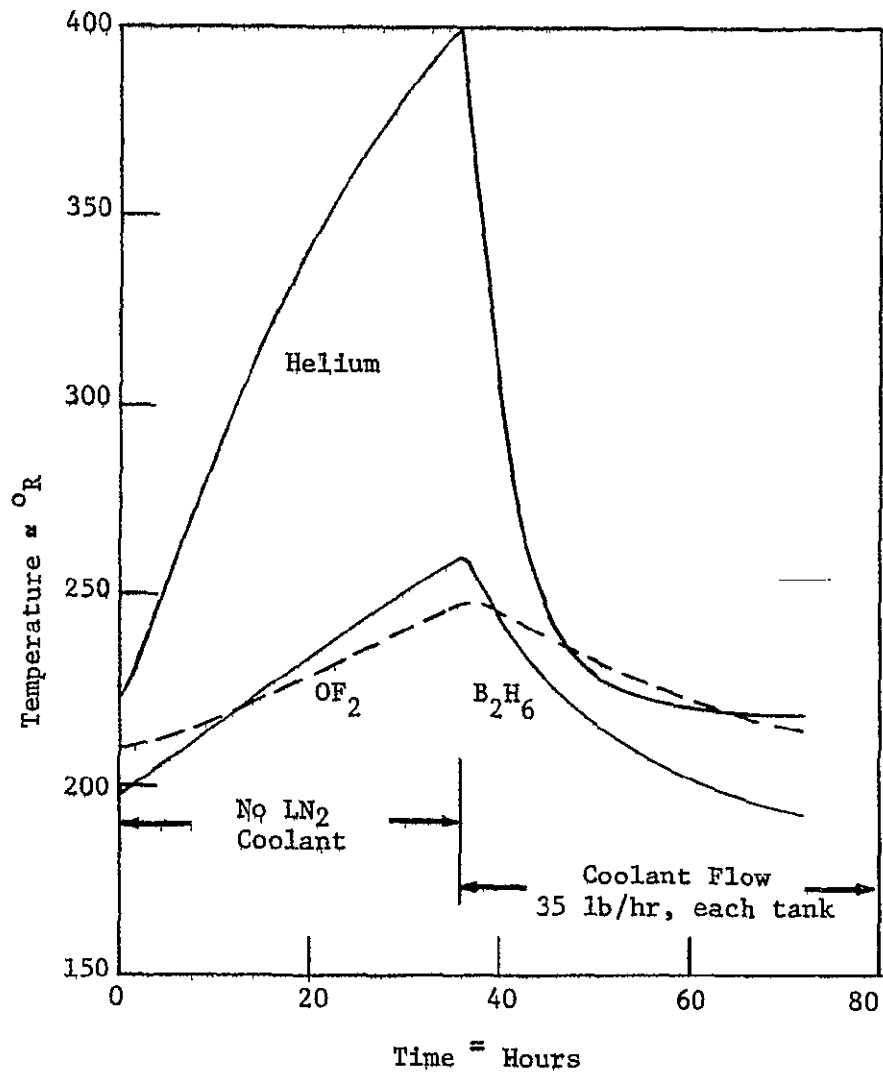
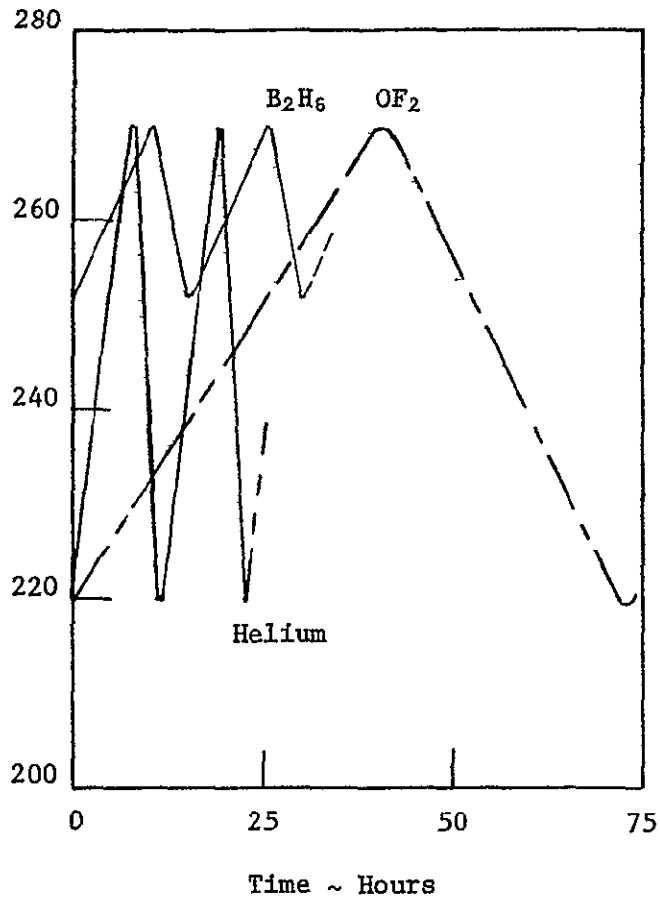


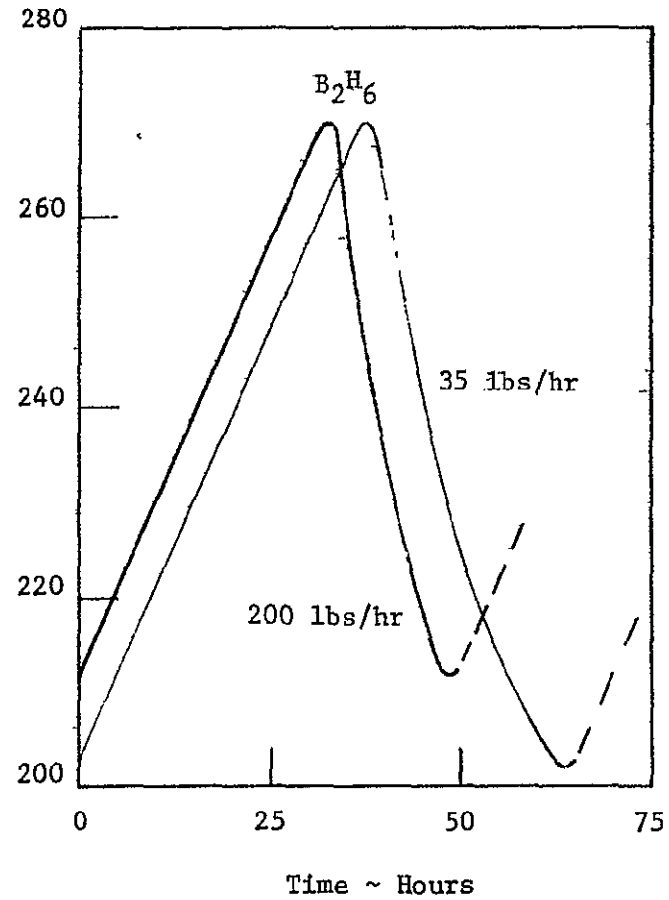
Figure 5-2 Transient Warm-Up and Cooldown
 During Groundhold Outside Film Coefficient = $1.0 \frac{\text{Btu}}{\text{ft}^2\text{-hr-}^\circ\text{F}}$

Notes: Helium and OF_2 Temperatures Controlled Between $220^{\circ}R$ and $270^{\circ}R$ by Immersion Temperature Sensors

B_2H_6 Maximum Temperature Controlled by Immersion Sensor Set at $270^{\circ}R$, and Low Temperature controlled by Sensor Attached to the Cooling Coil Set at $190^{\circ}R$



Graph "A" Coolant Flow Rate of 1000 lbs/hr



Graph "B" Coolant Flow Rate of 35 and 200 lbs/hr

Figure 5-3 Fluid Temperature Characteristics with Cyclic Control

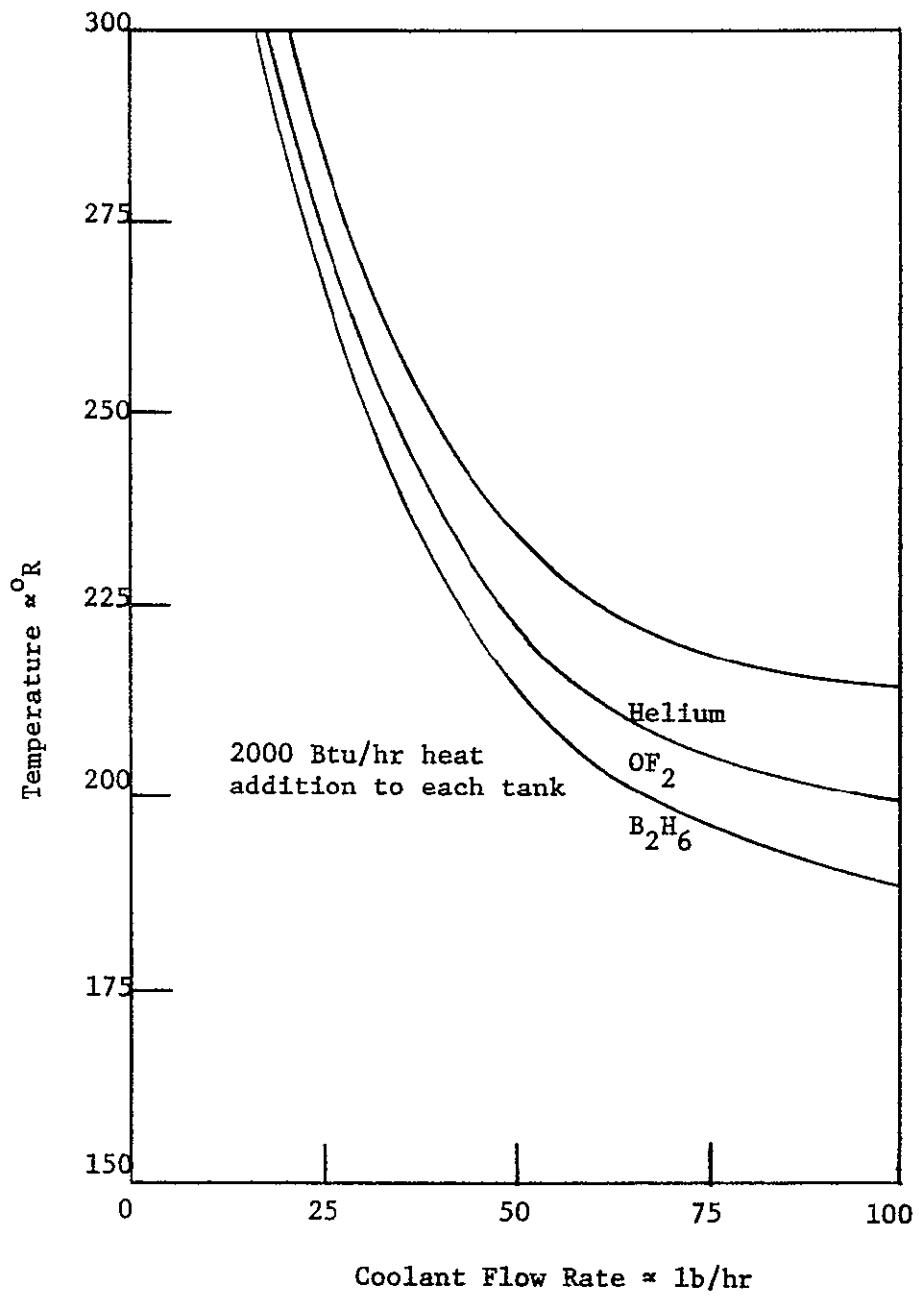


Figure 5-4 Tank Temperature With 2000 Btu/hr Heat Addition

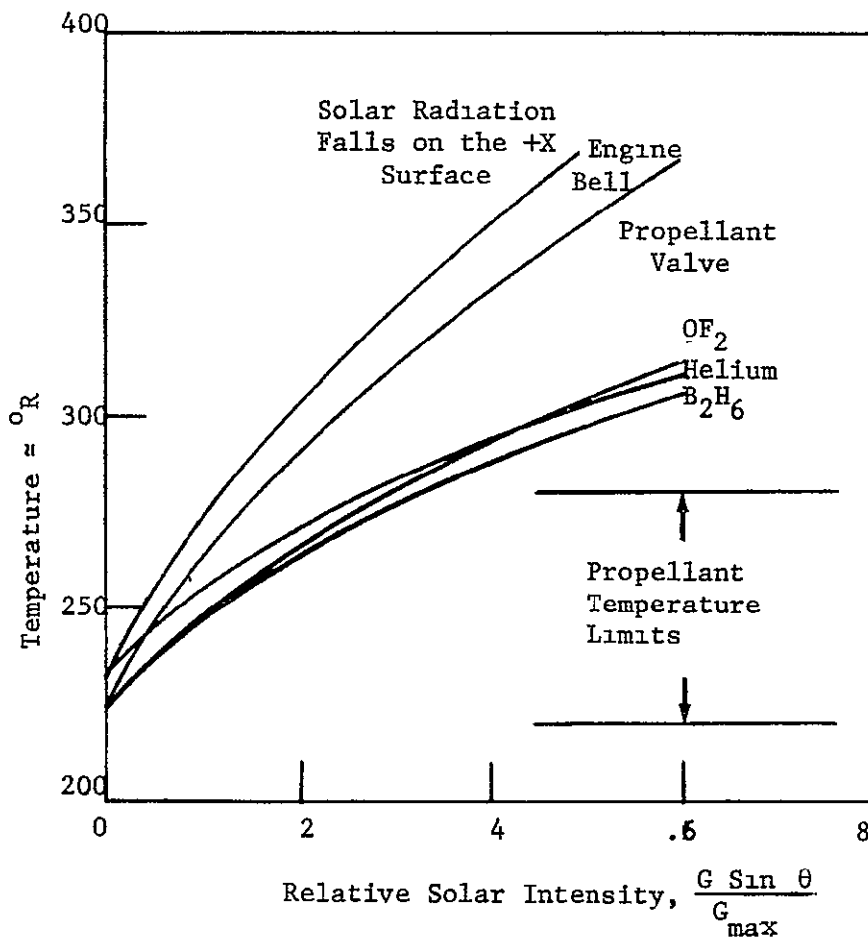
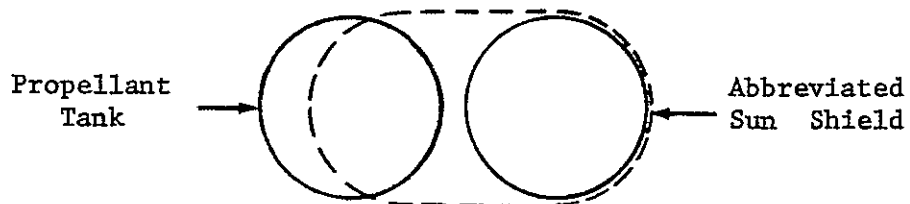


Figure 5-5 Steady State Temperatures for Varying Solar Radiation, 960°R RTG, Abbreviated Shield

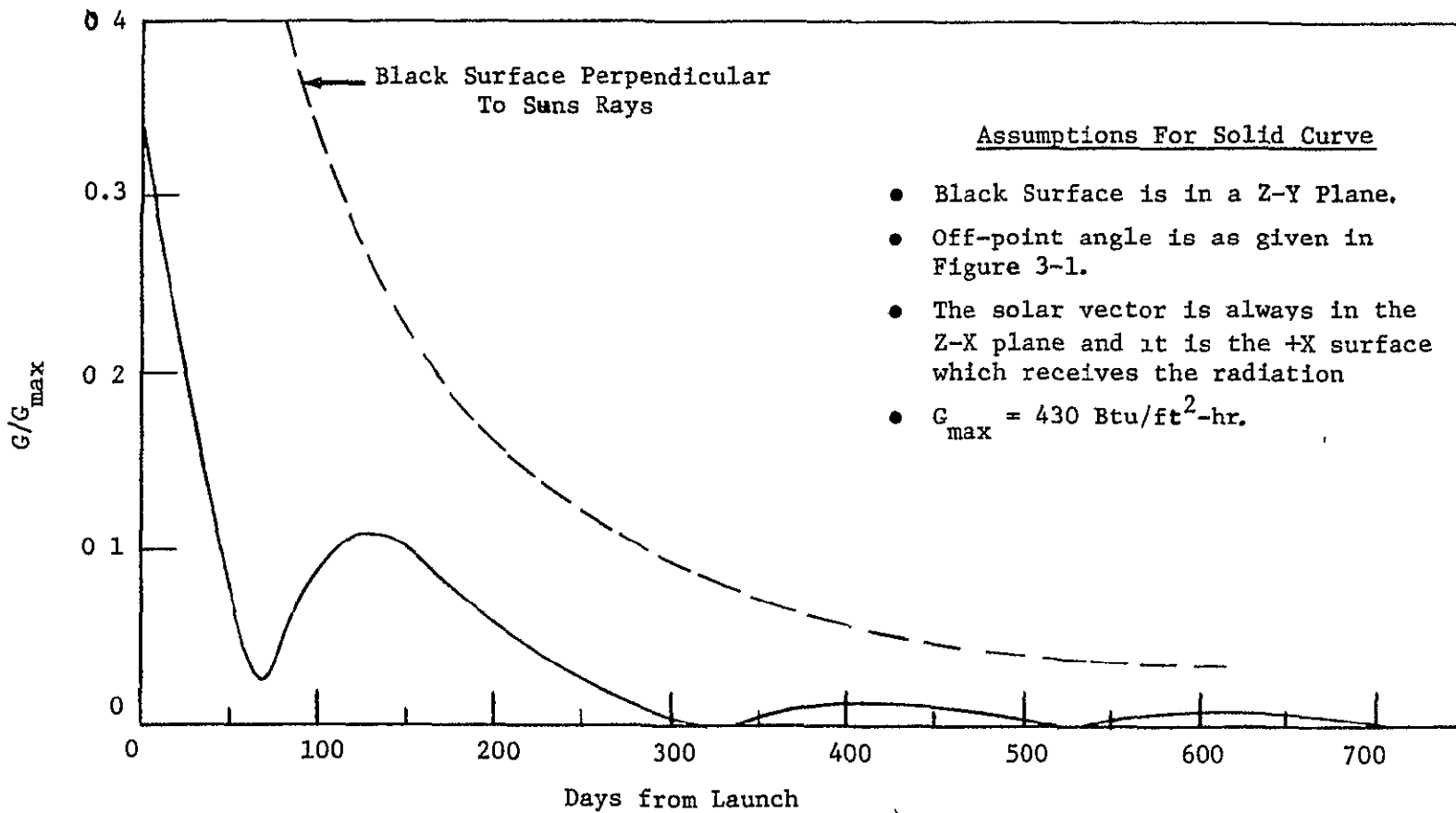


Figure 5-6 Relative Solar Heating Rate On a Black Surface During Normal Mission

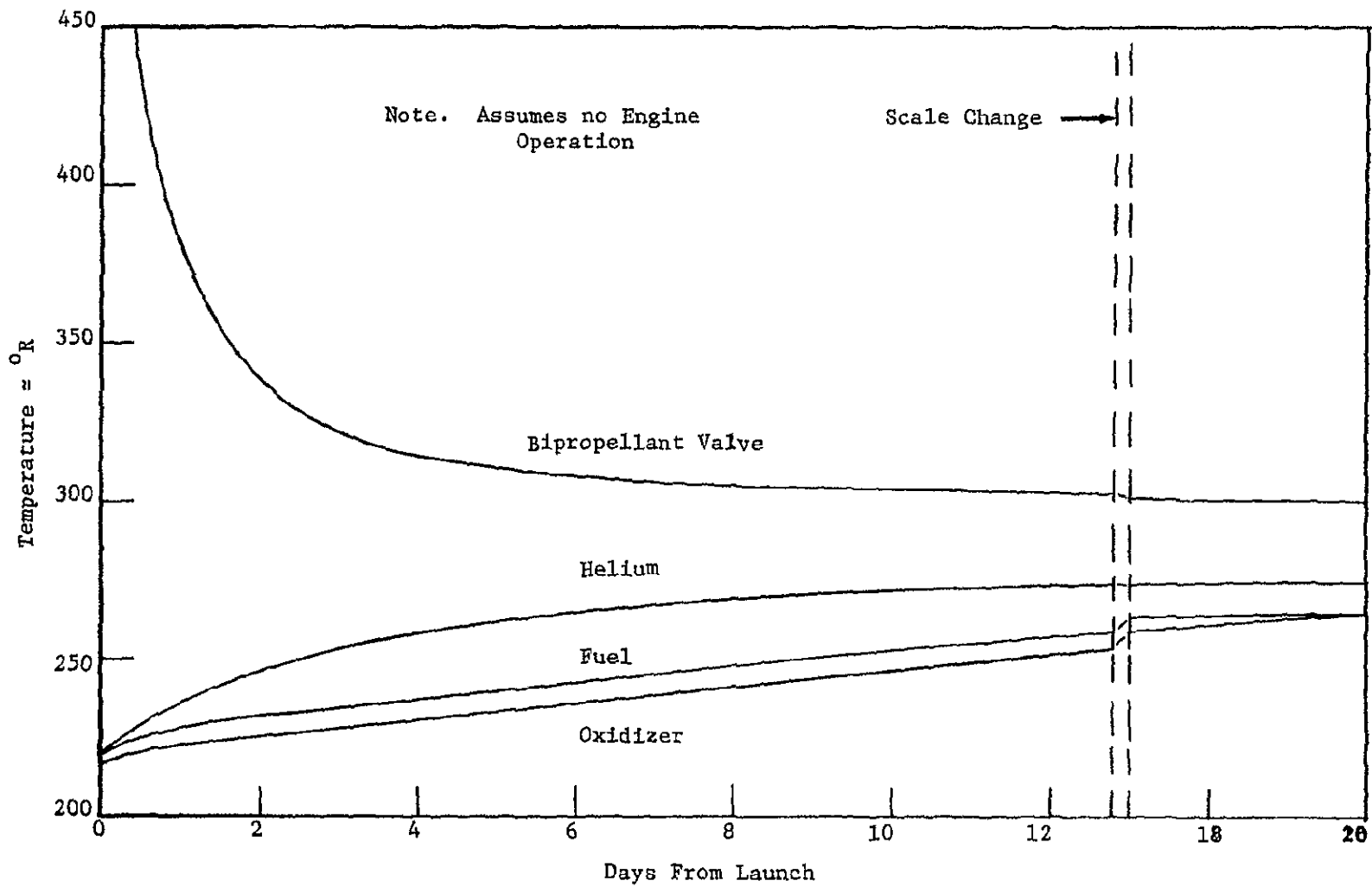


Figure 5-7 Module Temperatures After Launch on Normal Mission; 960°R RTG, Abbreviated Sun Shield

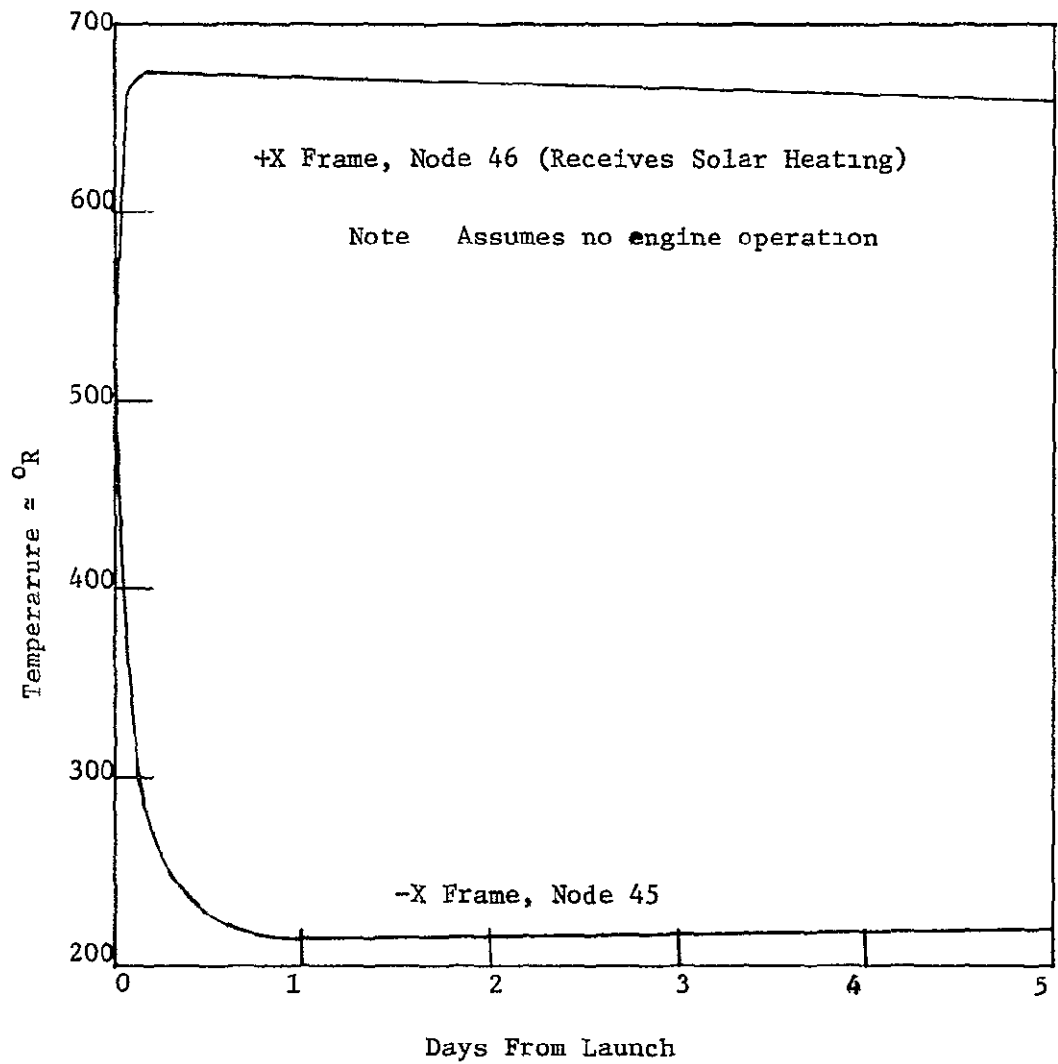


Figure 5-8 Module Frame Temperatures After Launch on Normal Mission; 960°R RTG, Abbreviated Sun Shield

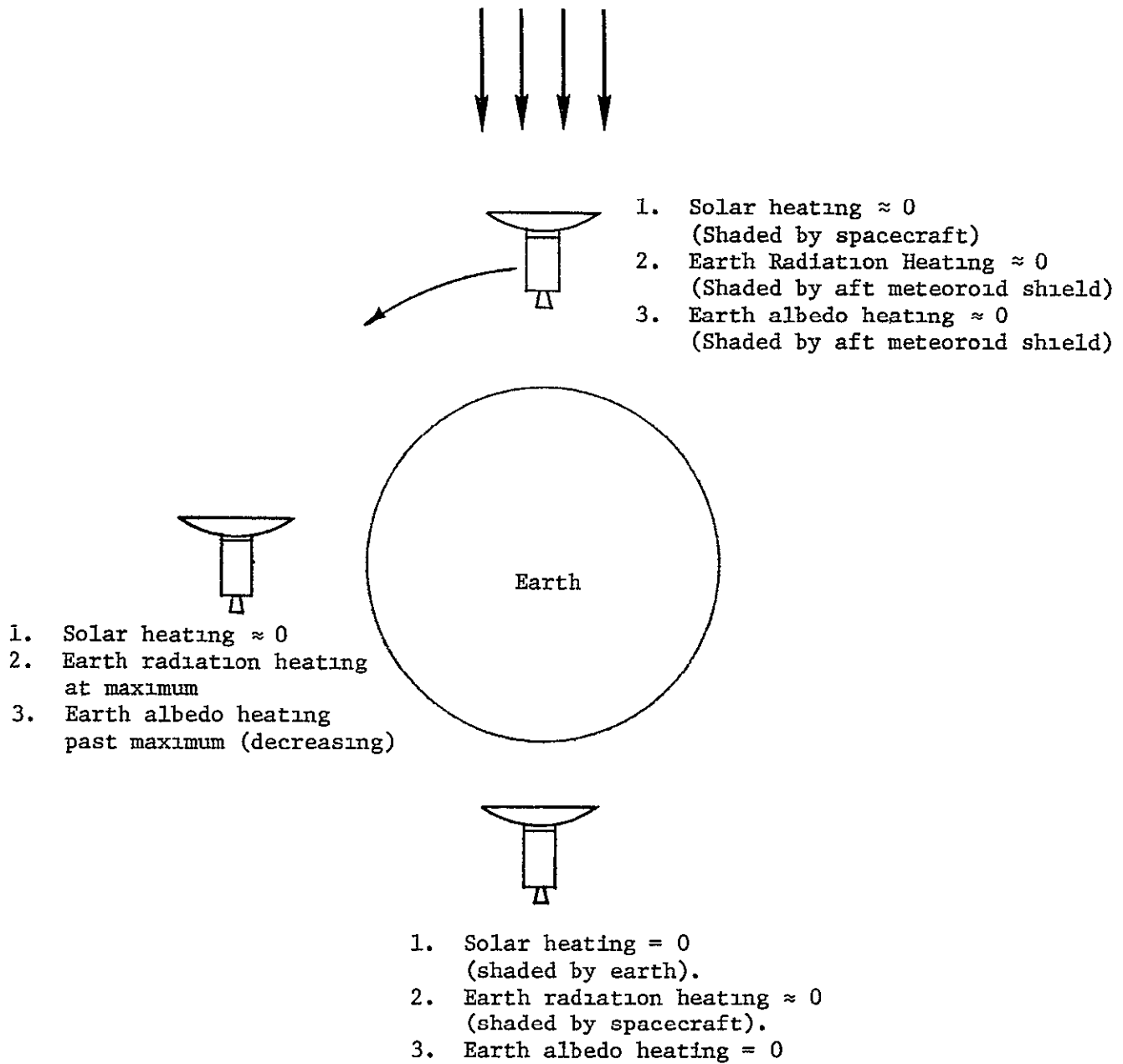


Figure 5-9 Sources of Module Heating While in Earth Orbit

Note: These curves are for full helium and propellant tanks. For only partially filled tanks, the response rate of the helium and propellants would be higher but the propellant valve curve would remain unaltered.

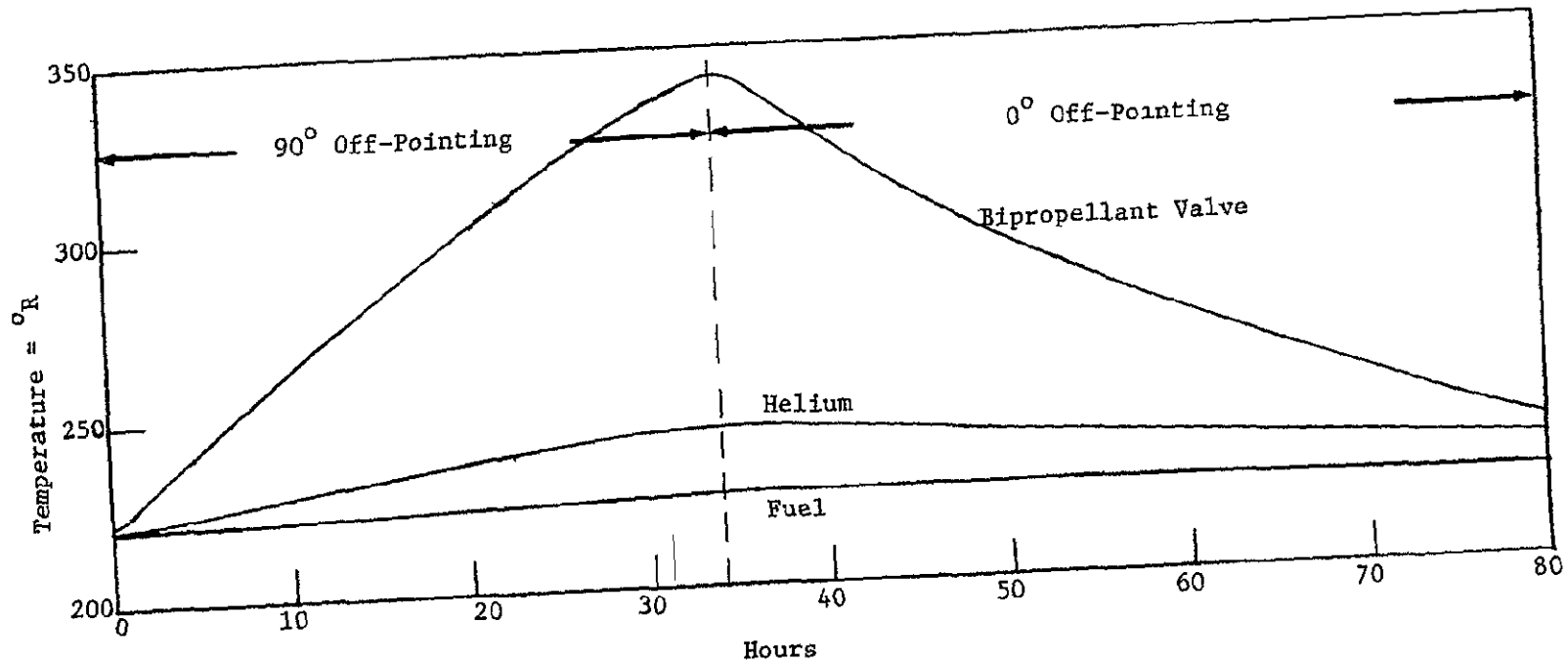


Figure 5-10 Effect of Orienting from 0° Off-Pointing to 90° Off-Pointing While Near Earth

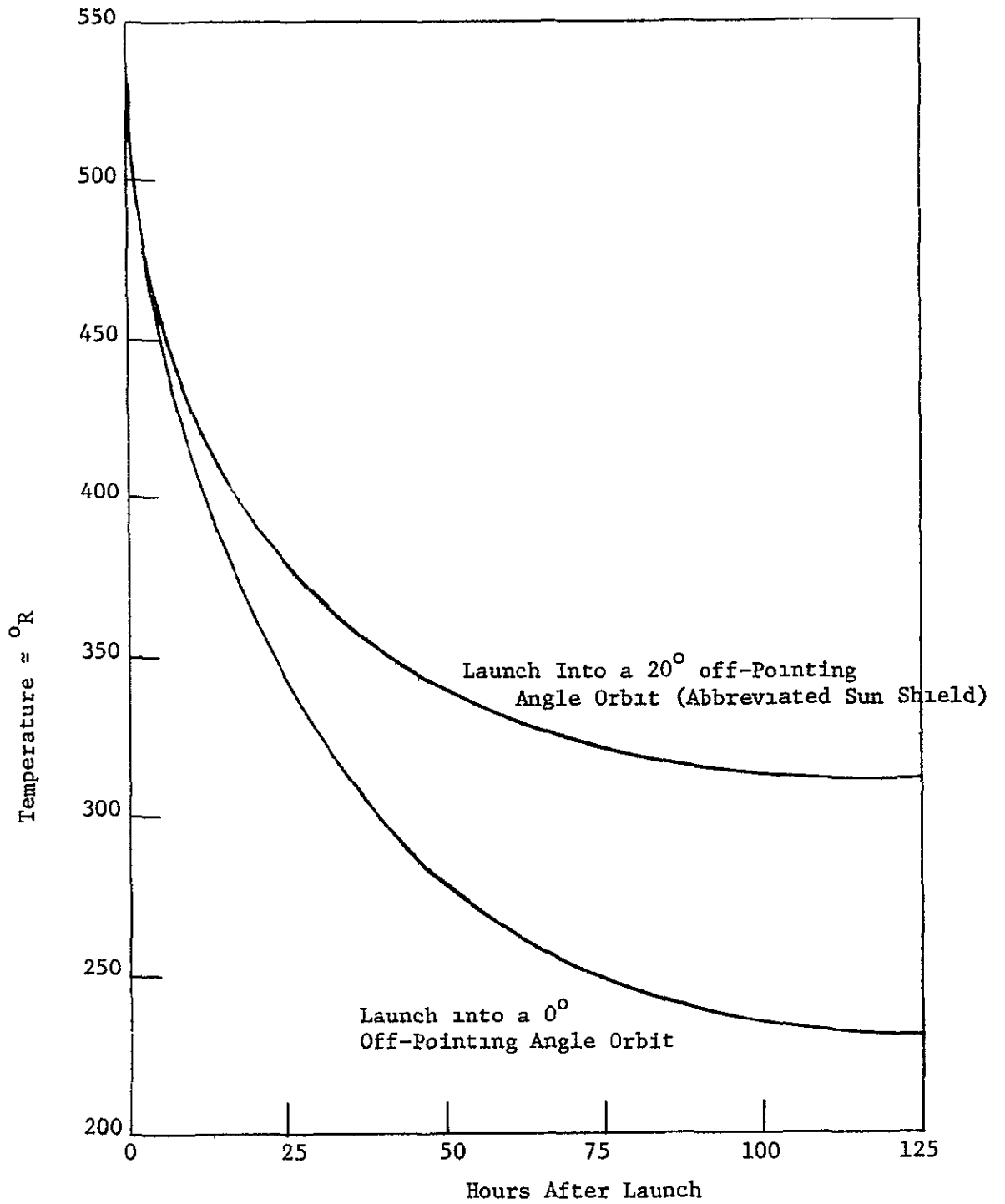


Figure 5-11 Temperature History of Bipropellant Valve Immediately After Launch

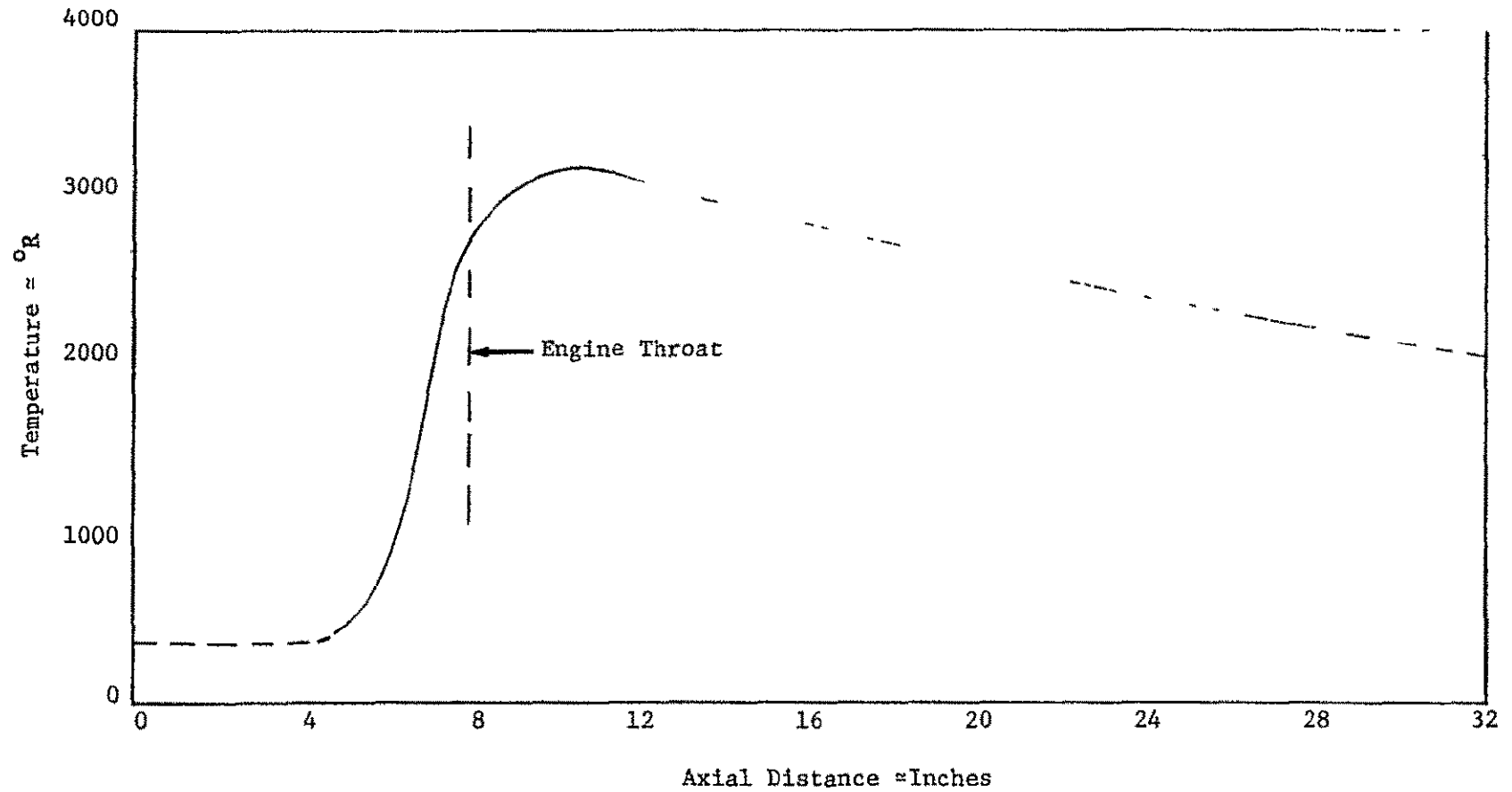


Figure 5-12 Outside Surface Temperature of Engine During Operation

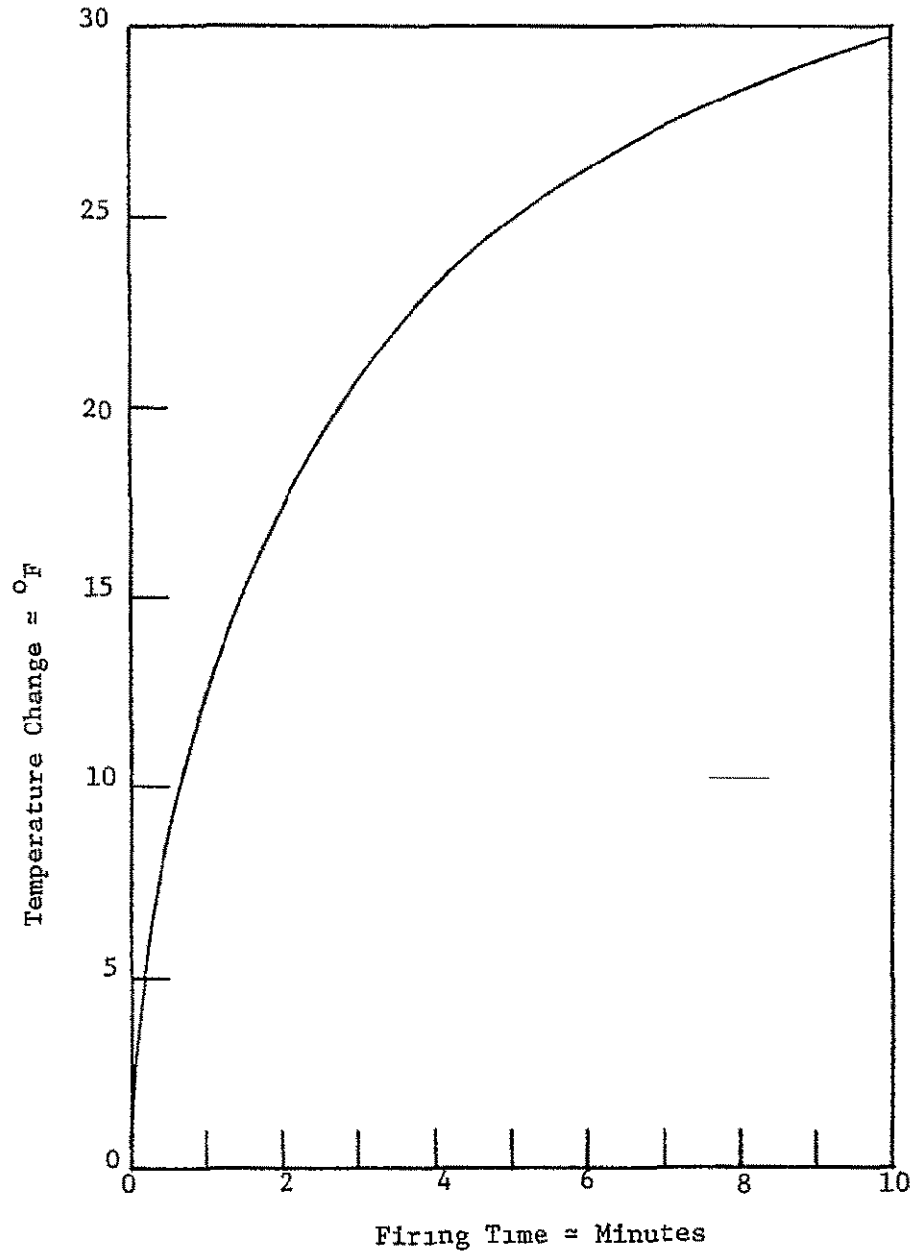


Figure 5-13 Helium Temperature Drop During Engine Firing

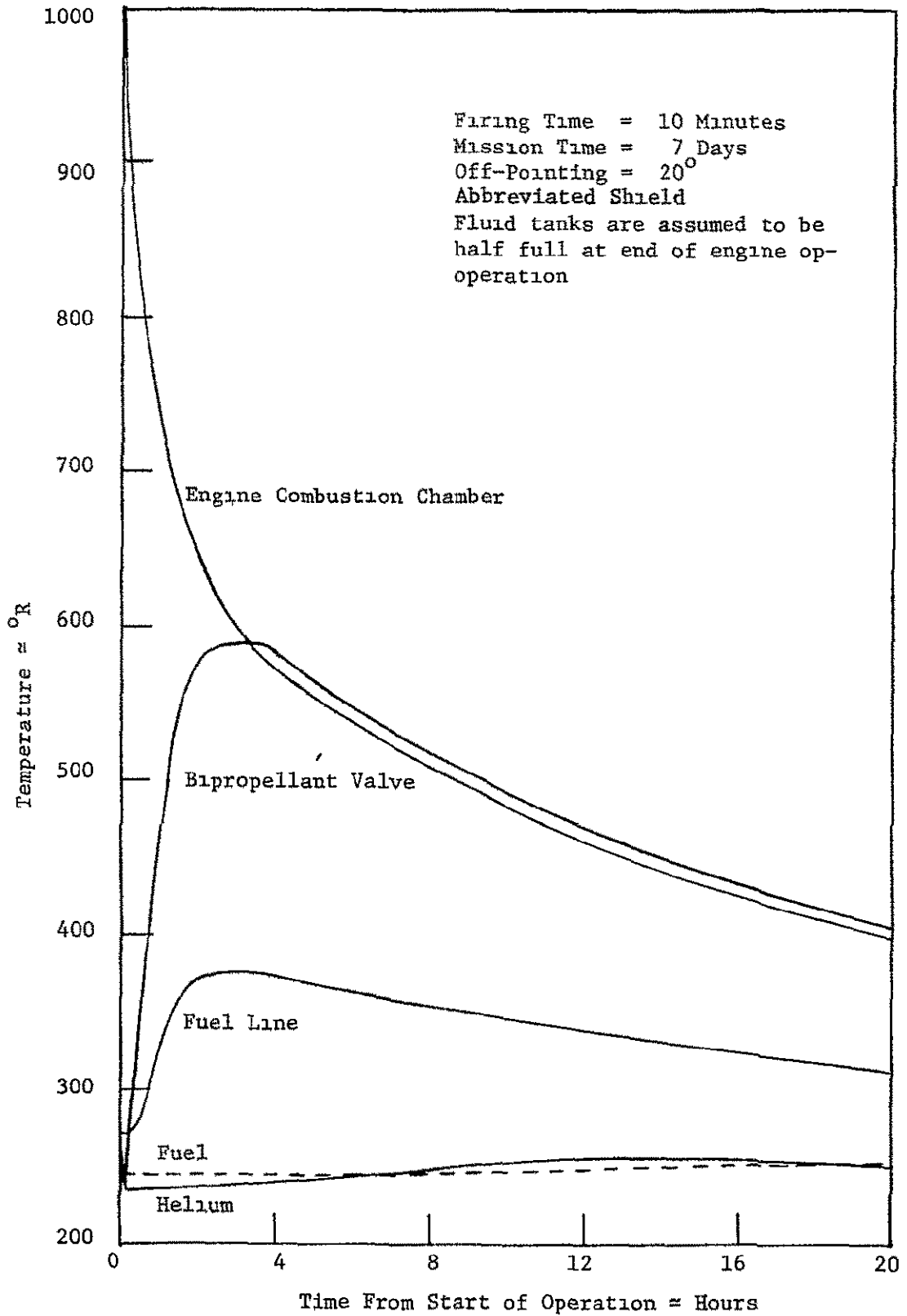


Figure 5-14 Temperature Histories During and After Engine Operation

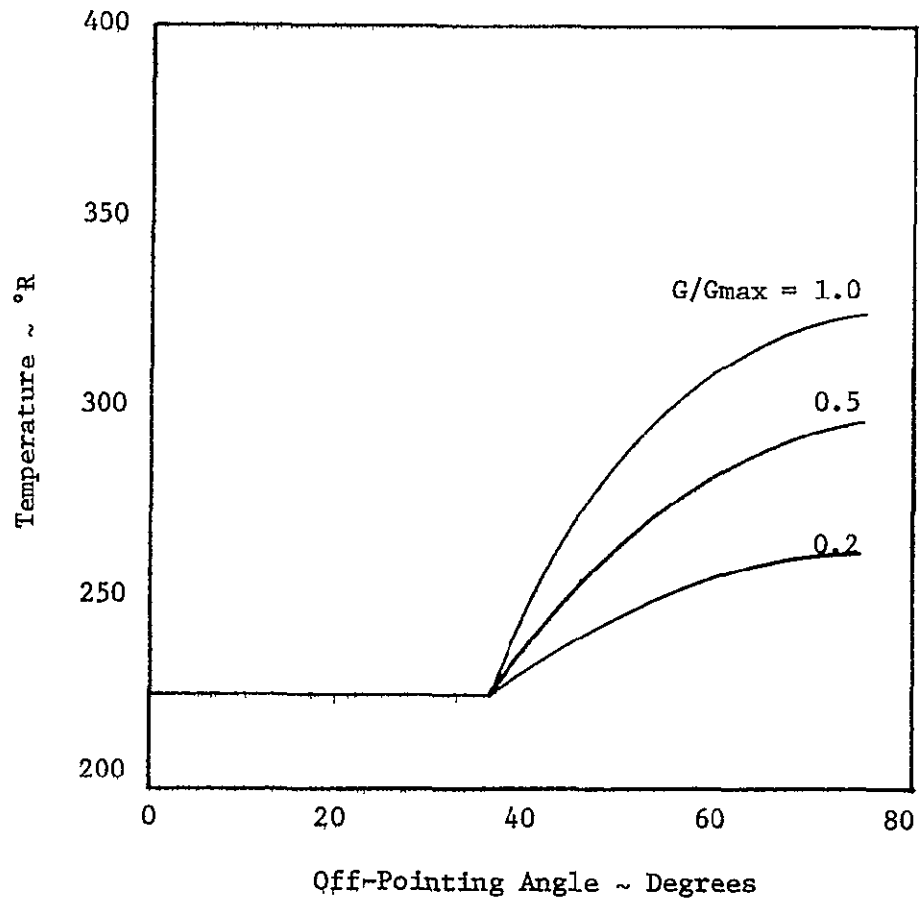


Figure 5-15 Steady-State Fuel Temperatures
for Varying Off-Pointing Angles,
Standard 10 ft dia. Shield, 960°R RTG

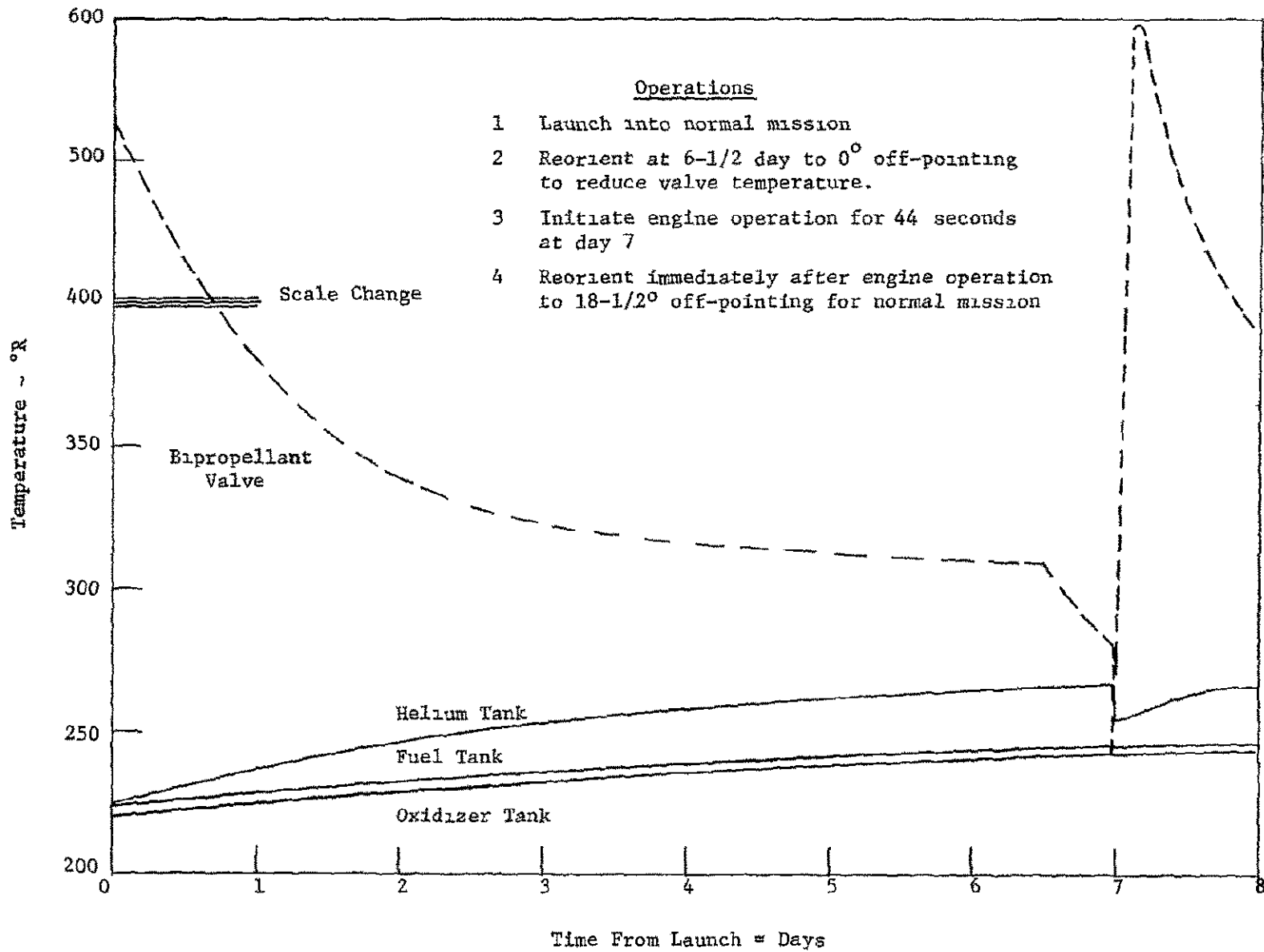


Figure 5-16A Thermal History of Major Components During Normal Mission; Module with Abbreviated Shield

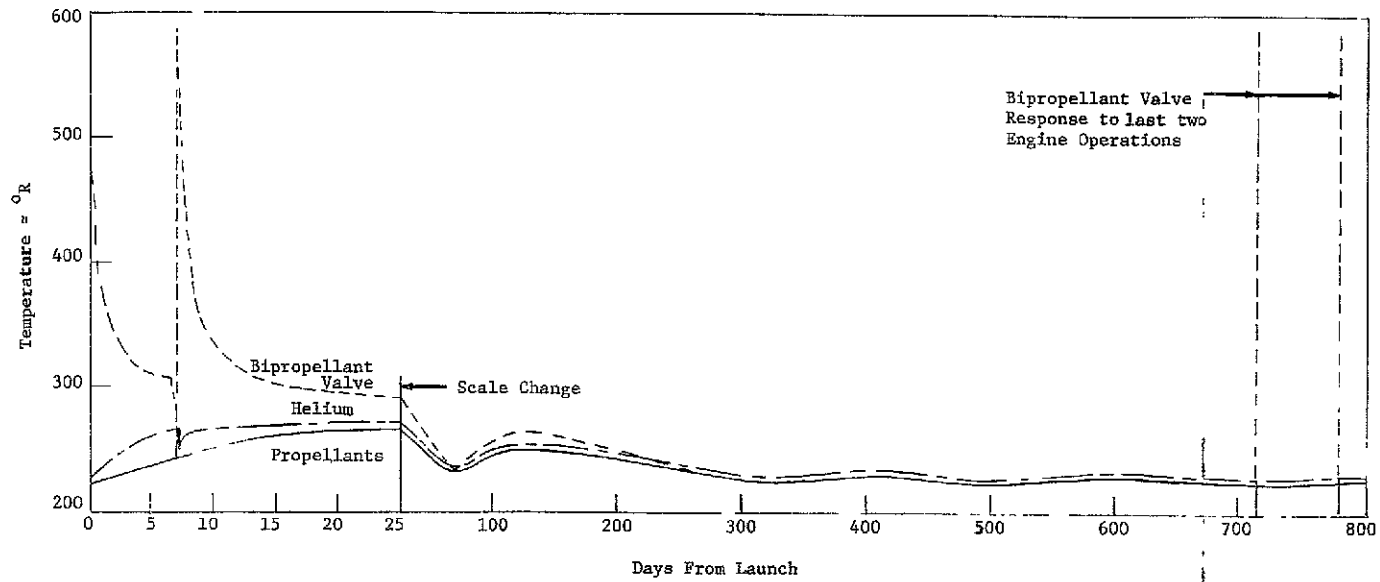


Figure 5-16B Thermal History of Major Components During Normal Mission; Module with Abbreviated Shield

FOLDOUT ERAME /

FOLDOUT ERAME 2

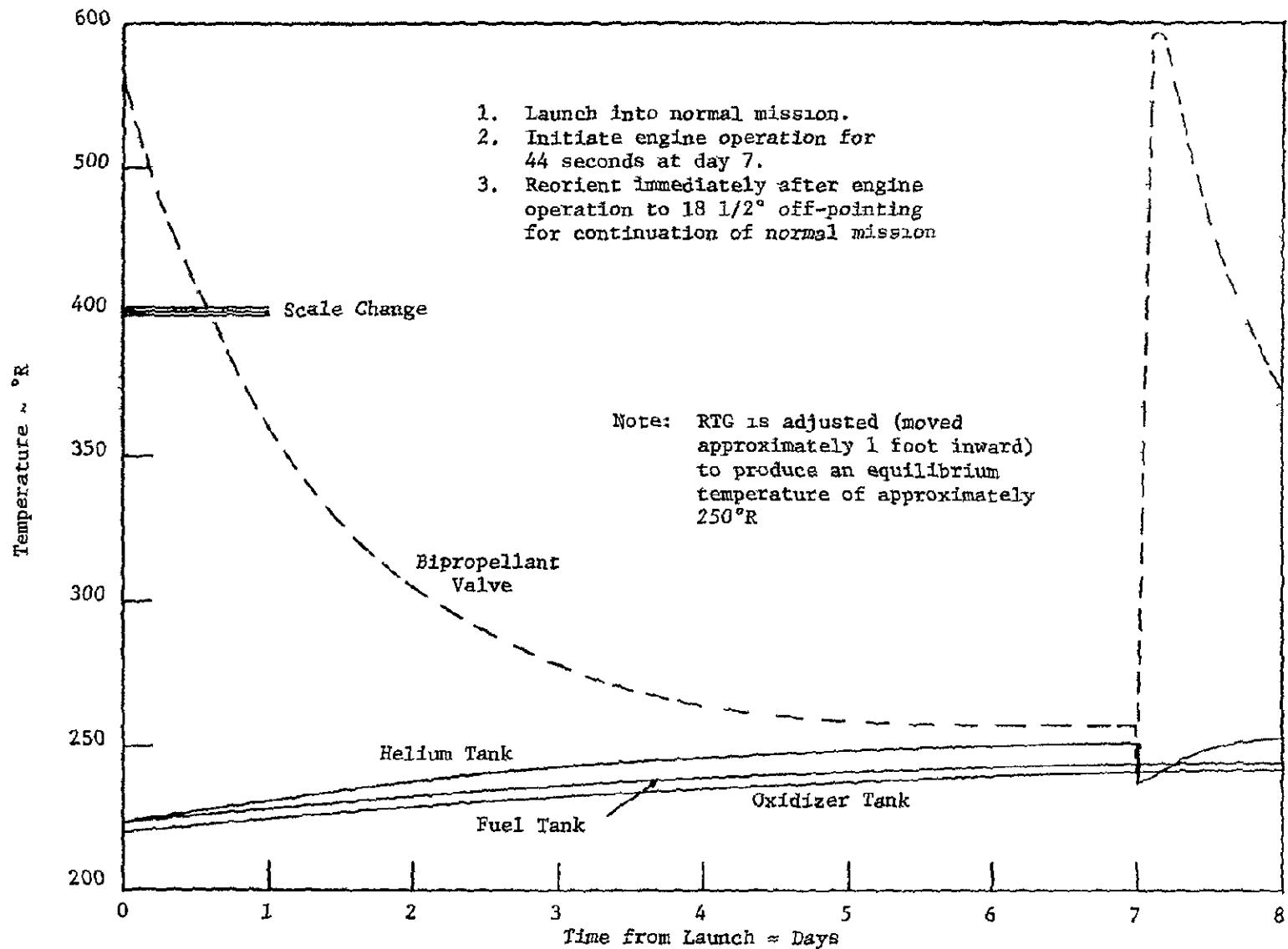


Figure 5-17A Thermal Histories of Major Components During Normal Mission; Standard Shield

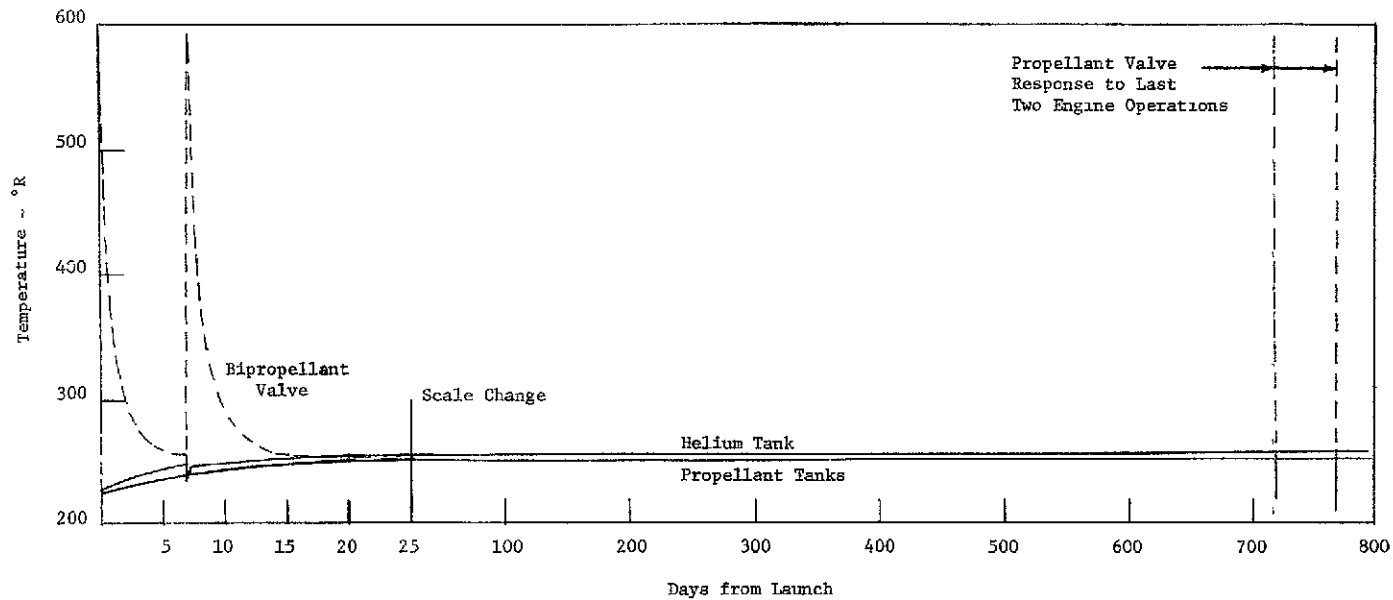


Figure 5-17B Thermal Histories of Major Components During Normal Mission; Standard Shield

10 10 10 10 10 /

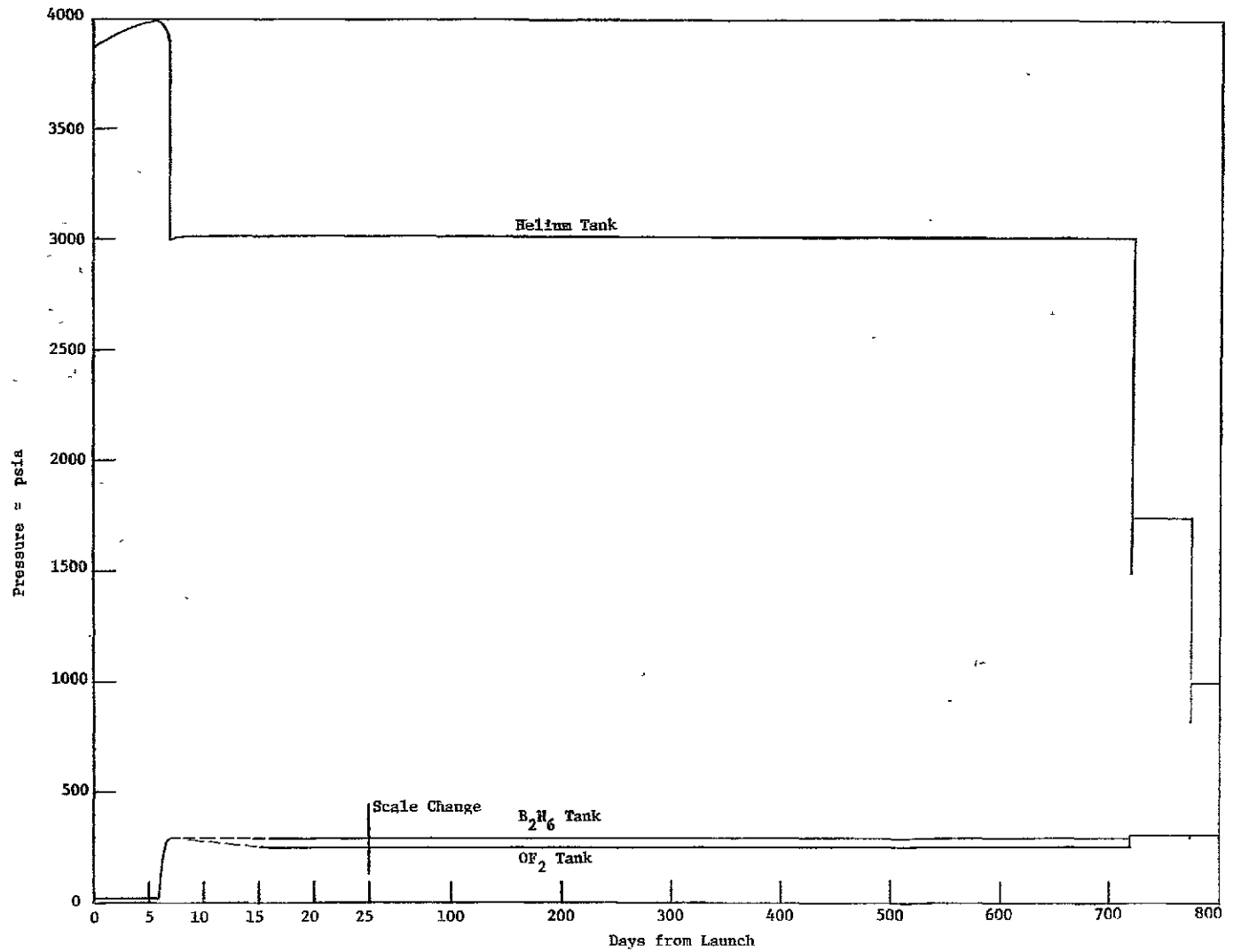


Figure 5-17C Pressure Histories of Major Components During Normal Mission; Standard Shield

FOLDOUT FRAME 1

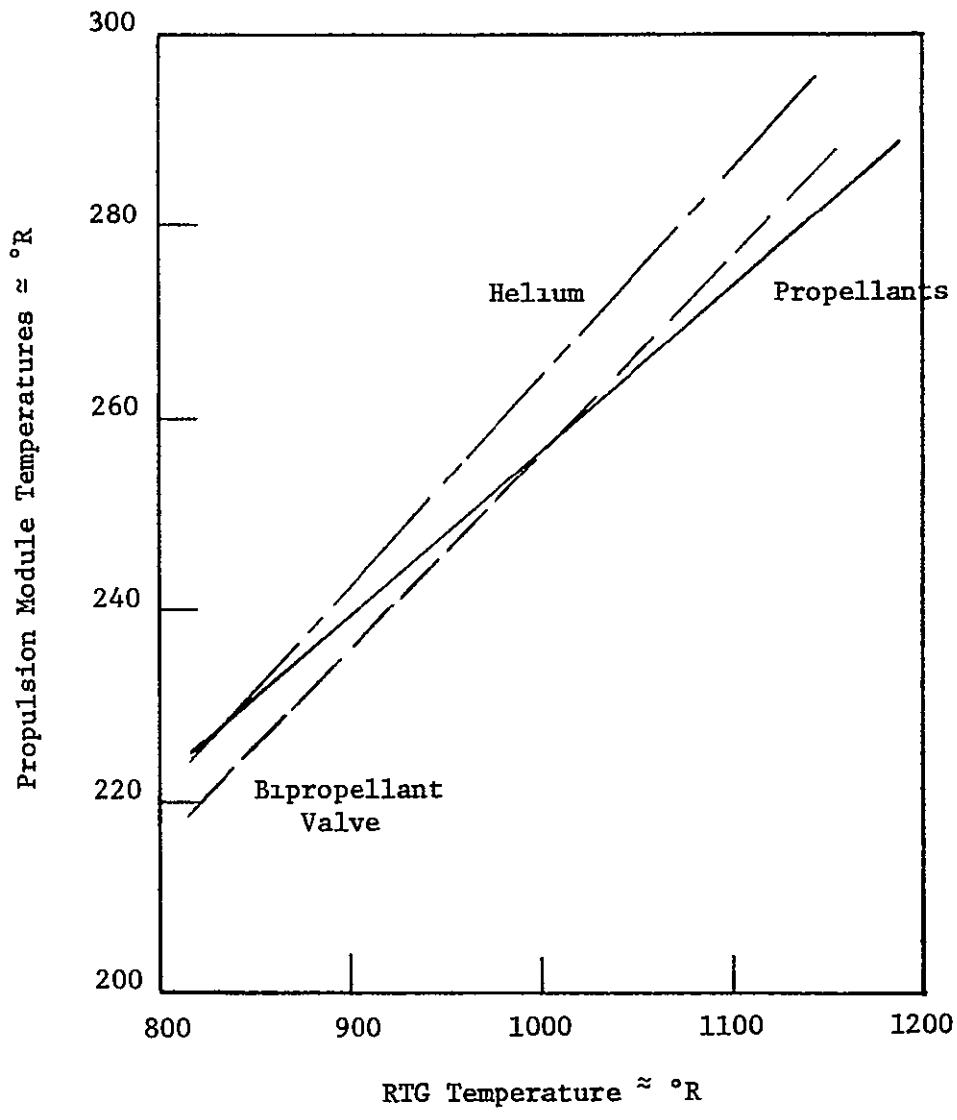


Figure 5-18 Effect of Varying RTG Temperature on Quasi-Steady State Module Temperature, Standard Shield

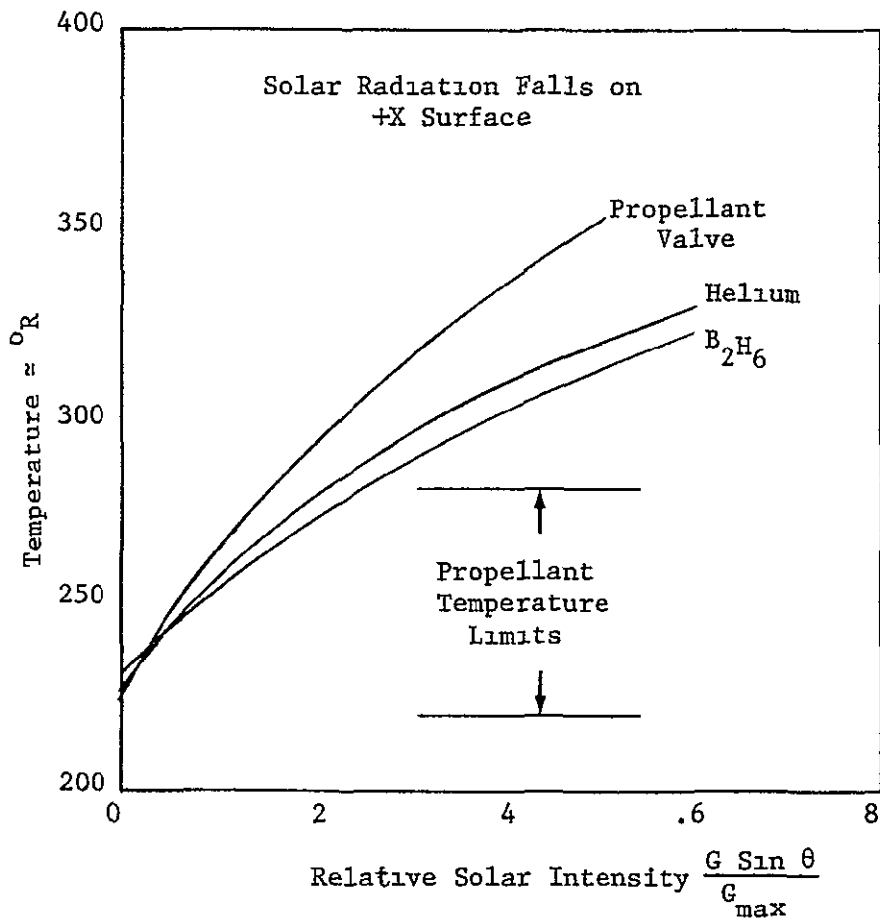


Figure 5-19 Steadystate Temperatures For Varying Solar Radiation, 960°R RTG, Louvers Replaced by Radiator Plates

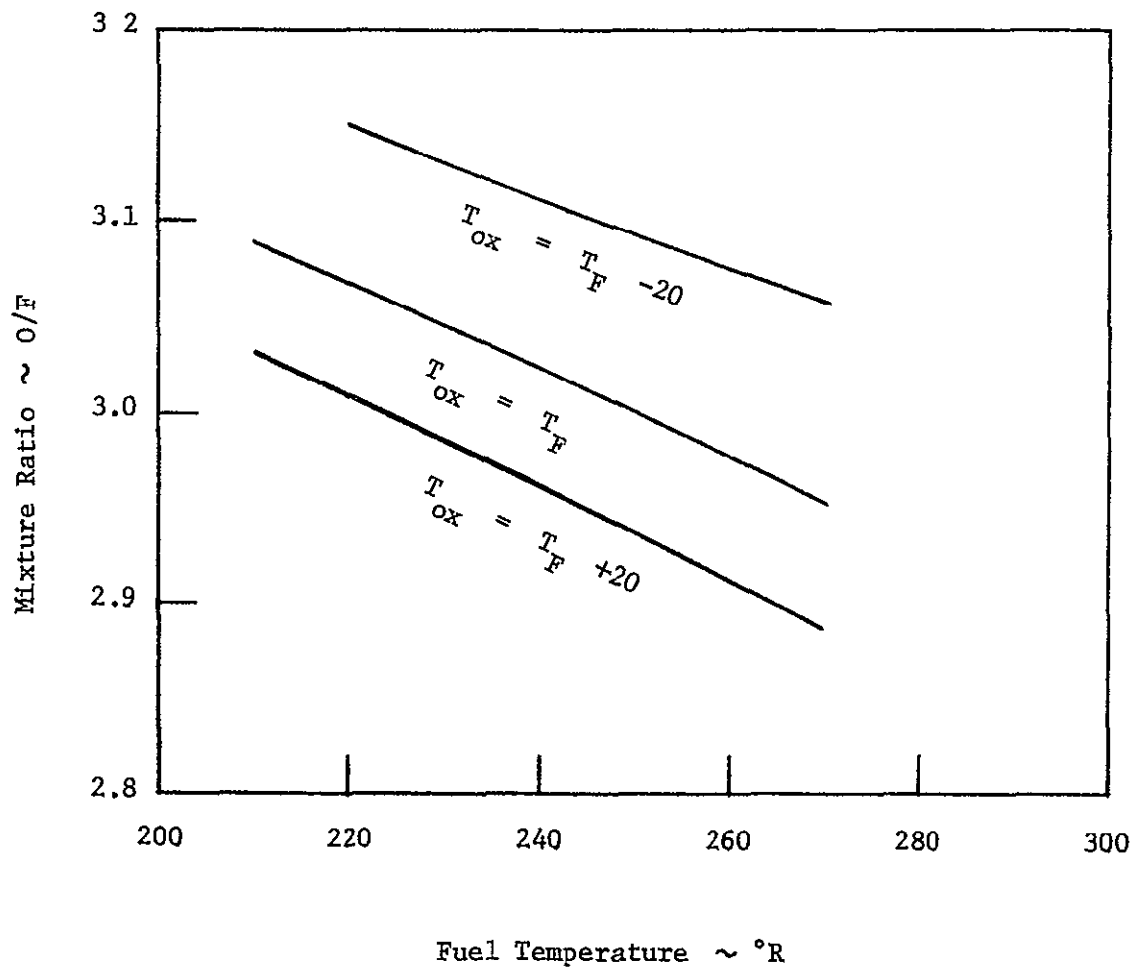


Figure 5-20 Mixture Ratio vs.
Propellant Temperatures

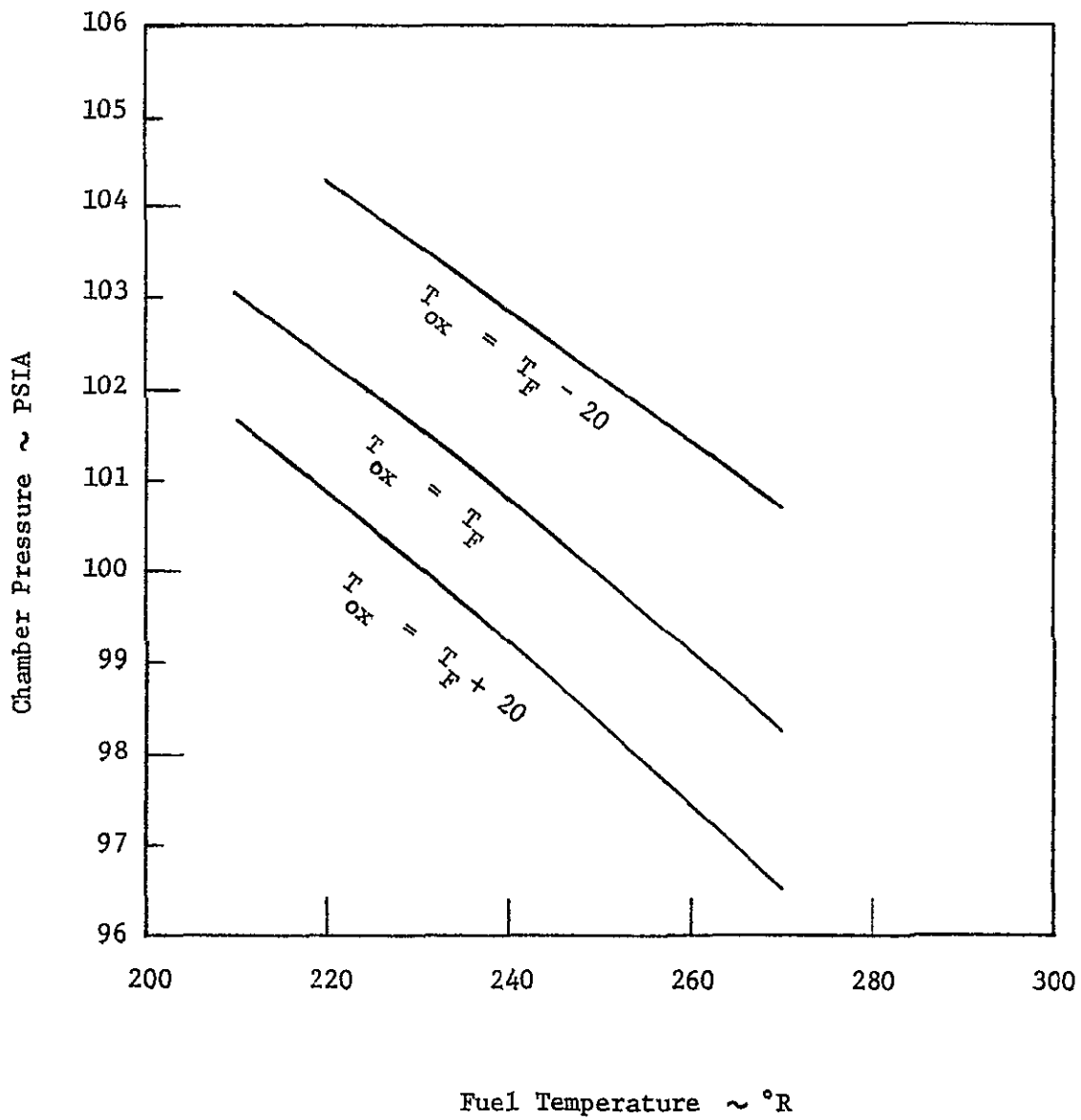


Figure 5-21 Chamber Pressure vs. Propellant Temperatures

6 0 CONCLUSIONS AND RECOMMENDATIONS

From the data that has been presented, it is possible to draw several important conclusions

- 1) Liquid nitrogen circulated through coils, submerged in the fluids inside the tanks, has ample capacity to maintain the fluids within their prescribed temperature limits during groundhold even if a sizeable insulation failure occurs.
- 2) Freezing of the fuel on the surface of the cooling coil is possible if the average fuel temperature is sufficiently near the fuel freezing temperature and the velocity of the liquid nitrogen in the coil is too high.
- 3) To avoid fuel freezing, it will be necessary to design the liquid nitrogen supply system so that it will supply the nitrogen in liquid form at a rate not exceeding 1500 lbs/hr. For better temperature control, the liquid nitrogen flow rate should be variable with a minimum flow rate of about 175 lbs/hr and a manual override.
- 4) To avoid freezing of the fuel, it will also be necessary to control the on/off flow of the liquid nitrogen by temperature sensors. The sensor for controlling when flow is initiated should be immersed in the fuel just below the surface. The sensor for controlling flow stoppage should be attached to the coil at or near its lowest point.
- 5) To avoid frost or moisture collection on portions of the frame, foam insulation will be required on all members and lines which contact the three tanks. Metal parts must be insulated for a distance of about one foot from the tanks and non-metal members insulated for about four inches.
- 6) The helium and propellant temperatures during the first six or seven days of flight are, to a large extent, determined by the temperatures which exist at launch because of the fluid heat capacitance.

- 7) The allowable steady-state, off-pointing angle which may be tolerated for the first 100 days is dependent on the amount of sun shielding provided. For the module as designed, the allowable off-pointing is approximately 20° at launch, increasing to 90° about day 100.
- 8) The module will be kept within the desired temperature limits if the louvers are replaced by radiator plates. However, the margin of safety will be slightly less.
- 9) The design of the pin joints at the bottom of each tank is not critical from the standpoint of thermal control. Since it is necessary to insulate the attaching frame as indicated above in (5), a joint having a high thermal conductance does not result in excessive heat transfer via the frame because of the frame insulation.
- 10) Unless it is allowable to initiate engine operation when the valve temperature is above the allowable fuel temperature, the first engine firing may not be made prior to day 3 because it takes that long for the valve to cool down from the ambient temperature of groundhold. In addition, if the module is launched into an orbit which causes the engine bell to be exposed to solar radiation, it may be necessary to orient the craft in a 0° off-pointing position for several hours prior to engine firing in order to drop the valve temperature.
- 11) Heat soak-back from the engine after engine firing is of minor consequence except for the bipropellant valve and connecting propellant lines. The valve will rise to approximately 600°R and small amounts of propellants will be vaporized and return to the tank to avoid high pressure.
- 12) The propellant lines and other control components will stay within the required temperature limits.
- 13) For the normal mission, the propulsion system functions properly with sufficient helium for the mission.

In the light of the conclusions and also the basic conclusions reached in the previous task reports, References 1 and 2, the following recommendations are given.

1. Radiator plates should be used and not louvers. This choice is based upon four items
 - a) The amount of sun shielding provided.
 - b) The degree of off-pointing
 - c) The complexity of the removable louver insulation design
 - d) The expected variation in RTG temperature

The added capability to accommodate mission and/or design variations which is furnished by the louvers is small. This marginal increase might be justified if a smaller shield were to be used. But with the large shield and the mission as now contemplated, the inclusion of louvers adds little to the overall module capability. In addition, when louvers are used, a rather complicated mechanism for removing the insulation on top of the louvers must be provided and this is a decided disadvantage. It is true that the insulation will still have to be removed if a radiator is used, but the mechanism can be substantially less complicated.

It should also be pointed out that if it becomes desirable to exercise greater control over the module temperature, it will also become necessary to consider using louvers which are located near the RTG but which still sense and operate according to the propellant temperature.

2. The standard sun shield (10-foot diameter) should be used. Although a much smaller shield is acceptable and lighter, the larger shield allows considerably more latitude in mission operation. More important, however, is that with a larger shield the thermal control system has a much larger safety factor.
3. To establish that a reliable flight model has actually been designed, it is recommended that a series of module thermal

control tests be made. These tests should have the following objectives:

- o Establish operational capability for the hottest portion of the mission
- o Establish operational capability for the coldest portion of the mission.
- o Establish the simplest manner of "trimming" the craft for a particular mission
- o Establish operational characteristics during groundhold

In conjunction with this last item, it is earnestly suggested that a simple groundhold test be made which utilizes only a single insulated container. This test should investigate thermal gradients in the fluids during groundhold and methods of LN₂ coolant control. If properly run, this small initial test will insure the success of the module thermal test and actually save funds and time.

4. A study program should be initiated which investigates boiling of the propellants in the feed lines upon engine shutdown. Side effects such as vapor venting back into the tanks should be considered. However, this study should not be initiated until the bipropellant valve design is started.
5. The engine thrust structure should be designed to stabilize the bipropellant valve temperature. Ordinarily, the gimbals brackets and the gimbal mounting supports are designed to prevent heat transfer to the structure from the engine during firing. From the standpoint of thermal control of the module, this is of little concern since the entire thrust structure is effectively isolated from the rest of the module by the long, thin boron filament tubes which support the thrust structure. It is impossible to state explicit design guidelines at this time, since they are highly dependent upon the design of the valve and the manner in which it is secured to the engine.

6 Attention must be given to the helium control system. In Sections 4.2 and 5.3, it was pointed out that pressurization, sufficiently in advance of firing to allow thermal equilibrium to be achieved prior to the firing, may conserve helium. However, to accomplish this, the helium valves must be reusable (not squib type) and must be leak tight. This may be difficult to reliably achieve. Obviously, unless the quantity of helium which can be saved is "appreciable" there is no advantage to early pressurization. The quantity of helium which would constitute an "appreciable" amount can be determined only by considering all facets of the module including its cost to development and manufacture. From the calculations made, it would seem that the helium savings would at most, be one to three pounds. With this amount of saving in helium consumption, it is hard to justify going to the effort to save it. But, in some cases, it could be critical. It is therefore recommended that as soon as the mission parameters are firm, a study in the area of helium conservation and required components be made.

7. A study should be initiated which will have the objective of establishing a reliable means of remotely controlling louvers. If such a mechanism existed, louvers could be placed at their most effective position (near the RTG) and still fluid temperatures could control their operation. This would be a tremendous advantage in that very little restriction by thermal control, if any, would be placed on the module design (shield requirements) and module orientation relative to the sun.

REFERENCES

1. TRW Report No. 14051-6004-T0-00, "Summary Report, Task III Space Storable Propellant Module Environmental Control Technology," R. E. DeLand, O. O. Haroldsen, and R. N. Porter, dated 1 June 1970.
2. TRW Report No. 14051-6002-R0-00, "Summary Report, Task II Space Storable Propellant Module Environmental Control Technology," R. E. DeLand, O. O. Haroldsen, and R. N. Porter, dated 1 April 1970
3. Heat Transmission, W. H. McAdams, McGraw-Hill Book Co., 1942.
4. "Stratification in a Pressurized Container with Sidewall Heating," Joseph M. Ruder, ATAA Journal, Vol. 2, No. 1, January 1964
5. Convair, San Diego Report No. 7-9516 Model 7, "Heat Transmission in Liquid Oxygen," H W Wigner and T H Buckley, dated 1955.
6. TRW Report No. 14051-6006-T0-00, "Propulsion Module Thermal Test Plan," O O. Haroldsen, to be issued
7. "Pressurization Systems Design Guide, Volume III," McDonnell Douglas Report No. DAC-60510-F1, Contract NAS 7-548, July 1968
8. "An Analytical Investigation of the Blowdown and Charging Processes in a Single Gas Receiver, Including Effects of Heat Transfer," Technical Report No T-1, Stanford University, Contract NF-065-104, dated 1 October 1955.
9. "Calculation of Real-Gas Effects in the Depressurization of Air Storage Cylinders," Journal of Spacecraft and Rockets, Volume 7, No. 7, T. G. Keith, Jr., dated July 1970
10. "Design Guide for Pressurized Gas Systems, Anonymous, Contract NAS 7-388, IIT Research Institute, dated March 1966.
11. "Determining Pressure Drop in Flexible Metal Hose," Machine Design, C. M. Daniels and J. R. Cleveland, dated 25 November 1965.

APPENDIX A THERMAL COMPUTER MODEL DETAILS

1.0 NODAL ARRANGEMENT

The thermal computer model is a nodal model of the propulsion module shown in Drawing SK 406876 included at the end of this Appendix. A general description of the module is given in Section 2 of this report. A description of all nodes is given in Table A-1.

The computer model is complete from the standpoint of a thermal analysis. It is not complete from a structural viewpoint. For example, representative nodes for the small boron filament struts which support the engine thrust frame from the main platform are not provided. The reason for this is that thermally, they are of no consequence since they are small and have extremely low thermal conductivities. The components located at the base of the oxidizer tank (isolation valve, check valve, filter, etc.) are represented by a node as is the oxidizer line leading to the engine propellant valve. However the comparable equipment for the fuel is not nodally represented since such a deletion does not materially alter the thermal characteristics of the module and the temperature of the "unrepresented" fuel components will be very near the temperatures established for the oxidizer components. The same reasoning was used in justifying the decision to delete nodes representing the helium pressurization line going to the fuel tank.

There are several places where "perfect" insulation is assumed in the model, that is, it is assumed that no insulation exists on the hardware surface and the hardware losses no heat to the surroundings by convection or radiation. This approach is taken in regards to the insulation around nodes 9, and the ends of nodes 14 through 19.

2.0 MATERIAL PROPERTIES

Material properties utilized in the computer model are based on published data where it is available. Where such data is not available, approximations have been made. Table A-2 is a table of the general properties used in the analysis.

3 0 RADIATION VIEW FACTORS

Radiation view factors to a large extent were obtained by readings taken with a form factometer on quarter and third scale models of the module. Where possible, these values were also checked against analytically determined view factors. To assure any errors in these values would be eliminated, a summation of all $F_a A$ (view factor times area) values for each node was made and compared with the area of the node. If these values did not compare favorably, a recheck of all $F_a A$ values was made.

4 0 COMPUTER PROGRAM FORMAT

The format of the computer model is the standard CINDA format. A typical output for the flight analysis computer model is included at the end of this Appendix. A review of this output will reveal that there are seven basic sections of input information.

A Node Data

This consists of a listing of all nodes together with their initial fahrenheit temperatures and their heat capacitances, wc_p . Nodes do not need to be arranged in numerical order. They do need to be arranged in three groups. first, regular nodes, second, zero-capacitance nodes (node which have $wc_p = 0$), third, constant temperature boundary nodes. Zero-capacitance nodes are denoted by a -1 0 in the wc_p column and constant temperature nodes are denoted by a minus node number.

B Conductor Data

This consists of a listing of all conduction and radiation conductors together with the nodes connected by the conductor and the value of the conductor. For conduction, the conductor value is kA/X . For radiation, the conductor is " ϵ " A, and it is denoted as a radiation conductor by a minus in front of the conductor number. Conductors -300 to -303 are the variable radiation conductors of the four louvers. The program obtains the value of these conductors by first looking in Table A-2 or A-1 for a value as a function of the temperature of the first listed node and then multiplying that value by 0.136×10^{-8} . The minus in the listed constant denotes that the first

listed node is the independent variable of the look-up array table and the constant multiplier accounts for the size of the louver, the view factor between the two listed nodes, and the Stefan-Boltzmann constant. The dependent variable of the table lists the varying emissivity of the louvers as a function of tank temperature

C Constants Data

This block of input data includes convergence criteria requirements, damping criteria and constant input heating in Btu/hr.

D Array Data

This block lists all array tables to be used. In the printout there are listed four such arrays. Arrays 1 and 2 are for variable emissivity for the louvers, referred to as A1 and A2 in conductors -300 to -303. Array A1 merely states that the emissivity is 0.72 at -240°F , 0.13 at -215°F and that it varies linearly between these two points. The third array is an array of multiplying factors as a function of time in hours. The fourth array varies the damping factors

E Execution

This block establishes the specific problems to be solved and the order of solution. First, the instruction is given to multiply all (420) radiation conductors starting with -305 by the Stefan-Boltzmann constant. CINDSL then instructs it to make a steady-state run. To do this, it must refer to the VARIABLES 1 and VARIABLES 2 blocks. These blocks are described below.

Upon completion of the steady-state solution, that is the CINDSL instruction, the program proceeds by resetting the several constants as listed and then making a transient analysis as commanded by the instruction CNFRDL. ITEST and LTEST values are required for instruction purposes in the VARIABLES BLOCKS. "LINECT-100" instructs the machine to skip a page on the printout at this point. TIMEND sets the time duration of the transient analysis and OUTPUT specifies the time interval for printout.

F. VARIABLE 1

Upon a command to perform a computational sequence the program scans through the various statements and subroutines listed in VARIABLES 1 and responds according to the information contained there. The first two listed subroutines command the program to use variable damping factors as a function of the reiterations performed (LOOPCT) according to the array A99. The next two Fortran "IF" statements give instructions as to skipping various subroutines according to whether ITEST or LTEST are equal to 1. Thus, if both ITEST and LTEST are NOT equal to 1, as is the case when the CINDSL function is being performed, the first block of 6 STFSEP subroutines will be performed in accomplishing CINDSL but the second set of DIDIWM subroutines will be skipped by jumping to statement 20. The STFSEP (K12,Q55) is an instruction to take the 12th constant in the CONSTANTS DATA, 88., and apply it as a constant heat addition to node 55. Note that all 17 of the constants are not used. It is through this manner that constant solar heating of any node is simulated.

If ITEST has been set to 1 0 in the EXECUTION block, the program will skip the STFSEP subroutines but will pick up the DIDIWM subroutines. This occurred in the example case after computing the steady-state CINDSL case in preparation for computing the transient CNFRDL case. In this particular transient case, the subroutine DIDIWM (TIMEN, A3, K1, Q24) instructs to use the actual time as the independent variable in array 3, multiply the first constant in the CONSTANTS block by the corresponding dependent variable of array 3 and use the result as a varying heat input to Node 24.

It should be observed that by utilizing the EXECUTION block and the VARIABLES 1 block, it is possible to compute several steady-state and/or transient cases successively, each having a different input. However, unless other provisions are made, the node temperatures obtained at the end of any particular case are used as the initial node temperatures for the next case.

G. Output Calls

This block is used to specify the printed output. In the example, temperatures are printed (TPRINT) only once for the CINDSL. However, by use of the several "IF" statements, the JTEST function, and the KTEST function, the program is made to print out the temperatures at the time specified by OUTPUT = X.

There are many other subroutines which may be called in order to accomplish a desired result. To fully utilize the capacity of the CINDA program, the reader must consult a CINDA manual.

A sensitivity analysis was made to determine which nodes and associated conductors are controlling. Table A-3 lists these major conductors. The nodes associated with each listed conductor are of necessity the controlling nodes. Table A-3 also lists the basis for the values of each conductor.

Table 1 Nodal Arrangement

<u>NODE</u>	<u>DESCRIPTION</u>
1	B ₂ H ₆ Tank -X
2	B ₂ H ₆ Tank Center
3	B ₂ H ₆ Tank +X
4	OF ₂ Tank -X
5	OF ₂ Tank Center
6	OF ₂ Tank +X
7	B ₂ H ₆ Top Fitting
8	OF ₂ Top Fitting
(9)	Spacecraft Support (5)
10	Bottom Vertical Strut -X, -Y
11	
12	
13	
14	B ₂ H ₆ Side Strut
15	B ₂ H ₆ Center Strut
16	OF ₂ Center Strut
17	OF ₂ Side Strut
18	Center, Vertical Strut -X
19	Center, Vertical Strut +X
20	Top, Diagonal Strut +X
21	Top, Vertical Strut +X, +Y
22	Upper, Diagonal Strut +X
23	Upper, Vertical Strut +X, +Y

Table 1 (Continued)

<u>NODE</u>	<u>DESCRIPTION</u>
24	Center, Diagonal Strut +X
25	Center, Vertical Strut +X, +Y
26	Top, Vertical Strut +X, -Y
27	Top, Vertical Strut -X, -Y
28	Top, Diagonal Strut -X
29	Upper, Vertical Strut -X, -Y
30	Upper, Diagonal Strut -X
31	Center, Vertical Strut -X, -Y
32	Center, Diagonal Strut -X
33	Center, Vertical Strut -X, +Y
34	Lower, Diagonal Strut -X
35	Lower, Vertical Strut -X, +Y
36	Bottom, Diagonal Strut -X
37	Bottom, Vertical Strut -X, +Y
38	Frame -X, +Y
39	Bottom, Vertical Strut +X, -Y
40	Bottom, Diagonal Strut +X
41	Frame, +X, -Y
42	Bottom, Vertical Strut +X, +Y
43	Frame +X, +Y
44	Frame -X, -Y

Table 1 (Continued)

<u>NODE</u>	<u>DESCRIPTION</u>
45	Frame -X
46	Frame +X
47	Frame +Y
48	Frame -Y
49	Helium Control Panel
50	OF ₂ Control Panel
51	B ₂ H ₆ Control Panel
52	Insulation Exterior, Node 1
53	Insulation Exterior, Node 2, -Y
54	Insulation Exterior, Node 2, +Y
55	Insulation Exterior, Node 3
56	Insulation Exterior, Node 4
57	Insulation Exterior, Node 5, -Y
58	Insulation Exterior, Node 5, +Y
59	Insulation Exterior, Node 6
60	Insulation Exterior, Helium Panel
61	Mating Foot +X, +Y
62	Insulation Exterior, B ₂ H ₆ Panel
63	Mating Foot +X
64	OF ₂ Bottom Fitting Insulation
65	Insulation Exterior, OF ₂ Panel
66	Louver B ₂ H ₆ +X

Table 1 (Continued)

<u>NODE</u>	<u>DESCRIPTION</u>
67	Louver B_2H_6 -X
68	Louver OF_2 +X
69	Louver OF_2 -X
70	Mylar Insulation Interior, OF_2 Panel
71	Mylar Insulation Exterior, OF_2 Panel
72	Mylar Insulation Interior, B_2H_6 Panel
73	Mylar Insulation Exterior, B_2H_6 Panel
74	Mylar Insulation Interior, Helium Panel
75	Mylar Insulation Exterior, Helium Panel
76	Propellant Valves
77	Propellant Valves, Insulation Interior
78	Propellant Valves, Insulation Exterior
79	OF_2 Feed Line, Upper
80	OF_2 Feed Line, Middle
81	OF_2 Feed Line, Lower
82	Bipropellant Valve
83	OF_2 Feed Line Insulation, Lower
84	OF_2 Feed Line Insulation, Middle
85	OF_2 Feed Line Insulation, Upper
86	OF_2 Bottom Fitting
87	B_2H_6 Bottom Fitting
88	Mating Foot +X, -Y
89	Mating Foot -Y
90	Mating Foot -X, -Y

Table 1 (Continued)

<u>NODE</u>	<u>DESCRIPTION</u>
91	Mating Foot -X
92	Mating Foot -X, +Y
93	Mating Foot +Y
94	Aluminum Beam
95	Aluminum Beam
96	Aluminum Beam
97	Aluminum Beam
98	Aluminum Beam
99	Mating Foot Insulation, Node 61
100	Beam Insulation, Node 94
101	Beam Insulation, Node 95
102	Beam Insulation, Node 96
103	
104	Beam Insulation, Node 97
105	Beam Insulation, Node 98
106	Mating Foot Insulation, Node 88
107	B ₂ H ₆ Bottom Fitting Insulation
108	Cross Beam +X
109	Cross Beam -X
110	
111	
112	Helium Tank, Upper
113	Helium Tank, Center

Table 1 (Continued)

<u>NODE</u>	<u>DESCRIPTION</u>
114	Helium Tank, Lower
115	Helium Tank Insulation, Upper
116	Helium Tank Insulation, Center
117	Helium Tank Insulation, Lower
118	Helium Tank Lower Fitting
119	Thrust Frame +X
120	Thrust Frame -X
121	Upper Thrust Ring
122	Thrust Cylinder
123	Lower Thrust Ring
124	Combustion Chamber
125	Thrust Cone
126	Engine Purge Line, Upper
127	Engine Purge Line, Lower
128	Actuator, +Y
129	Actuator, +X
130	OF ₂ Vent Line, Upper
131	OF ₂ Vent Line, Middle
132	OF ₂ Vent Line, Lower
133	OF ₂ Vent Line Insulation, Upper
134	OF ₂ Vent Line Insulation, Center
135	OF ₂ Vent Line Insulation, Lower
136	Engine Purge Line Insulation, Upper, Node 126

Table 1 (Continued)

137	Engine Purge Line Insulation, Lower, Node 127
138	Engine Valve Line, Upper
139	Engine Valve Line, Lower
140	Engine Valve Line Insulation, Upper, Node 138
141	Engine Valve Line Insulation, Lower, Node 139
142	Shield -Y
143	Shield -X
144	Shield +Y
145	Shield +X
146	Aft Shield
147	
148	
149	
150	
151	
152	
153	Spacecraft Insulation Exterior -Y
154	Spacecraft Insulation Exterior -X
155	Spacecraft Insulation Exterior +Y
156	Spacecraft Insulation Exterior +X
157	RTG
158	Space
159	Helium Line, Upper

Table 1 (Continued)

<u>NODE</u>	<u>DESCRIPTION</u>
160	Helium Line, Middle
161	Helium Line, Bottom
162	Helium Line Insulation, Upper
163	Helium Line Insulation, Middle
164	Helium Line Insulation, Lower
165	
166	Insulation Exterior, Top, Node 1
167	Insulation Exterior, Top, Node 2
168	Insulation Exterior, Top, Node 3
169	Insulation Exterior, Bottom, Node 1
170	Insulation Exterior, Bottom, Node 2
171	Insulation Exterior, Bottom, Node 3
172	Insulation Exterior, Top, Node 4
173	Insulation Exterior, Top, Node 5
174	Insulation Exterior, Top, Node 6
175	Insulation Exterior, Bottom, Node 4
176	Insulation Exterior, Bottom, Node 5
177	Insulation Exterior, Bottom, Node 6
178	
179	
180	LN ₂ Coolant
181	B ₂ H ₆ Coolant Coil

Table 1 (Continued)

<u>NODE</u>	<u>DESCRIPTION</u>
182	OF ₂ Coolant Coil
183	He Coolant Coil
184	Ambient Air
185	Air, OF ₂ Control Panel Box
186	Air, B ₂ H ₆ Control Panel Box
187	Air, He Control Panel Box
188	Air, Propellant Valve Box

NOTES

1. () Denotes constant temperature node for flight thermal analysis
2. [] Denotes constant temperature node for groundhold analysis.
- 3 Delete Nodes 66, 67, 68, 69 and all associated resistances for groundhold analysis.
- 4 Assume RTG in stowed position for groundhold analysis
5. Background radiation changed from 0°R for flight analysis to 525°R for groundhold analysis

Table A-2 Material Properties

Material	$k \frac{\text{Btu}}{\text{ft}^2 \cdot \text{ft} \cdot ^\circ\text{F}}$	$C_p \frac{\text{Btu}}{\text{lb} \cdot ^\circ\text{F}}$	Solar Adsorbitivity	Emissivity
Boron Filament (Parallel to Fiber)	1.17	0.28	0.80	0.80
Foam Insulation	0.1*	0.16	0.80	0.90
Silvered Teflon	-	-	0.20	0.90
Second Surface Mirrors	-	-	0.10	0.80
Aluminized Mylar Blanket	0.01	-	0.24	0.80
Titanium	20.00	0.095	0.30	0.10
Columbium	35.00	0.06	0.40	0.30
Aluminum	90.00	0.20	0.40	0.05
Stainless Steel	0.10	0.10	-	-
Fiberglass	0.12	0.15	0.80	0.80
LN ₂	0.08	0.49	-	-
Helium	0.07	1.30	-	-
B ₂ H ₆	0.72	0.65	-	-
OF ₂	0.175	0.35	-	-
RTG	-	-	-	0.90

* There is a good indication that this value may be as small as 0.02.

Table A-3 Controlling Conductors and Nodes

<u>Conductor No.</u>	<u>Node-to-Node</u>	<u>Conductor Value, kA/1</u>
1	1-2	75 x 11.3/.8
2	1-52	0.00625 x 5.76/0.0625
4	2-3	same as No. 1
6	2-53	0.00625 x 3/0.0625
7	2-54	same as No. 6
9	3-55	0.00625 x 6.1/0.0625
10	4-5	0.175 x 11.3/.75
11	4-56	0.00625 x 4.75/0.0625
13	5-6	same as No. 10
15	5-57	same as No. 6
16	5-58	same as No. 6
20	6-59	same as No. 2
116	94-95	90 x 0.0037/0.75
118	95-96	same as No. 116
120	96-97	same as No. 116
124	96-112	90 x 0.016/0.125
126	97-98	90 x 0.0037/0.7
132	112-115	0.00625 x 8.05/0.0625
134	113-116	0.00625 x 3.1/0.0625
136	114-117	same as No. 132

<u>Conductor No.</u>	<u>Node-to-Node</u>	<u>Radiation Conductor, (μA) $\epsilon_1 \epsilon_2$</u>
-455	52-158	4.92 x 0.9 x 1
-460	53-158	3.84 x 0.9 x 1.
-471	54-158	2.44 x 0.9 x 1
-483	55-157	0.062 x 0.9 x 0.9
-484	55-158	4.90 x 0.9 x 1.
-494	56-158	4.0 x 0.9 x 1.
-504	57-158	1.8 x 0.9 x 1.
-509	58-158	4.13 x 0.9 x 1.

Table A-3 (Continued)

<u>Conductor No.</u>	<u>Node-to-Node</u>	<u>Radiation Conductor, (A)$\epsilon_1\epsilon_2$</u>
-522	59-157	0.059 x 0.9 x 0.9
-523	59-158	3.94 x 0.9 x 1
-622	115-158	1.14 x 0.9 x 1
-630	116-157	0.0303 x 0.9 x 0.9
-631	116-158	3.22 x 0.9 x 1
-637	117-157	0.015 x 0.9 x 0.9
-638	117-158	0.5 x 0.9 x 1
-665	125-158	4.56 x 0.3 x 1. 2.18 x 0.8 x 1
-697	166-158	1.45 x 0.9 x 1
-707	168-157	0.0086 x 0.9 x 0.9
-708	168-158	1.29 x 0.9 x 1.
-722	174-157	0.0049 x 0.9 x 0.9

Computer Format Input

BCD 3THERMAL LPCS
 BCD 9TASK 4 STcADY NEAR EARTH
 END
 BCD 3NODE DATA

Node	→	1,	-210°,	147.	
		2,	-210°,	175.	
Initial		3,	-210°,	147.	
Temperature	→	4,	-210°,	243.	← Heat
		5,	-210°,	260.	Capacitance
		6,	-210°,	243.	
		10,	-250°,	.1	
		14,	-200°,	.034	
		16,	-200°,	.036	
		17,	-230°,	.053	
		18,	-300°,	.56	
		19,	-100°,	.50	
		20,	10°,	.09	
		21,	10°,	.07	
		22,	-200°,	.12	
		23,	-230°,	.001	
		24,	-50°,	.435	
		25,	-50°,	.296	
		26,	-50°,	.14	
		27,	-10°,	.00	
		28,	-20°,	.00	
		29,	-200°,	.001	
		30,	-200°,	.078	
		31,	-250°,	.308	
		32,	-250°,	.126	
		33,	-250°,	.105	
		34,	-200°,	.132	
		35,	-200°,	.059	
		36,	-250°,	.00	
		38,	-250°,	.074	
		39,	-50°,	.11	
		40,	-50°,	.11	
		41,	-50°,	.077	
		42,	-50°,	.09	
		43,	1°,	.055	
		44,	-100°,	.065	
		45,	-100°,	.076	
		46,	1°,	.102	
		47,	-200°,	.086	
		48,	-200°,	.065	
		49,	-200°,	2.75	
		50,	-200°,	.44	
		51,	-200°,	.44	
		52,	-300°,	.19	
		53,	-200°,	.092	

Computer Input

54,	-200°,	.132	
55,	-100°,	.246	
56,	-300°,	.16	
57,	-200°,	.132	
58,	-200°,	.092	
59,	-100°,	.142	
60,	-200°,	.046	
66,	-200°,	.1	
67,	-200°,	.1	
68,	-200°,	.1	
69,	-200°,	.1	
76,	-200°,	1.3	
82,	-200°,	1.5	
94,	-200°,	.09	
95,	-200°,	.09	
97,	-200°,	.09	
98,	-200°,	.09	
112,	-200°,	18.6	
113,	-200°,	26.2	
114,	-200°,	18.6	
115,	-200°,	.16	
116,	-200°,	.126	
117,	-200°,	.16	
119,	-200°,	.038	
120,	-200°,	.038	
121,	-200°,	.171	
123,	-300°,	.3	
124,	-200°,	2.08	
125,	-200°,	.96	
128,	-300°,	.33	
129,	-300°,	.33	
142,	-300°,	.9	
143,	-300°,	.9	
144,	-300°,	.9	
145,	-300°,	.9	
169,	-200°,	.032	
170,	-200°,	.019	
171,	-200°,	.032	
172,	-200°,	.032	
173,	-200°,	.019	
174,	-200°,	.032	
175,	-200°,	.032	
176,	-200°,	.019	
177,	-200°,	.032	
7,	-210°,	-1.	← Zero
8,	-210°,	-1.	Capacitance
15,	-200°,	-1.	
37,	-200°,	-1.	
61,	-300°,	-1.	

Computer Input

62,	-200°,	-1.
63,	-300°,	-1.
64,	-200°,	-1.
65,	-200°,	-1.
70,	-200°,	-1.
71,	-60°,	-1.
72,	-200°,	-1.
73,	-300°,	-1.
74,	-200°,	-1.
75,	-300°,	-1.
77,	-200°,	-1.
78,	-200°,	-1.
79,	-200°,	-1.
80,	-200°,	-1.
81,	-200°,	-1.
83,	-200°,	-1.
84,	-200°,	-1.
85,	-200°,	-1.
86,	-200°,	-1.
87,	-200°,	-1.
88,	-300°,	-1.
89,	-300°,	-1.
90,	-300°,	-1.
91,	-300°,	-1.
92,	-300°,	-1.
93,	-300°,	-1.
96,	-200°,	-1.
99,	-300°,	-1.
100,	-200°,	-1.
101,	-200°,	-1.
102,	-200°,	-1.
104,	-200°,	-1.
105,	-200°,	-1.
106,	-200°,	-1.
107,	-200°,	-1.
108,	-200°,	-1.
109,	-200°,	-1.
122,	-200°,	-1.
126,	-200°,	-1.
127,	-200°,	-1.
130,	-200°,	-1.
131,	-200°,	-1.
132,	-200°,	-1.
133,	-200°,	-1.
134,	-200°,	-1.
135,	-200°,	-1.
136,	-200°,	-1.
137,	-200°,	-1.
138,	-200°,	-1.
139,	-200°,	-1.

Computer Input

	140,	-200°,	-1.
	141,	-200°,	-1.
	146,	-300°,	-1.
	153,	-200°,	-1.
	154,	-200°,	-1.
	155,	-200°,	-1.
	156,	-200°,	-1.
	159,	-200°,	-1.
	160,	-200°,	-1.
	161,	-200°,	-1.
	162,	-200°,	-1.
	163,	-200°,	-1.
	164,	-200°,	-1.
	166,	1°,	-1.
	167,	1°,	-1.
	168,	-30°,	-1.
Constant	-9,	65°,	3.0
Temperature	→ -157,	500°,	0.0
Node	-158,	-460°,	0.0

Conductor Number	3CONDUCTOR DATA			Conductance
	1,	1,	2,	10.15
	2,	1,	52,	.576
	3,	1,	62,	.1
	4,	2,	3,	10.15
	5,	2,	7,	64.8
	6,	2,	53,	.304
	7,	2,	54,	.440
	8,	2,	87,	81.5
	9,	3,	55,	.610
	10,	4,	5,	3.0
	11,	4,	56,	.475
	12,	4,	60,	.275
	13,	5,	6,	3.0
	14,	5,	8,	64.8
	15,	5,	57,	.440
	16,	5,	58,	.307
	17,	5,	76,	.08
	18,	5,	86,	81.5
	19,	5,	130,	.0033
	20,	6,	59,	.555
	21,	6,	65,	.1

→
←
←

Computer Input

22,	6,	131,	•0033
23,	7,	14,	•0005
24,	7,	14,	•0005
25,	8,	16,	•0005
26,	8,	17,	•0005
27,	8,	130,	•001
28,	9,	14,	•0005
29,	9,	15,	•0005
30,	9,	16,	•0006
31,	9,	17,	•0009
32,	9,	18,	•0009
33,	9,	19,	•0009
34,	9,	20,	•064
35,	9,	21,	•064
36,	9,	26,	•064
37,	9,	27,	•064
38,	9,	28,	•064
39,	9,	33,	•0009
40,	9,	153,	•056
41,	9,	154,	•056
42,	9,	155,	•056
43,	9,	156,	•056
44,	10,	31,	•004
45,	10,	44,	•064
46,	18,	45,	•0009
47,	19,	46,	•0009
48,	20,	22,	•0036
49,	21,	23,	•003
50,	22,	24,	•001
51,	22,	50,	•004
52,	23,	25,	•001
53,	23,	50,	•004
54,	24,	40,	•001
55,	25,	42,	•001
56,	27,	29,	•003
57,	28,	30,	•0036
58,	29,	31,	•001
59,	29,	51,	•004
60,	30,	32,	•0017
61,	30,	51,	•004
62,	32,	34,	•0017
63,	33,	35,	•0004
64,	34,	36,	•002
65,	34,	49,	•006
66,	35,	37,	•0011
67,	35,	49,	•006
68,	36,	38,	•064
69,	37,	38,	•064
70,	38,	45,	•013
71,	38,	47,	•019

Computer Input

72,	38,	92,	•029
73,	39,	41,	•064
74,	40,	41,	•064
75,	41,	46,	•023
76,	41,	48,	•012
77,	41,	88,	•029
78,	42,	43,	•064
79,	43,	46,	•023
80,	43,	47,	•019
81,	43,	61,	•029
82,	44,	45,	•013
83,	44,	48,	•012
84,	44,	90,	•029
85,	45,	91,	•029
86,	46,	63,	•029
87,	47,	86,	•318
88,	47,	93,	•029
89,	47,	94,	•45
90,	47,	99,	•006
91,	48,	87,	•318
92,	48,	89,	•029
93,	48,	98,	•45
94,	48,	106,	•006
95,	49,	126,	•0006
96,	49,	138,	•0006
97,	49,	159,	•0006
98,	50,	132,	•001
99,	64,	86,	•0033
100,	70,	71,	•005
101,	72,	73,	•005
102,	74,	75,	•01
103,	76,	79,	•025
104,	77,	78,	•167
105,	79,	80,	•025
106,	79,	85,	•015
107,	80,	81,	•025
108,	80,	84,	•0002
109,	80,	113,	•0025
110,	81,	82,	•025
111,	81,	83,	•015
112,	82,	124,	2•0
113,	82,	127,	•001
114,	82,	139,	•001
115,	87,	107,	•0033
116,	94,	95,	•45
117,	94,	100,	•008
118,	95,	96,	•45
119,	95,	101,	•008
120,	96,	97,	•45
121,	96,	102,	•008

Computer Input

122,	96,	108,	.02
123,	96,	109,	.02
124,	96,	112,	11.5
125,	96,	161,	.001
126,	97,	98,	.48
127,	97,	104,	.008
128,	98,	105,	.008
129,	108,	46,	.02
130,	109,	45,	.02
131,	112,	113,	.84
132,	112,	115,	.536
133,	113,	114,	.84
134,	113,	116,	.207
136,	114,	117,	.53
137,	114,	119,	.0001
138,	114,	120,	.0001
139,	119,	121,	.039
140,	120,---	121,	.039---
141,	121,	122,	.26
142,	121,	128,	.043
144,	121,	129,	.043
145,	122,	123,	.26
146,	123,	124,	.026
147,	124,---	125,	.2---
148,	124,	128,	.035
149,	124,	129,	.035
150,	126,	127,	.001
151,	126,--	136,	.0006
152,	127,	137,	.0006
153,	130,---	131,	.001---
154,	130,	133,	.00017
155,	131,	132,	.001
156,	131,	134,	.00017
157,	132,---	135,	.0006-
158,	138,	139,	.001
159,	138,--	140,	.0006--
160,	139,	141,	.0006
161,	159,	160,	.001
162,	159,	162,	.0006
163,	160,	161,	.001
164,	160,	163,	.0006
165,	161,---	164,	.0006---
166,	166,	1,	.128
167,	167,	2,	.067
168,	168,	3,	.144
169,	169,	1,	.128
170,	170,	2,	.067
171,	171,	3,	.145-
172,	172,	4,	.119
173,	173,	5,	.067

Computer Input

	174,	174,	6,	.140	
	175,	175,	4,	.119	
Radiation	176,	176,	5,	.067	Array Table
Conductor	177,	177,	6,	.140	
CGS	-300,	1,	67,	A2,	--.395E-8
CGS	-301,	3,	66,	A1,	--.316E-8
CGS	-302,	4,	69,	A2,	--.316E-8
CGS	-303,	6,	68,	A1,	--.316E-8
	-305,	14,	168,	.022	
	-306,	14,	153,	.036	Multiplier
	-307,	14,	156,	.005	
	-308,	14,	157,	.00025	
	-309,	14,	158,	.051	
	-310,	15,	166,	.0026	
	-311,	15,	54,	.0095	
	-312,	15,	168,	.0026	
	-313,	15,	57,	.0052	
	-314,	15,	153,	.027	
	-315,	15,	154,	.0031	
	-316,	15,	156,	.0031	
	-317,	15,	157,	.0003	
	-318,	15,	158,	.032	
	-319,	16,	54,	.0052	
	-320,	16,	172,	.0026	
	-321,	16,	57,	.0095	
	-322,	16,	174,	.0026	
	-323,	16,	154,	.0031	
	-324,	16,	155,	.027	
	-325,	16,	156,	.0031	
	-326,	16,	157,	.0003	
	-327,	16,	158,	.032	
	-328,	17,	172,	.0275	
	-329,	17,	173,	.0119	
	-330,	17,	154,	.037	
	-331,	17,	155,	.037	
	-332,	17,	158,	.084	
	-333,	18,	19,	.172	
	-334,	18,	52,	.202	
	-335,	18,	54,	.121	
	-336,	18,	56,	.202	
	-337,	18,	57,	.121	
	-338,	18,	115,	.081	
	-339,	18,	154,	.115	
	-340,	18,	158,	.08	
	-341,	19,	54,	.121	
	-342,	19,	55,	.201	
	-343,	19,	57,	.121	
	-344,	19,	59,	.202	
	-345,	19,	115,	.081	

Computer Input

-346,	19,	156,	.115
-347,	19,	157,	.0125
-348,	19,	158,	.94
-349,	22,	23,	.0027
-350,	22,	50,	.013
-351,	22,	65,	.019
-352,	22,	70,	.0012
-353,	23,	50,	.013
-354,	23,	65,	.019
-355,	23,	70,	.0012
-356,	24,	55,	.40
-357,	24,	59,	.266
-358,	24,	66,	.153
-359,	24,	68,	.153
-360,	24,	115,	.108
-361,	24,	156,	.071
-362,	24,	157,	.0085
-363,	24,	158,	1.6
-364,	25,	59,	.57
-365,	25,	68,	.1
-366,	25,	157,	.0055
-367,	25,	158,	1.2
-368,	29,	30,	.0027
-369,	29,	51,	.013
-370,	29,	62,	.019
-371,	29,	72,	.0012
-372,	30,	51,	.013
-373,	30,	62,	.019
-374,	30,	72,	.0012
-375,	31,	52,	.57
-376,	31,	67,	.1
-377,	31,	158,	1.21
-378,	32,	52,	.229
-379,	32,	56,	.222
-380,	32,	67,	.064
-381,	32,	69,	.064
-382,	32,	154,	.038
-383,	32,	158,	.346
-384,	33,	56,	.57
-385,	33,	69,	.1
-386,	33,	158,	1.21
-387,	34,	35,	.0042
-388,	34,	49,	.035
-389,	34,	60,	.050
-390,	34,	74,	.015
-391,	35,	49,	.023
-392,	35,	60,	.028
-393,	35,	74,	.008

Computer Input

-394,	36,	37,	.023
-395,	36,	38,	.004
-396,	36,	175,	.062
-397,	36,	158,	.216
-398,	37,	38,	.003
-399,	37,	175,	.045
-400,	37,	158,	.144
-401,	38,	175,	.036
-402,	38,	115,	.023
-403,	38,	144,	.016
-404,	38,	158,	.11
-405,	41,	171,	.036
-406,	41,	115,	.023
-407,	41,	142,	.016
-408,	41,	157,	.001
-409,	41,	158,	.11
-410,	43,	177,	.036
-411,	43,	115,	.023
-412,	43, 144,	.016	
-413,	43,	157,	.001
-414,	43,	158,	.11
-415,	44,	169,	.036
-416,	44,	115,	.023
-417,	44,	142,	.016
-418,	44,	158,	.17
-419,	45,	169,	.009
-420,	45,	175,	.009
-421,	45,	115,	.011
-422,	45,	143,	.016
-423,	45,	158,	.05
-424,	46,	171,	.009
-425,	46,	177,	.009
-426,	46,	115,	.011
-427,	46,	145,	.016
-428,	46,	157,	.001
-429,	46,	158,	.05
-430,	47,	176,	.018
-431,	47,	115,	.011
-432,	47,	144,	.016
-433,	47,	158,	.05
-434,	48,	170,	.018
-435,	48,	115,	.011
-436,	48,	142,	.016
-437,	48,	158,	.05
-438,	49,	60,	.49
-439,	49,	74,	.07
-440,	50,	65,	.155
-441,	50,	70,	.003
-442,	51,	62,	.155

Computer Input

-443,	51,	72,	.003
-444,	52,	56,	.955
-445,	52,	57,	.332
-446,	169,	104,	.021
-447,	169,	105,	.021
-448,	169,	109,	.008
-449,	52,	115,	.10
-450,	52,	142,	.076
-451,	52,	143,	.293
-452,	52,	153,	.076
-453,	52,	154,	.044
-454,	166,	155,	.014
-455,	52,	158,	4.43
-456,	53,	142,	.092
-457,	53,	143,	.074
-458,	53,	145,	.074
-459,	167,	153,	.036
-460,	53,	158,	3.46
-461,	54,	56,	.33
-462,	54,	57,	1.62
-463,	54,	59,	.33
-464,	54,	104,	.036
-465,	54,	105,	.036
-466,	54,	108,	.005
-467,	54,	109,	.005
-468,	54,	115,	.46
-469,	54,	153,	.18
-470,	54,	155,	.007
-471,	54,	158,	2.20
-472,	55,	57,	.33
-473,	55,	59,	.955
-474,	171,	104,	.021
-475,	171,	105,	.021
-476,	171,	109,	.021
-477,	55,	115,	.10
-478,	55,	142,	.076
-479,	55,	145,	.293
-480,	55,	153,	.076
-481,	55,	156,	.044
-482,	168,	155,	.014
-483,	55,	157,	.050
-484,	55,	158,	4.42
-485,	175,	100,	.021
-486,	175,	101,	.021
-487,	175,	108,	.021
-488,	56,	115,	.044
-489,	56,	144,	.076
-490,	56,	143,	.293
-491,	172,	153,	.021
-492,	56,	154,	.09

Computer Input

-493,	56,	155,	.05
-494,	56,	158,	3.60
-495,	57,	100,	.036
-496,	57,	101,	.035
-497,	57,	108,	.005
-498,	57,	109,	.005
-499,	57,	115,	.46
-500,	57,	153,	.014
-501,	57,	154,	.115
-502,	57,	155,	.44
-503,	57,	156,	.115
-504,	57,	158,	1.62
-505,	58,	143,	.144
-506,	58,	144,	.792
-507,	58,	145,	.144
-508,	58,	155,	.54
-509,	58,	158,	3.72
-510,	177,	100,	.021
-511,	177,	101,	.021
-512,	177,	108,	.021
-513,	59,	115,	.044
-514,	174,	133,	.076
-515,	174,	134,	.076
-516,	159,	135,	.076
-517,	59,	144,	.076
-518,	59,	145,	.293
-519,	174,	153,	.021
-520,	59,	155,	.052
-521,	59,	156,	.09
-522,	59,	157,	.040
-523,	59,	158,	3.55
-524,	60,	74,	.05
-525,	61,	116,	.002
-526,	61,	125,	.00013
-527,	61,	146,	.0014
-528,	61,	158,	.012
-529,	62,	72,	.02
-530,	63,	116,	.002
-531,	63,	146,	.0014
-532,	63,	158,	.012
-533,	65,	70,	.02
-534,	66,	156,	.077
-535,	66,	157,	.018
-536,	66,	158,	1.27
-537,	67,	154,	.077
-538,	67,	158,	1.70
-539,	68,	156,	.077
-540,	68,	157,	.018
-541,	68,	158,	1.15
-542,	69,	154,	.077

Computer Input

-543,	69,	158,	1.22
-544,	71,	157,	.0043
-545,	71,	158,	.8
-546,	73,	158,	.8
-547,	75,	158,	2.4
-548,	76,	77,	.099
-549,	78,	115,	.29
-550,	78,	158,	1.08
-551,	82,	117,	.027
-552,	82,	121,	.003
-553,	82,	122,	.0016
-554,	82,	123,	.0008
-555,	82,	158,	.008
-556,	83,	117,	.011
-557,	83,	158,	.012
-558,	84,	157,	.0011
-559,	84,	158,	.05
-560,	85,	115,	.014
-561,	85,	158,	.008
-562,	88,	116,	.002
-563,	88,	146,	.0014
-564,	88,	158,	.012
-565,	89,	116,	.002
-566,	89,	146,	.0014
-567,	89,	158,	.012
-568,	90,	116,	.002
-569,	90,	146,	.0014
-570,	90,	158,	.012
-571,	91,	116,	.002
-572,	91,	146,	.0014
-573,	91,	158,	.012
-574,	92,	116,	.002
-575,	92,	125,	.00013
-576,	92,	146,	.0014
-577,	92,	158,	.012
-578,	93,	116,	.002
-579,	93,	146,	.0014
-580,	93,	158,	.012
-581,	99,	144,	.093
-582,	99,	158,	.144
-583,	100,	115,	.123
-584,	100,	143,	.064
-585,	100,	144,	.051
-586,	100,	145,	.064
-587,	100,	158,	.08
-588,	101,	115,	.123
-589,	101,	143,	.092
-590,	101,	145,	.092
-591,	101,	137,	.003

Computer Input

-592,	101,	158,	.08
-593,	102,	115,	.10
-594,	102,	143,	.071
-595,	102,	145,	.071
-596,	102,	157,	.001
-597,	102,	158,	.064
-598,	104,	115,	.123
-599,	104,	143,	.092
-600,	104,	145,	.092
-601,	104,	157,	.0015
-602,	104,	158,	.08
-603,	105,	115,	.123
-604,	105,	142,	.051
-605,	105,	143,	.064
-606,	105,	145,	.064
-607,	105,	158,	.08
-608,	106,	142,	.093
-609,	106,	158,	.144
-610,	108,	142,	.048
-611,	108,	144,	.048
-612,	108,	158,	.03
-613,	109,	142,	.048
-614,	109,	144,	.048
-615,	109,	158,	.03
-616,	115,	136,	.072
-617,	115,	140,	.072
-618,	115,	142,	.21
-619,	115,	143,	.21
-620,	115,	144,	.21
-621,	115,	145,	.21
-622,	115,	158,	1.03
-623,	115,	162,	0.58
-624,	115,	163,	.079
-625,	115,	164,	.108
-626,	116,	142,	.505
-627,	116,	143,	.505
-628,	116,	144,	.505
-629,	116,	145,	.505
-630,	116,	157,	.0245
-631,	116,	158,	2.9
-632,	117,	119,	.011
-633,	117,	120,	.011
-634,	117,	137,	.072
-635,	117,	141,	.072
-636,	117,	146,	5.15
-637,	117,	157,	.012
-638,	117,	158,	.45
-639,	119,	121,	.0003
-640,	119,	146,	.0096
-641,	120,	121,	.0003
-642,	120,	146,	.0096

Computer Input

-643,	121,	128,	.00014
-644,	121,	129,	.00014
-645,	121,	146,	.0011
-646,	121,	158,	.011
-647,	122,	123,	.0006
-648,	122,	128,	.0003
-649,	122,	129,	.0003
-650,	122,	146,	.001
-651,	122,	158,	.02
-652,	123,	124,	.0044
-653,	123,	125,	.0017
-654,	123,	128,	.00014
-655,	123,	129,	.00014
-656,	123,	146,	.0004
-657,	123,	158,	.041
-658,	124,	125,	.0012
-659,	124,	158,	.04
-660,	125,	128,	.00003
-661,	125,	129,	.00003
-662,	125,	144,	.0024
-663,	125,	146,	.084
-664,	125,	157,	.008
-665,	125,	158,	3.11
-666,	128,	146,	.002
-667,	128,	158,	.004
-668,	129,	146,	.002
-669,	129,	158,	.004
-670,	133,	155,	.04
-671,	133,	158,	.034
-672,	134,	155,	.013
-673,	134,	158,	.067
-674,	135,	155,	.013
-675,	135,	158,	.067
-676,	136,	158,	.08
-677,	137,	158,	.08
-678,	140,	158,	.08
-679,	141,	158,	.08
-680,	142,	158,	1.28
-681,	144,	158,	1.28
-682,	146,	158,	7.35
-683,	153,	158,	4.6
-684,	154,	158,	3.92
-685,	155,	158,	3.54
-686,	156,	157,	.0025
-687,	156,	158,	3.94
-688,	162,	158,	.096
-689,	163,	158,	.072
-690,	164,	158,	.04
-691,	169,	115,	.24

Computer Input

-692,	169,	142,	.19
-693,	169,	143,	.29
-694,	166,	153,	.22
-695,	166,	154,	.28
-696,	169,	158,	.51
-697,	166,	158,	1.30
-698,	170,	142,	.70
-699,	170,	143,	.07
-700,	170,	145,	.07
-701,	167,	158,	.90
-702,	171,	115,	.24
-703,	171,	142,	.19
-704,	171,	145,	.29
-705,	168,	153,	.22
-706,	168,	154,	.28
-707,	168,	157,	.007
-708,	168,	158,	1.16
-709,	171,	158,	.51
-710,	175,	115,	.28
-711,	175,	144,	.19
-712,	175,	143,	.29
-713,	172,	154,	.50
-714,	172,	155,	.35
-715,	172,	158,	.70
-716,	175,	158,	.51
-717,	177,	115,	.28
-718,	177,	144,	.19
-719,	177,	145,	.29
-720,	174,	155,	.03
-721,	174,	156,	.50
-722,	174,	157,	.0040
-723,	174,	158,	.70
-724,	177,	158,	.51

END

Computer Program

FOLDOUT FRAME

```

BCD 3CONSTANTS DATA
  NLOOP,1000
  ARLXCA,.01, ARLXCA,.01
  DAMPD,.1, DAMPA,.1
  1,340., 2,250., 3,86., 4,473., 5,75., 6,75.
  7,145., 8,125., 9,172., 10,64., 11,430.
  12,88., 13,15., 14,15., 15,29., 16,17., 17,26.
END
BCD 3ARRAY DATA
  1,=240.,.72,=.216,=.13,END ← Louver Emissivity Table
  2,=205.,.13,=.180,=.72,END
  3 $ Q TABLE AS A FUNCTION OF TIME
    0,0, 0,0
    .042, .13
    .083, .26
    .167, .5
    .25, .71
    .33, .86
    .5, 1.
    .94,0., 1.0
  END
  99, 0.,.1, 100.,.9, END $ DAMPING FACTORS AS A FUNCTION OF LOOPCT
END
BCD 3EXECUTION
DIMENSION X(2000) / Fortran Statement → F
NIN=0 F
NDIM=2000 F
  ARYHPY(420,6305,.1714E-8,6305)
  *** CASE 1 S/S Comment Statement → C
  CINDSL
  *** CASE 7 TRANS
  NLOOP=100
  ARLXCA=.05
  ITEST=1
  JTEST=1
  LINECT=100
  TIMEND=96.
  OUTPUT=.167
  CNPRDL
  END
BCD 3VARIABLES 1
  RTEST=LOOPCT
  DIDEG(I RTEST,A99,DAMPD)
  STFSEP(DAMPD,DAMPA)
  IF (ITEST.EQ.1) GO TO 10 F
  IF (JTEST.EQ.1) GO TO 20 F
  STFSEP(K12,Q55)
  STFSEP(K13,Q41)
  STFSEP(K14,Q43)
  STFSEP(K15,Q46)
  STFSEP(K16,Q115)
  STFSEP(K17,Q125)
  GO TO 20 F
10 CONTINUE F
  DID1WH (TIMEH,A3,K1,Q24)
  DID1WH (TIMEH,A3,K2,Q25)
  DID1WH (TIMEH,A3,K3,Q68)
  DID1WH (TIMEH,A3,K4,Q55)
  DID1WH (TIMEH,A3,K5,Q41)
  DID1WH (TIMEH,A3,K6,Q43)
  DID1WH (TIMEH,A3,K7,Q46)
  DID1WH (TIMEH,A3,K8,Q116)
  DID1WH (TIMEH,A3,K9,Q125)
  DID1WH (TIMEH,A3,K10,Q71)
  DID1WH (TIMEH,A3,K11,Q69)
20 CONTINUE F
  END
BCD 3VARIABLES 2
  END
BCD 3OUTPUT CALLS
  TPRINT
  IF (JTEST.EQ.0) GO TO 10 F
  KTEST=KTEST+1 F
  IF (KTEST.EQ.2) OUTPUT=.333 F
  IF (KTEST.EQ.3) OUTPUT=.5 F
  IF (KTEST.EQ.4) OUTPUT=1. F
  IF (KTEST.EQ.5) OUTPUT=2. F
  IF (KTEST.EQ.6) OUTPUT=4. F
  IF (KTEST.EQ.8) OUTPUT=12. F
10 CONTINUE F
  END
  
```

FOLDOUT FRAME

Computer Output, Initial Node Temperatures

TIME=	0.00000	DTIMEU=	0.00000	CSGMIN(0)=	0.00000	TEMPCC(0)=	0.00000	RELXCC(0)=	0.00000					
T	1#	-2.10000+02	T	2#	-2.10000+02	T	3#	+2.10000+02	T	4#	-2.10000+02	T	5#	-2.10000+02	T	6#	-2.10000+02
T	10#	+2.50000+02	T	19#	-2.30000+02	T	16#	=2.00000+02	T	17#	-2.00000+02	T	18#	=3.00000+02	T	19#	=1.00000+02
T	20#	1.00000+01	T	21#	1.00000+01	T	22#	-2.00000+02	T	23#	+2.00000+02	T	24#	=5.00000+01	T	25#	=5.00000+01
T	26#	-5.00000+01	T	27#	-1.00000+01	T	28#	-2.80000+01	T	29#	+2.00000+02	T	30#	+2.00000+02	T	31#	-2.50000+02
T	32#	-2.50000+02	T	33#	-2.50000+02	T	34#	-2.00000+02	T	35#	-2.00000+02	T	36#	-2.50000+02	T	38#	-2.50000+02
T	39#	-5.00000+01	T	40#	-5.00000+01	T	41#	-5.00000+01	T	42#	-5.00000+01	T	43#	1.00000+00	T	44#	-1.00000+02
T	45#	-1.00000+02	T	46#	1.00000+00	T	47#	+2.00000+02	T	48#	-2.00000+02	T	49#	-2.00000+02	T	50#	-2.00000+02
T	51#	-2.00000+02	T	52#	=3.00000+02	T	53#	+2.00000+02	T	54#	=2.00000+02	T	55#	=1.00000+02	T	56#	=3.00000+02
T	57#	-2.00000+02	T	58#	-2.00000+02	T	59#	-1.00000+02	T	60#	-2.00000+02	T	66#	-2.00000+02	T	67#	-2.00000+02
T	68#	-2.00000+02	T	69#	-2.00000+02	T	76#	+2.00000+02	T	82#	-2.00000+02	T	94#	-2.00000+02	T	95#	-2.00000+02
T	97#	-2.00000+02	T	98#	-2.00000+02	T	112#	+2.00000+02	T	113#	-2.00000+02	T	114#	-2.00000+02	T	115#	-2.00000+02
T	116#	-2.00000+02	T	117#	-2.00000+02	T	119#	+2.00000+02	T	120#	-2.00000+02	T	121#	-2.00000+02	T	123#	-3.00000+02
T	124#	-2.00000+02	T	125#	-2.00000+02	T	128#	+3.00000+02	T	129#	+3.00000+02	T	142#	-3.00000+02	T	143#	-3.00000+02
T	144#	-3.00000+02	T	145#	-3.00000+02	T	169#	+2.00000+02	T	170#	=2.00000+02	T	171#	-2.00000+02	T	172#	=2.00000+02
T	173#	-2.00000+02	T	174#	-2.00000+02	T	175#	-2.00000+02	T	176#	-2.00000+02	T	177#	-2.00000+02	T	7#	-2.10000+02
T	8#	-2.10000+02	T	15#	-2.00000+02	T	37#	-2.00000+02	T	61#	-3.00000+02	T	62#	-2.00000+02	T	63#	-3.00000+02
T	64#	-2.00000+02	T	65#	-2.00000+02	T	70#	-2.00000+02	T	71#	=6.00000+01	T	72#	-2.00000+02	T	73#	-3.00000+02
T	74#	-2.00000+02	T	75#	-3.00000+02	T	77#	-2.00000+02	T	78#	-2.00000+02	T	79#	-2.00000+02	T	80#	-2.00000+02
T	81#	-2.00000+02	T	83#	-2.00000+02	T	84#	+2.00000+02	T	85#	-2.00000+02	T	86#	-2.00000+02	T	87#	-2.00000+02
T	88#	+3.00000+02	T	89#	-3.00000+02	T	90#	+3.00000+02	T	91#	-3.00000+02	T	92#	-3.00000+02	T	93#	-3.00000+02
T	96#	-2.00000+02	T	99#	-3.00000+02	T	100#	-2.00000+02	T	101#	-2.00000+02	T	102#	-2.00000+02	T	104#	-2.00000+02
T	105#	-2.00000+02	T	106#	-2.00000+02	T	107#	=2.00000+02	T	108#	-2.00000+02	T	109#	-2.00000+02	T	122#	-2.00000+02
T	126#	-2.00000+02	T	127#	-2.00000+02	T	130#	-2.00000+02	T	131#	-2.00000+02	T	132#	-2.00000+02	T	133#	-2.00000+02
T	134#	+2.00000+02	T	135#	-2.00000+02	T	136#	-2.00000+02	T	137#	=2.00000+02	T	138#	-2.00000+02	T	139#	-2.00000+02
T	140#	+2.00000+02	T	141#	-2.00000+02	T	146#	-3.00000+02	T	153#	-2.00000+02	T	154#	-2.00000+02	T	155#	-2.00000+02
T	156#	+2.00000+02	T	159#	-2.00000+02	T	160#	-2.00000+02	T	161#	-2.00000+02	T	162#	-2.00000+02	T	163#	=2.00000+02
T	164#	+2.00000+02	T	166#	1.00000+00	T	167#	1.00000+00	T	168#	+3.00000+01	T	9#	+6.50000+01	T	157#	5.00000+02
T	158#	+4.60000+02															

130204 FRAME

130204 FRAME 2

Computer Output, Steady-State Temperatures

```

*****
TIME= 0.00000 DTIMEU= 0.00000 CSGMIN( 0)= 0.00000 TEMPC( 0)= 0.00000 RELXCC( 4)= 9.24301-03

```

T	1#	-2.08920+02	T	2#	-2.06429+02	T	3#	-2.01797+02	T	4#	-2.18493+02	T	5#	-2.12541+02	T	6#	-2.04915+02
T	10#	-2.47544+02	T	14#	-2.03932+02	T	16#	-1.84528+02	T	17#	-2.38920+02	T	18#	-2.50687+02	T	19#	-1.56739+02
T	20#	5.49407+01	T	21#	5.62437+01	T	22#	1.23900+02	T	23#	-1.30567+02	T	24#	-1.76110+02	T	25#	-1.91070+02
T	26#	6.50000+01	T	27#	5.57324+01	T	28#	6.41222+01	T	29#	-1.41975+02	T	30#	-1.39260+02	T	31#	-2.89674+02
T	32#	-2.66615+02	T	33#	-2.92353+02	T	34#	-2.36965+02	T	35#	-2.34441+02	T	36#	-2.56067+02	T	38#	-2.48762+02
T	39#	1.21893+01	T	40#	9.29235+00	T	41#	1.21895+01	T	42#	4.98486+01	T	43#	3.49018+00	T	44#	-2.44911+02
T	45#	-2.38926+02	T	46#	1.20998+02	T	47#	-2.02672+02	T	48#	-2.00570+02	T	49#	-2.29490+02	T	50#	-1.70964+02
T	51#	-1.79296+02	T	52#	-2.40289+02	T	53#	-2.45040+02	T	54#	-2.22994+02	T	55#	-1.29330+02	T	56#	-2.45147+02
T	57#	-2.20149+02	T	58#	-2.46275+02	T	59#	-1.71475+02	T	60#	-2.20985+02	T	66#	-1.43571+02	T	67#	-2.97616+02
T	68#	1.40558+02	T	69#	-2.97787+02	T	74#	-2.15259+02	T	82#	-1.84275+02	T	94#	-2.00704+02	T	95#	-1.98569+02
T	97#	-1.97555+02	T	98#	-1.99110+02	T	112#	-1.96246+02	T	113#	-1.98721+02	T	114#	-2.09226+02	T	115#	-1.91663+02
T	116#	1.86411+02	T	117#	-2.12955+02	T	119#	-1.97808+02	T	120#	-1.97808+02	T	121#	-1.95978+02	T	122#	-1.96630+02
T	124#	1.84015+02	T	125#	-1.75218+02	T	128#	1.91234+02	T	129#	1.91234+02	T	142#	-2.22637+02	T	143#	-2.12056+02
T	144#	-2.32147+02	T	145#	-1.76118+02	T	169#	-2.21920+02	T	170#	-2.12057+02	T	171#	-1.96863+02	T	172#	-2.39316+02
T	173#	-2.12931+02	T	174#	-2.06363+02	T	175#	-2.26979+02	T	176#	-2.12240+02	T	177#	-1.98418+02	T	7#	-2.06431+02
T	8#	-2.12524+02	T	15#	-1.86579+02	T	37#	-2.54008+02	T	61#	-2.77162+01	T	62#	-2.01719+02	T	63#	5.68835+01
T	64#	-2.12464+02	T	65#	-1.94721+02	T	70#	1.93038+02	T	71#	-2.00050+02	T	72#	-3.08622+02	T	7#	-3.49504+02
T	74#	-2.97783+02	T	75#	-3.52572+02	T	77#	-2.69229+02	T	78#	-2.71533+02	T	79#	-2.08664+02	T	80#	-2.01185+02
T	81#	-1.94826+02	T	83#	-2.01821+02	T	84#	-9.35250+01	T	85#	-2.10154+02	T	86#	-2.12486+02	T	87#	-2.06408+02
T	88#	-2.08643+01	T	89#	-2.03705+02	T	90#	-2.46025+02	T	91#	-2.40254+02	T	92#	-2.49706+02	T	93#	-2.05675+02
T	96#	1.96282+02	T	99#	-2.53696+02	T	100#	-2.11243+02	T	101#	-2.07265+02	T	102#	-1.75854+02	T	104#	-1.75930+02
T	105#	-2.10214+02	T	106#	-2.49406+02	T	107#	-2.06413+02	T	108#	-1.19656+02	T	109#	-2.21577+02	T	122#	-1.96629+02
T	126#	-2.25112+02	T	127#	-2.15490+02	T	130#	-2.12223+02	T	131#	-2.08087+02	T	132#	-2.08739+02	T	133#	-2.29132+02
T	134#	-2.41801+02	T	135#	-2.72833+02	T	136#	-2.36779+02	T	137#	-2.51482+02	T	138#	-2.25240+02	T	139#	-2.15812+02
T	140#	-2.36787+02	T	141#	-2.52630+02	T	146#	-2.60279+02	T	153#	-2.37553+02	T	154#	-2.36068+02	T	155#	-2.31064+02
T	156#	-2.15711+02	T	159#	-2.55360+02	T	160#	-2.34237+02	T	161#	-2.14526+02	T	162#	-2.02145+02	T	163#	-2.31899+02
T	164#	-2.12084+02	T	166#	-2.44264+02	T	167#	-2.50395+02	T	168#	-2.03020+02	T	9#	6.50000+01	T	157#	5.00000+02
T	158#	-4.60000+02															

APPENDIX B PROPULSION SYSTEM ANALYSIS EQUATIONS

1.0 FIRING SIMULATION PROGRAM

This is a "time-advancing" program which computes propellant flow rates, the resultant changes in the ullage volumes, the gas flow rates into the ullages, the temperatures, and the pressures that result. That is to say, the result of time is simulated by repeating the entire sequence of calculations for as many increments of time as necessary to cover a totalized time interval equal to the predicted burning time, calculated values are carried forward as necessary and cumulative totals maintained. The equations used in the program are listed here in a logical order but it should be recognized that they could be solved in any other mathematically logical order without significantly changing the answers. Furthermore, this listing is not the actual computer program per se, but only the engineering equations, the computer program itself must of necessity, include certain instructions, checks, etc., which have been omitted there for the sake of clarity.

Table B-1 lists the symbols, their meaning, and the units used in these computations. Values of "given" and constant quantities are shown in parenthesis

Propellant flow rates to the engine are calculated by a trial-and-error process using these equations

$$(1) \quad \dot{m}_{ox} = \sqrt{\frac{g\rho_{lox} (P_{tox} - P_c)}{R_{ox}}}$$

$$(2) \quad \dot{m}_f = \sqrt{\frac{g\rho_{lf} (P_{tff} - P_c)}{R_f}}$$

$$(3) \quad r = \frac{\dot{m}_{ox}}{\dot{m}_f}$$

$$(4) \quad P_c = 14.4 I_s (\dot{m}_{ox} + \dot{m}_f)$$

$$(5) \quad N_{\text{ox}} = \frac{1.273 \dot{m}_{\text{ox}}}{D_{\text{ox}} \mu_{\text{ox}}}$$

$$(6) \quad N_{\text{f}} = \frac{1.273 \dot{m}_{\text{f}}}{D_{\text{f}} \mu_{\text{f}}}$$

$$(7) \quad R_{\text{ox}} = 0.8105 \left[\frac{f_{\text{ox}} L_{\text{ox}}}{D_{\text{ox}}^5} + \frac{1}{C_{\text{ox}}^2 D_{\text{ox}}^4} \right]$$

$$(8) \quad R_{\text{f}} = 0.8105 \left[\frac{f_{\text{f}} L_{\text{f}}}{D_{\text{f}}^5} + \frac{1}{C_{\text{f}}^2 D_{\text{f}}^4} \right]$$

To solve these equations, the propellant densities (ρ_{lox} and ρ_{lf}) and viscosities (μ_{ox} and μ_{f}) are calculated from equations or look up in tables as functions of temperature. The trial-and-error process is started by assuming values for chamber pressure (P_{c}) and the resistance coefficients (R_{ox} and R_{f}), which allows equations (1) and (2) to be solved to get first estimates of oxidizer and fuel flow rates (\dot{m}_{ox} and \dot{m}_{f}). After mixture ratio (r) is computed (equation 3), specific impulse (I_{g}) is looked up in a table as a function of mixture ratio (r). Next, the first iteration on chamber pressure (P_{c}) is obtained from equation (4). If this value differs from the initial estimate by more than the allowed error, iteration is necessary. A new estimate for chamber pressure is then calculated (a method which causes very fast convergence on the correct value is to let the next estimate of P_{c} equal 0.2 of the previous estimate plus 0.8 of the calculated P_{c}). Before a recalculation is made, however, the resistance coefficients should be reestimated by solving equations (5) and (6) for the Reynolds Numbers (N_{ox} and N_{f}), looking up the friction factors (f_{ox} and f_{f}) in a table as a function of those Reynolds Numbers, and then solving equations (7) and (8) for the new estimates of the resistance coefficients (R_{ox} and R_{f}). (In passing, it might be noted that these resistance coefficients have been formulated to account for both constant and variable discharge coefficients.)

If it is assumed that the propellant temperatures are constant throughout the particular firing being simulated, then the above calculation of chamber pressure, mixture ratio, and propellant flow rates needs to be made only once.

Next, the remaining masses of liquid propellants in the tanks and the ullage volumes are calculated using these simple relations

$$(9) \quad dm_{lox} = \dot{m}_{ox} d\theta + dm_{vox}$$

$$(10) \quad dm_{lf} = m_f d\theta + dm_{vof}$$

$$(11) \quad m_{lox} = m_{lox}(0) - \int_0^\theta dm_{lox}$$

$$(12) \quad m_{lf} = m_{lf}(0) - \int_0^\theta dm_{lf}$$

$$(13) \quad V_{uox} = V_{tox} - \frac{m_{lox}}{\rho_{lox}}$$

$$(14) \quad V_{uf} = V_{tf} - \frac{m_{lf}}{\rho_{lf}}$$

The value of $d\theta$ is equal to the length of the time step used in the calculation (e.g., if the computation is made for each successive second of burning time, $d\theta = 1$ sec). An estimate of the rate of propellant vapor evolution is necessary for the first time step computation only in order to get dm_{vox} and dm_{vof} , but for small time steps the errors resulting from setting these equal to zero for the first time step is very small. Values of the liquid propellant masses at the beginning of the firing ($m_{lox}(0)$ and $m_{lf}(0)$) are, of course, basic inputs as are the propellant tank volumes (V_{tox} and V_{tf}).

Next, the partial masses of helium in the propellant tank ullages and the helium flow rates to the ullages are calculated. If the total

pressure of a propellant tank exceeds regulated pressure (P_r), then the existing pressure is used in the calculations, otherwise, it is set to 300 psia on the assumption that the pressure regulator will control the pressure by admitting just enough gas to keep total pressure in the tank at the regulated level (i.e., total pressure equals the vapor pressure plus a partial pressure of helium sufficient to make the sum exactly 300 psia)

Propellant tank total pressures are calculated as follows. First, propellant vapor pressures are computed from equations or looked up in tables as functions of the ullage temperatures (see discussion above on the validity of this assumption). Approximate equations for OF_2 and B_2H_6 vapor pressure were obtained by curve fitting to selected empirical data.

$$P_{\text{vox}} = 2.7847 \times 10^{7.3474 - \frac{1029.15}{T_{\text{uox}}}}$$

$$P_{\text{vf}} = e^{17.5151 - \frac{3217.09}{T_{\text{uf}}}}$$

Next, the helium partial pressures are computed using the gas law. For the first time step, the initial or estimated values of the partial helium masses and ullage temperatures are used. For later time steps, the values from the previous time step are used. In both cases, the current ullage volumes, calculated as mentioned above, are used. Errors in the order of 2% will result unless the compressibility factors are correct. These factors are most simply obtained from a table as a function of helium pressure and temperature. For the first time step, it is necessary to provide an estimated ullage temperature and helium partial pressure, or an estimate of the compressibility factor; thereafter, it is sufficiently accurate to use the helium partial pressure and ullage temperature calculated during the previous time step. The partial pressures of helium, then are

$$(15) \quad P_{\text{heox}} = \frac{M_{\text{heox}} Z_{\text{ox}} R T_{\text{uox}}}{V_{\text{uox}}}$$

$$(16) \quad P_{\text{hef}} = \frac{M_{\text{hef}} Z_f R T_{\text{uf}}}{V_{\text{uf}}}$$

Propellant tank total pressures are assumed to be the simple sums of the vapor pressures of the propellants and the respective partial pressures of helium,

$$(17) \quad P_{\text{tox}} = P_{\text{vox}} + P_{\text{heox}}$$

$$(18) \quad P_{\text{tf}} = P_{\text{vof}} + P_{\text{hef}}$$

Whenever the calculated total pressure is less than regulated pressure ($P_r = 300 \text{ psia} - 43200 \text{ psfa}$), it is discarded and replaced with the regulated pressure valve. In that case, it is necessary to calculate the corresponding partial masses of helium in the ullage volume

$$(19) \quad M_{\text{heox}} = \frac{(P_{\text{tox}} - P_{\text{vox}}) V_{\text{uox}}}{Z_{\text{ox}} R T_{\text{uox}}}$$

$$(20) \quad M_{\text{hef}} = \frac{(P_{\text{tf}} - P_{\text{vof}}) V_{\text{uf}}}{Z_f R T_{\text{uf}}}$$

By subtracting the partial masses of helium for the previous time step from these current masses, a difference is obtained which is the mass change during this time step. The sum of the changes in the partial masses of helium in the oxidizer and fuel tanks is the change in the helium mass within the helium tank (by the conservation of mass law) (Note that none of these differential masses can be less than zero in a real system)

$$(21) \quad dm_{\text{heox}} = m_{\text{heox}_\theta} - m_{\text{heox}_{\theta-1}}$$

$$(22) \quad dm_{\text{hef}} = m_{\text{hef}_\theta} - m_{\text{hef}_{\theta-1}}$$

$$(23) \quad dm_{he} = dm_{heox} + dm_{hef}$$

The current mass of helium in the helium tank is simply the initial mass minus the sum of all the changes from time 0 to θ

$$(24) \quad m_{he} = m_{he(0)} - \int_0^\theta dm_{he}$$

In order to calculate the ullage temperatures, it is necessary to know the temperature of the incoming helium. This helium temperature can be estimated by assuming it is at the current average temperature of the helium in the helium tank (T_{he}) plus any changes in temperature incurred as the gas flows through the connecting plumbing, such as heating due to the Joule-Thomson effect within the regulator and convective heat transfer. The average temperature of the helium in the helium tank is assumed to be the initial temperature (time 0) plus the sum of all the incremental changes in temperature to time θ . These incremental changes are due to the net sum of the energy changes caused by expansion of the residual gas as helium flows from the tank, and to the transfer of heat from the tank wall to the gas. In order to estimate the heat transfer rate, a simplified free-convection model was adopted. This model requires a value for the convection coefficient, h_c , so an expression was set up using the average properties of helium

$$(25) \quad h_c = 1.39 \times 10^{-4} \left[G \left(\frac{P_{he}}{T_{he}} \right)^2 \left(\frac{T_w}{T_{he}} - 1 \right) \right]^{0.4}$$

where "G" is the acceleration of the spacecraft in "g's"

$$(26) \quad G = \frac{F}{m_{sc}} = \frac{F}{m_{sc(0)} - \int_0^\theta dm_{ox} - \int_0^\theta dm_f}$$

This convection coefficient changes very slowly during a firing so the values used for the variables can be those calculated during the previous time step, the coefficient can be zero at start without incurring any error.

The incremental change in temperature of the helium due to the convective heat transfer is then obtained by rearrangement of the conventional equation

$$q = \frac{dQ}{d\theta} = \frac{m_{he} C_{v_{he}} \partial T_{he}}{d\theta}$$

$$\partial T_{he} = \frac{d\theta}{\frac{m_{he} C_{v_{he}}}{q}}$$

but $q = h_c A (T_w - T_{he})$ (convection heat transfer)

so
$$\partial T_{he} = \frac{d\theta}{\frac{m_{he} C_{v_{he}}}{h_c S (T_w - T_{he})}}$$

The change in energy within the helium tank due to withdrawal of dm_{he} pounds of helium is

$$dE = \frac{Z_{he} R T_{he} dm_{he}}{J}$$

And the resultant incremental temperature change is

$$\alpha T_{he} = - \frac{1}{\frac{m_{he} C_{v_{he}}}{\left[\frac{Z_{he} R T_{he} dm_{he}}{J} \right]}}$$

Adding these two increments of temperature change together yields the total change affected during each time step $d\theta$.

$$(27) \quad dT_{he} = \frac{\left[h_c A (T_w - T_{he}) \right] d\theta - \frac{1}{J} (Z_{he} R T_{he}) d m_{he}}{m_{he} C_{v_{he}}}$$

The compressibility factor (Z_{he}) may be looked up in a table as a function of T_{he} and P_{he} ; omitting this step (i.e., letting $Z = 1$) leads to errors in excess of 20 percent when tank pressures are highest.

Current helium temperature (at time θ) is the initial temperature plus the algebraic sum of all the changes calculated for the individual time steps

$$(28) \quad T_{\text{he}} = T_{\text{he}(0)} + \int_0^{\theta} dT_{\text{he}}$$

The current helium tank pressure is calculated using the gas law

$$(29) \quad P_{\text{he}} = \frac{M_{\text{he}} Z_{\text{he}} R T_{\text{he}}}{V_{\text{he}}}$$

The above convective heat transfer calculation also included a value for the tank wall temperature, T_w . In the presently outlined order of computation, a new wall temperature is calculated next so it is available as an input for the following time step calculation. To obtain T_w , a simple mathematical model of the helium tank thermal balance was set up. Figure B-1 illustrates the nomenclature.

Imagining the wall to be composed of three discrete layers within which the temperatures are uniform and from which the heat flows uniformly, the model of the wall reduces to three heat capacitances (C1, C2 and C3) separated by three thermal resistances (R1W, R21 and R32). All parts of the tank and gas are assumed to be at the same temperature at start (time = 0). As gas is withdrawn, the remaining gas expands and is thus cooled to a lower temperature. This creates a temperature difference between the gas and the wall which drives heat from the wall to the gas. As the wall cools, it receives heat across resistance R1W from layer 1 (represented by capacitance C1). Heat extracted from C1 lowers its temperature so it in turn receives heat from C2, and so forth. The set of equations representing this model, and with which the temperature changes and temperatures are calculated, are based on the fundamental conduction relation,

$$q = kA\Delta T/x$$

and the thermal capacity definition,

$$dT = \frac{dQ}{mC_p}$$

Introducing the thermal resistance, R_t , equal to $\frac{X}{KA}$, and the thermal capacitance, C , equal to mc_p , gives the equations

$$q = \frac{\Delta T}{R_t}$$

and
$$dT = \frac{dQ}{C}$$

These two relations may be combined in an expression for the conservation of energy law, which in this case says that the net heat flow into any thermal capacitance must be equal to the rate of change in its energy content

$$q_{in} - q_{out} = \frac{dE}{d\theta} = \frac{dQ}{d\theta} = \frac{CdT}{d\theta}$$

or
$$dT = \frac{(q_{in} - q_{out})}{C} d\theta$$

For any layer, n , in the tank,

$$(30) \quad dT_n = \left[\left(\frac{\Delta T}{R_t} \right)_{in} - \left(\frac{\Delta T}{R_t} \right)_{out} \right] \frac{d\theta}{C_n} = \left(\frac{T_{n+1} - T_n}{R_{t(n+1 \rightarrow n)}} - \frac{T_n - T_{n-1}}{R_{t(n \rightarrow n-1)}} \right) \frac{d\theta}{C_n}$$

For the outermost layer, which receives no heat, the heat flow out results in a change of.

$$(31) \quad dT_m = - \left(\frac{T_m - T_{m-1}}{R_{t(m \rightarrow m-1)}} \right) \frac{d\theta}{C_m}$$

and the current temperature (at time θ) is

$$(32) \quad T_n = T_n(0) \int_0^\theta dT_n$$

After having solved these equations for all three layers in the tank, the inside wall temperature (T_w) can be calculated on the basis that the rate at which heat arrives at a surface is the same as the rate at which

heat leaves a surface (i e , a surface has no thermal capacity and therefore cannot store energy)*

$$q_{in} = q_{out}$$

$$q_{in} = \frac{T_l - T_w}{R_t lW}$$

$$q_{out} = h_c A (T_w - T_{he})$$

Rearranging and solving for T_w gives,

$$(33) \quad T_w = \frac{T_l + T_{he} h_c A R_t lW}{1 + h_c A R_t lW}$$

Having the temperature of the gas leaving the helium tank, T_{he} (equation 28), it is now possible to estimate the temperature of the gas entering the propellant tank ullages (T_g). Heat transferring to this flow of gas from the gas circuitry hardware (lines, valves, filters, etc) was ignored in the present model although the effect of this extra heat could be appreciable during the initial moments of flow. An attempt was made, however, to approximate the Joule-Thomson effect by constructing a table of temperature rise through the regulator (ΔT_{jt}) as a function of regulator inlet pressure and temperature (P_{he} and T_{he}). The values of temperature rise for the table were obtained from a temperature-entropy diagram by following constant enthalpy lines from their point of intersection with the chosen inlet pressure and temperature conditions to their intersection with the 300 psia line, reading the temperature value there and subtracting from it the inlet temperature. Outlet temperature from the regulator (and inlet temperature for the propellant tank ullages) then is

$$(34) \quad T_g = T_{he} + \Delta T_{jt}$$

* Thermophysical properties such as surface energy is ignored in this model

Propellant vapor densities, rates of vapor evolution, and total vapor masses are required to calculate the average ullage temperature. Vapor densities can be looked up in tables as a function of ullage temperature or calculated from equations. An equation for OF_2 vapor density was obtained by curve fitting selected empirical data

$$\rho_{\text{VOX}} = e^{8.2 - \frac{2180}{T_{\text{uox}}}}$$

The rates of vapor evolution or condensation are the differentials of the mass equation (expressed here for a single component for clarity, but must be solved for both propellants)

$$(35) \quad m_v = \rho_v V_u$$

$$(36) \quad \text{therefore,} \quad dm_v = \rho_v dV_u + V_u d\rho_v$$

Initial estimates of ullage volume (V_u) and vapor density (ρ_v) at time 0 must be supplied for the first time step calculations of dV_u and $d\rho_v$ but thereafter, the previous time step values are used (i.e., $dV_u = V_{u\theta} - V_{u\theta-1}$).

Changes in the ullage temperatures can be calculated from the energy balances. A number of simplifications and assumptions were accepted in order to make the calculation reasonably easy. These were discussed above. The differential quantities of energy brought into the ullage by the incoming helium and evolving vapor are

$$dH_{\text{he}} = dm_{\text{he}} C_{p_{\text{he}}} T_g$$

$$dH_v = dm_v C_{p_v} T_l$$

The differential quantities of internal energy possessed by these fluids after they come to equilibrium with the ullage gases are

$$dU_{\text{he}} = dm_{\text{he}} C_{v_{\text{he}}} T_u$$

$$dU_v = dm_v C_{V_v} T_u$$

The differential quantity of work done by the ullage gas in expelling the differential volume of propellant is

$$dW = \frac{P}{J} dV_u$$

The energy balance equates the changes in energy of the incoming helium and the propellant vapor being evolved minus the expulsion work done, to the change in internal energy of the ullage gases

$$(dH_{he} - dU_{he}) + (dH_v - dU_v) - JW = dU_{he + v} = (m_{he} C_{V_{he}} + m_v C_{V_v}) dT_u$$

Rearranging the terms gives an explicit expression for the change in ullage temperature.

$$(37) \quad dT_u = \frac{(dH_{he} - dU_{he}) + (dH_v - dU_v) - dW}{m_{he} C_{V_{he}} + m_v C_{V_v}} = \frac{dm_{he} (C_{P_{he}} T_g - C_{V_{he}} T_g) + dm_v (C_{P_v} T_l - C_{V_v} T_u) - \frac{P}{J} dV_u}{m_{he} C_{V_{he}} + m_v C_{V_v}}$$

Finally, the new ullage temperatures are calculated by adding the sums of the differential changes (dT_u) to the initial temperatures (at time = 0).

$$(38) \quad T_{uox} = T_{uox}(0) + \int_0^\theta dT_{uox}$$

$$(39) \quad T_{uf} = T_{uf}(0) + \int_0^\theta dT_{uf}$$

This completes the entire calculation for one time step (value of θ). The process is, of course, repeated as often as necessary to reach the required total burn time by carrying forward all the values calculated

2.0 CRUISE-MODE PROGRAM

Equations which determine the equilibrium pressures and masses in the ullages were programmed for a digital computer so that the effects of temperature changes and helium solubility in the propellants could be analyzed. This analysis is specifically designed to determine the magnitude of problems which may arise because equilibrium temperatures may change with time during a mission, or because at the end of a firing, the ullage gas temperatures and helium partial pressures may be substantially different than the equilibrium values. Either of these situations may cause excessive tank pressures to develop. Therefore, it is necessary to investigate (1) the effect of reaching thermal equilibrium in the propellant tanks, and (2) the helium partial pressure which will remain after reaching the equilibrium concentration of dissolved helium in the liquids.

The approach outlined below uses mass balance, gas law and solubility relations. These are steady-state equations (time is not a variable). Identical calculations are made for fuel and oxidizer. In the description below, the input values (those constants or variables which are known for one temperature condition such as at the end of a firing) are labeled condition (1). The desired values (unknowns being solved for) are labeled condition (2),

First, the propellant liquid and vapor densities are looked up in tables or calculated as functions of the condition (2) liquid and ullage gas temperatures. (Presumably, for equilibrium conditions, the liquid and ullage gas temperatures are identical.) Ullage volumes are then computed on the basis of the conservation of mass which means that the total mass of a propellant (liquid plus vapor) remains unchanged although the amounts existing as liquid and vapor change with temperature.

$$\text{At condition (1)} \quad m_1 = m_{L1} + m_{V1}$$

$$\text{At condition (2)} \quad m_2 = m_{L2} + m_{V2}$$

$$m_1 = m_2 \quad (\text{from the conservation of mass})$$

$$\therefore m_{L1} + m_{v1} = m_{L2} + m_{v2}$$

$$V_{u2} = V_t - V_{L2}$$

$$V_{L2} = \frac{m_{L2}}{\rho_{L2}}$$

$$m_{L2} = m_{L1} + m_{v1} - m_{v2}$$

$$m_{v2} = V_{u2} \rho_{v2}$$

$$V_{u2} = V_t - \frac{m_{L1} + m_{v1} - V_{u2} \rho_{v2}}{\rho_{L2}}$$

Solving for V_{u2}
(40)

$$V_{u2} = \frac{V_t \rho_{L2} - m_{L1} - m_{v1}}{\rho_{L2} - \rho_{v2}}$$

Mass of the liquid at condition (2) is

$$m_{L2} = m_{L1} + m_{v1} - m_{v2}$$

(41)

$$m_{L2} = m_{L1} + m_{v1} - V_{u2} \rho_{v2}$$

In order to determine the equilibrium partial pressure of helium, which is a function of helium solubility (s_2) or concentration (lb/lb) it is necessary to establish the solubility divided by the partial mass of helium in the ullage

$$ss_2 = \frac{s_2}{m_{hu2}}$$

But the solubility itself is a function of the partial pressure as well as temperature

$$S_2 = (C_1 + C_2 T_{L2} + C_3 T_{L2}^2) P_{hu2}$$

Data contained in Reference 7 were used to obtain the values of the constants, C_1 , C_2 , and C_3 by curve fitting. They are.

	C_1	C_2	C_3
OF_2	$+6.9361 \times 10^{-9}$	-9.8294×10^{-11}	$+3.698 \times 10^{-12}$
B_2H_6	$+1.9382 \times 10^{-8}$	-1.8383×10^{-10}	$+4.5944 \times 10^{-13}$

when the units are pounds, pounds per square foot, and rankine.

However, since
$$P_{hu2} = \frac{m_{hu2} Z_2 R T_{u2}}{V_{u2}},$$

$$s_2 = (C_1 + C_2 T_{L2} + C_3 T_{L2}^2) \frac{m_{hu2} Z_2 R T_{u2}}{V_{u2}}$$

Therefore,

$$(42) \quad ss_2 = (C_1 + C_2 T_{L2} + C_3 T_{L2}^2) \frac{Z_2 R T_{u2}}{V_{u2}}$$

During the cruise periods, no additional helium is added to the propellant tanks, so by the conservation of mass

$$m_{h1} = m_{h2}$$

Each of these total masses consists of two parts, the partial mass of helium in the ullage, and the mass of helium dissolved in the liquid

$$m_h = m_{hu} + m_{hs}$$

The amounts dissolved in the liquids are the solubilities times the liquid masses.

$$m_{hs} = sm_L$$

$$\therefore m_{hu1} + s_1 m_{L1} = m_{hu2} + s_2 m_{L2}$$

However, s is unknown, so set

$$s_2 = ss_2 m_{hu2}$$

then $m_{hu1} + s_1 m_{L1} = m_{hu2} + ss_2 m_{hu2} m_{L1} = m_{hu2} (1 + ss_2 m_{L2})$

Solving for m_{hu2}

$$(43) \quad m_{hu2} = \frac{m_{hu1} + s_1 m_{L1}}{1 + ss_2 m_{L2}}$$

With the partial mass of helium in the ullage at condition (2) known, it is now possible to calculate the helium partial pressure by the gas law.

$$(44) \quad P_{hu2} = \frac{m_{hu2} Z_2 R T_{u2}}{V_{u2}}$$

This pressure plus the propellant vapor pressure (looked up in a table or calculated as a function of T_{u2}) is the total pressure in the propellant tank at equilibrium condition (2)

$$(45) \quad P_{t2} = P_{v2} + P_{hu2}$$

Finally, the actual solubility can be computed now that the helium partial mass is known

$$(46) \quad s_2 = ss_2 m_{hu2}$$

The mass of helium dissolved in the liquid, and therefore lost as far as useful work is concerned, is

$$(47) \quad m_{hs2} = s_2 m_{L2}$$

Table B-1 Nomenclature

A	= inside surface area of helium tank (18 96), sq ft.
C	= thermal capacity, Btu/°R
C ₁	= thermal capacity of layer 1 of helium tank (7 67), Btu/°R
C ₂	= thermal capacity of layer 2 of helium tank (7 27), Btu/°R
C ₃	= thermal capacity of layer 3 of helium tank (7 27), Btu/°R
C _f	= flow resistance coefficient of fuel injector
C _{ox}	= flow resistance coefficient of oxidizer injector
C _p	= specific heat at constant pressure, Btu/lb-°R
C _{p_{he}}	= specific heat at constant pressure of helium (1.255), Btu/lb-°R
C _{p_{vf}}	= specific heat at constant pressure of fuel vapor (0 3), Btu/lb-°R
C _{p_{vox}}	= specific heat at constant volume of oxidizer vapor (0 1333), Btu/lb-°R
C _{v_{he}}	= specific heat at constant volume of helium (0.753), Btu/lb-°R
C _{v_{vf}}	= specific heat at constant volume of fuel vapor (0 2), Btu/lb-°R
C _{v_{vox}}	= specific heat at constant volume of oxidizer vapor (0 1333), Btu/lb-°R
dE	= differential amount of energy, Btu
D _f	= equivalent fuel feedline diameter (0.5667), ft
dH	= differential amount of enthalpy, Btu
dm _f	= differential mass of liquid fuel, lb
dm _{he}	= differential mass of helium, lb
dm _{ox}	= differential mass of liquid oxidizer, lb
dm _v	= differential mass of vapor, lb
dm _{vf}	= differential mass of fuel vapor, lb
dm _{vox}	= differential mass of oxidizer vapor, lb
D _{ox}	= equivalent oxidizer feedline diameter (0.05667), ft

Table B-1 (Con't.)

dQ	= differential amount of heat, Btu
dT	= differential change in temperature, $^{\circ}R$
dT_1	= differential change in temperature of layer 1 of helium tank, $^{\circ}R$
dT_2	= differential change in temperature of layer 2 of helium tank, $^{\circ}R$
dT_3	= differential change in temperature of layer 3 of helium tank, $^{\circ}R$
dT_{he}	= differential change in average temperature of helium in helium tank, $^{\circ}R$
dT_{uf}	= differential change in average temperature of ullage gases in fuel tank, $^{\circ}R$
dT_{uox}	= differential change in average temperature of ullage gases in oxidizer tank, $^{\circ}R$
dU	= differential amount of internal energy, Btu
dV_{uf}	= differential change in volume of ullage in fuel tank, cu ft
dV_{uox}	= differential change in volume of ullage in oxidizer tank, cu ft
dW	= differential amount of work, Btu
$d\theta$	= time interval between calculations, seconds
e	= 2 71828
F	= thrust, lb
f_f	= friction factor in fuel feed system, dimensionless
f_{ox}	= friction factor in oxidizer feed system, dimensionless
g	= gravitational constant (32 174), ft/sec^2
G	= acceleration, $g's$
h_c	= convective heat transfer coefficient, $Btu/^{\circ}R-ft^2-sec$
I_s	= specific impulse, lb_f-sec/lb_m
J	= mechanical equivalent of heat (778 16), $ft-lb/Btu$
k	= thermal conductivity, $Btu/ft-^{\circ}R-sec$
L_f	= number of equivalent L/D 's of fuel feedline and components, dimensionless

Table B-1 (Con't)

L_{ox}	= number of equivalent L/D's of oxidizer feedline and components, dimensionless
m_f	= mass flow rate of liquid fuel, lb/sec
\dot{m}_{ox}	= mass flow rate of liquid oxidizer, lb/sec
m_{he}	= mass of helium in helium tank, lb
m_{hef}	= mass of helium in ullage of fuel tank, lb
m_{heox}	= mass of helium in ullage of oxidizer tank, lb
m_{lf}	= mass of liquid fuel, lb
m_{lox}	= mass of liquid oxidizer, lb
m_{sc}	= mass of dry spacecraft, lb
m_{vf}	= mass of fuel vapor, lb
m_{vox}	= mass of oxidizer vapor, lb
N_f	= Reynolds Number in fuel feedlines, dimensionless
N_{ox}	= Reynolds Number in oxidizer feedline, dimensionless
P_c	= chamber pressure, lb/ft ² (absolute)
P_r	= regulated pressure (43200), lb/ft ² (absolute)
P_{tf}	= total pressure in fuel tank, lb/ft ² (absolute)
P_{tox}	= total pressure in oxidizer tank, lb/ft ² (absolute)
P_{vf}	= partial pressure of fuel vapor, lb/ft ² (absolute)
P_{vox}	= partial pressure of oxidizer vapor, lb/ft ² (absolute)
q	= heat flux, Btu/sec
r	= mixture ratio, o/f, dimensionless
R	= gas constant for helium (386), ft-lb/lb-°R
R_f	= flow resistance in fuel circuit, ft ⁻⁴
R_{ox}	= flow resistance in oxidizer circuit- ft ⁻⁴
R_t	= thermal resistance, °R-sec/Btu

Table B-1 (Con't.)

R_{t1w}	= thermal resistance between layer 1 center-of-mass and wall surface in helium tank (2 536), $^{\circ}\text{R-sec/Btu}$
R_{t21}	= thermal resistance between the centers-of-mass of layers 2 and 1 of the helium tank (5 072), $^{\circ}\text{R-sec/Btu}$
R_{t32}	= thermal resistance between the centers-of-mass of layers 3 and 2 of the helium tank (5.072), $^{\circ}\text{R-sec/Btu}$
T_1	= average temperature of layer 1 of helium tank wall, $^{\circ}\text{R}$
T_2	= average temperature of layer 2 of helium tank wall, $^{\circ}\text{R}$
T_3	= average temperature of layer 3 of helium tank wall, $^{\circ}\text{R}$
T_g	= temperature of helium entering propellant tank ullages, $^{\circ}\text{R}$
T_{he}	= average temperature of helium in helium tank, $^{\circ}\text{R}$
T_1	= temperature of liquid propellant, $^{\circ}\text{R}$
T_{1f}	= average temperature of liquid fuel, $^{\circ}\text{R}$
T_{1ox}	= average temperature of liquid oxidizer, $^{\circ}\text{R}$
T_{uf}	= average temperature of gases in fuel tank ullage, $^{\circ}\text{R}$
T_{uox}	= average temperature of gases in oxidizer tank ullages, $^{\circ}\text{R}$
T_w	= average temperature of inside wall surface of helium tank, $^{\circ}\text{R}$
V_{he}	= volume of helium tank (7.36), cu ft
V_{tf}	= volume of fuel tank (27.37), cu ft
V_{tox}	= volume of oxidizer tank (27 37), cu ft
V_{uf}	= ullage volume in fuel tank, cu ft
V_{uox}	= ullage volume in oxidizer tank, cu ft
X	= length of thermal path, ft
Z_f	= compressibility factor of helium in fuel tank ullage, dimensionless
Z_{he}	= compressibility factor of helium in helium tank, dimensionless
Z_{ox}	= compressibility factor of helium in oxidizer tank ullage, dimensionless

Table B-1 (CON't)

ΔT	= temperature difference across a thermal resistance, $^{\circ}R$
ΔT_{Jt}	= temperature change due to Joule-Thomson effect, $^{\circ}R$
ΔV	= velocity change during spacecraft maneuver, ft/sec
θ	= time when computation made, seconds
μ_f	= absolute viscosity of fuel, lb/sec-ft
μ_{ox}	= absolute viscosity of oxidizer, lb/sec-ft
ρ_{lf}	= density of liquid fuel, lb/cu ft
ρ_{lox}	= density of liquid oxidizer, lb/cu ft
ρ_{vf}	= density of fuel vapor, lb/cu ft
ρ_{vox}	= density of oxidizer vapor, lb/cu ft

Symbols used in Cruise simulation equations, not given above

$C1, C2, C3$	= coefficients in solubility equation, dimensionless
m_h	= total mass of helium in propellant (oxidizer or fuel) tank, lb
m_{h1}	= total mass of helium in propellant (oxidizer or fuel) tank at condition 1, lb
m_{h2}	= total mass of helium in propellant (oxidizer or fuel) tank at condition 2, lb
m_{hu}	= mass of helium in propellant (oxidizer or fuel) ullage, lb
m_{hu1}	= mass of helium in propellant (oxidizer or fuel) ullage at condition 1, lb
m_{hu2}	= mass of helium in propellant (oxidizer or fuel) ullage at condition 2, lb
m_{hs}	= mass of helium dissolved in propellant (oxidizer or fuel), lb
m_{hs1}	= mass of helium dissolved in propellant (oxidizer or fuel), lb

Table B-1 (Con't.)

m_{hs2}	= mass of helium dissolved in propellant (oxidizer or fuel), lb
m_{L1}	= mass of propellant (oxidizer or fuel) as liquid condition 1, lb
m_{L2}	= mass of propellant (oxidizer or fuel) as liquid at condition 2, lb
m_{v1}	= mass of propellant (oxidizer or fuel) vapor at condition 1, lb
m_{v2}	= mass of propellant (oxidizer or fuel) vapor at condition 2, lb
P_{hu2}	= partial pressure of helium in ullage at condition 2, lb/ft ²
s	= solubility of helium in propellant (oxidizer or fuel), lb/lb
s_1	= solubility of helium in propellant (oxidizer or fuel) at condition 1, lb/lb
s_2	= solubility of helium in propellant (oxidizer or fuel)
ss_1	= solubility of helium in propellant (oxidizer or fuel) divided by mass of helium in ullage at condition 1, lb/lb/lb
ss_2	= solubility of helium in propellant (oxidizer or fuel) divided by mass of helium in ullage at condition 2, lb/lb/lb
T_{L2}	= temperature of liquid propellant (oxidizer or fuel) at condition 2, °R
T_{u2}	= temperature of ullage gases at condition 2, °R
V_{L1}	= volume of liquid propellant (oxidizer or fuel) at condition 1, ft ³
V_{L2}	= volume of liquid propellant (oxidizer or fuel) at condition 2, ft ³
V_t	= volume of oxidizer or fuel tank, ft ³
V_{u1}	= volume of ullage (oxidizer or fuel) at condition 1, ft ³
V_{u2}	= volume of ullage (oxidizer or fuel) at condition 2, ft ³
Z_2	= compressibility factor of helium at condition 2, dimensionless
ρ_{L2}	= density of liquid propellant (oxidizer or fuel) at condition 2, lb _m /ft ³
ρ_{v2}	= density of propellant (oxidizer or fuel) vapor at condition 2, lb _m /ft ³

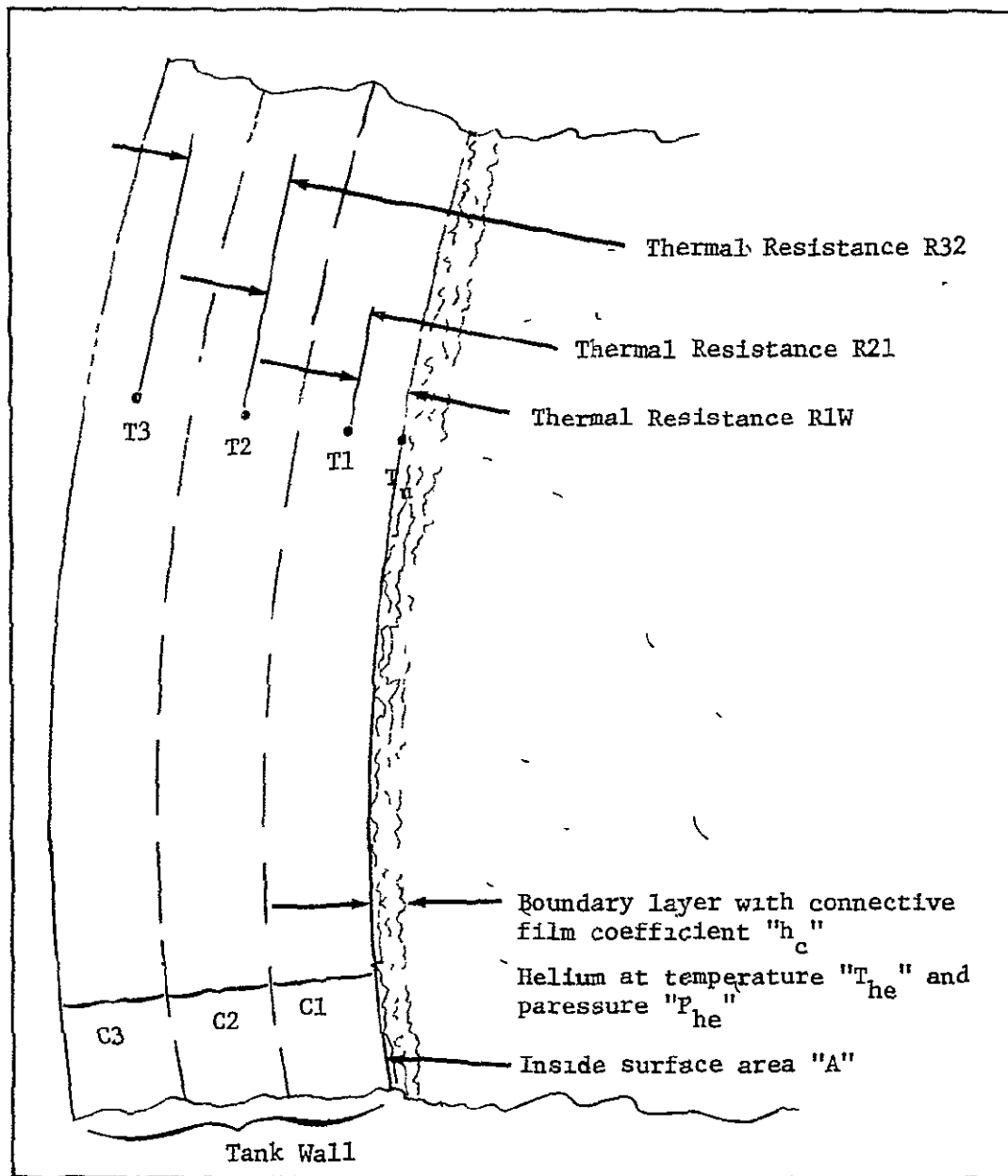


Figure B-1 Model Used in Calculating Heat Transfer from Tank Wall to Helium